THE ROLE OF THREE-DIMENSIONAL ECHOCARDIOGRAPHY IN THE EVALUATION OF PHYSIOLOGICAL AND PATHOLOGICAL RIGHT VENTRICULAR REMODELING

Doctoral Thesis

Doronina Alexandra M.D.

Semmelweis University
Doctoral School of Basic and Translational Medicine

Supervisors: Béla Merkely M.D., Ph.D., D.Sc.
Attila Kovács M.D., Ph.D.

Official Reviewers: Réka Faludi M.D., Ph.D.
Gergely Szabó M.D., Ph.D.

Head of Final Examination Committee:
Katalin Darvas M.D., Ph.D.

Members of Final Examination Committee:
Leila Seres M.D., Ph.D.
Viktor Horváth M.D., Ph.D.

Budapest
2018

TABLE OF CONTENTS

1. ABBREVIATIONS

2D	Two-dimensional
3DE	Three-dimensional echocardiography
A	Late wave of mitral inflow
a`	Late diastolic velocity
AC	Arrhythmogenic Cardiomyopathy
A4C	Apical 4-chamber view
A2C	Apical 2-chamber view
ANOVA	Analysis of variance
BMI	Body Mass Index
BSA	Body Surface Area
CMR	Cardiac Magnetic Resonance Imaging
CT	Computed Tomography
DCT	Deceleration time
DCM	Dilated Cardiomyopathy
E	Early wave of mitral valve inflow
e`	Early diastolic velocity
EDV	End-diastolic volume
EDVi	End-diastolic volume index
EF	Ejection Fraction
ESV	End-systolic volume
ESVi	End-diastolic volume index
FAC	Fractional Area Change
FFMI	Fat Free Mass Index
GCS	Global Circumferencial Strain
GLS	Global Longitudinal Strain
GRS	Global Radial Strain
ID	Internal Diameter
ICU	Intensive Care Unit

IFBB	International Federation of Bodybuilding and Fitness
IGF	Insulin-like Growth Factor
ISHLT	International Society for Heart&Transplantation
IVC	Inferior Vena Cava
IVSd	Interventricular Septum in end-diastole
HCM	Hypertrophic Cardiomyopathy
HR	Heart rate
HTX	Heart transplantation
LEF	Longitudinal ejection fraction
LV	Left Ventricle
LVEDV	Left Ventricular end-diastolic volume
LVESV	Left ventricular end-systolic volume
LVH	Left Ventricular Hypertrophy
IVIDd	Left Ventricular Internal Diameter
LVMi	Left Ventricular Mass index
LVOT	Left Ventricular Outflow Tract
LVPWd	Left Ventricular Posterior Wall Diameter in end-diastole
LVWT	Left Ventricular Wall Thickness
M-mode	Motion Mode
MRI	Magnetic Resonance Imaging
PA	Pulmonary Artery
$pAMR_2$	Pathologic antibody-mediated reaction
PASP	Pulmonary arterial systolic pressure
PVK	Pulmonary vascular resistance
PW	Posterior Wall
PW TDI s`	Pulsed-Wave Tissue Doppler Imaging systolic velocity
RA	Right Atrium
REF	Radial ejection fraction
ReVISION	Right VentrIcular Separate wall motIon quantificatiON
RV	Right Ventricle

RVOT	Right Ventricular Outflow Tract
RVTD	Right Ventricular Internal Diameter
RWT	Relative Wall Thickness
S	End-systole
SBP	Systolic blood pressure
SCD	Sudden Cardiac Death
SV	Stroke Volume
SVi	Stroke Volume index
TAPSE	Tricuspid Annular Plane Systolic Excursion
TEF	Total ejection fraction
TR	Tricuspid regurgitation

2. INTRODUCTION

The right ventricle (RV) is the heart chamber that receives deoxygenated blood from the right atrium (RA) and then pumps it into the pulmonary artery (PA) to maintain the pulmonary circulation. Although there is no doubt that the RV is important for normal physiology, the role of the RV in cardiac pathology is frequently underestimated. Currently, there is clear evidence showing that the RV is a strong predictor of outcomes in a range of pathologic conditions, such as RV myocardial infarction, heart failure, pulmonary hypertension, myocarditis, and cardiomyopathies, in addition to heart transplant (HTX) patients (1). Echocardiography remains the routine clinical examination of choice to assess RV structure, function and hemodynamics (2, 3). However, it is complicated to analyze RV dysfunction based on a conventional echocardiographic examination because it is located in an anterior position right behind the sternum and has a complex geometry, prominent trabeculations and a poorly delineated endocardial border. Hence, the myocardial mechanics of the RV are not fully understood. Novel modalities, such as three-dimensional echocardiography (3DE) and speckle-tracking echocardiography, can be useful for overcoming these limitations and may provide a better understanding of the mechanical aspects of RV performance under physiological conditions (e.g., in athlete's heart) and the mechanisms underlying cardiac diseases.

Athlete's heart' is an umbrella term that covers various cardiac effects resulting from regular intense exercise. It is a non-pathological complex of changes in the functional, structural and electrical characteristics of the heart and is also referred to as "athletic heart syndrome", "athletic bradycardia" or "exercise-induced cardiomegaly". It is a physiological, benign condition that makes intensive bouts of exercise more well-tolerated in athletes than in nonathletes in addition to playing an important physiological role heart adaptations that help a good athlete to become a great one. According to the law of Laplace, "a larger heart can fill and empty larger volumes more efficiently" than does a smaller heart (4). Athlete's heart has been a topic of great interest for cardiologists for almost two centuries and continues to be a popular topic today. The first study in the literature to describe the remarkable changes that occur in cardiac morphology in response to intensive

exercise appeared in the 19th century. The first such observations were initially presented in early 1890 by a Swedish clinician, Henschen (5) who described findings in elite Nordic skiers. Eugene Darling (6) from Harvard University used percussion and auscultation to determine whether cardiac dimensions were increased in university rowers. In the early 1900s, Paul Dudley White (7) provided the first report of sinus bradycardia at resting among long-distance runners. Chest X-rays later confirmed both Darling's and Henschen's findings by showing that the hearts of sportsmen are enlarged (4).

Sudden cardiac death (SCD) is a tragic event that occurs in professional athletes in all age groups. In athletes older than 35 years old, 80% of cases of SCD occur due to coronary artery disease, while in younger athletes (>35 years old), the most frequent causes of SCD are hypertrophic cardiomyopathy (HCM) and arrhythmogenic cardiomyopathy (AC) (8, 9). Elite athletes train and perform at levels that exceed the capabilities of most others groups. As a result, they may develop myocardial hypertrophy as a physiological response to intensive physical training. The degree of increased myocardial thickness as a result of athletic physiological adaptations is associated with the pathological hypertrophy observed in HCM, making it difficult to distinguish the two entities. Left ventricular (LV) wall thickness (LVWT) ranging between 12 and 16 mm represents the "gray zone" between the physiological adaptations exhibited by athletes and the pathological expression of HCM. AC is a progressive inherited muscle disorder characterized by ventricular arrhythmia, heart failure and SCD that manifests predominantly in younger individuals. Traditionally, AC has been associated with the Mediterranean basin; however, the growing incidence of AC, around the world suggests that this disease may not be associated with ethnicity or geography (10). AC accounts for approximately 5% of the incidence of SCD in athletes and has an overall incidence of 1/1,000 in the general population (8, 11).

In athletes, it can be difficult to distinguish physiological from pathological alterations. A misdiagnosis can be devastating to an athlete because it can result in an unnecessary interruption in training or elimination from competition. Conversely, a false negative diagnosis could jeopardize a young life and prevent further risk stratification or the evaluation of family members for genetic conditions. Currently, interest in clinical and research studies aimed at evaluating adaptations in the RV is growing because of awareness

about AC and exercise-induced RV dysfunction. The aim of the present thesis is to discuss the role of 3DE in evaluating RV remodeling and determine whether it can be utilized to help clinicians assess physiological and pathological cardiac processes.

2.1 Comparison of anatomical features and physiology of the left and right ventricles

2.1.1 Left ventricle

The LV forms the left-lateral and diaphragmatic surface of the heart and represents a large part of the apex. A normal LV geometry has been described as a prolate ellipsoid shape with the long-axis directed from the apex to the base (12). When the heart is viewed from the anterior, most of the LV is hidden by the RV, and the LV outflow tract (LVOT) overlaps its inflow tract. The LV is essentially divided into inlet and outlet tracts, which are separated by the anterior leaflet of the mitral valve. The hallmark of the LV inflow tract is the mitral (bicuspid) valve apparatus, which consists of the annulus fibrosus, the mitral valve itself, the chordate tendinae and the papillary muscles. The outlet portion of the LV, also called the aortic vestibule or subaortic area, is a narrow cavity in which the interventricular septum forms the anterior wall, and the anterior cusp of the mitral valve forms the posterior wall and the aortic valve orifice. The apical portion contains fine trabeculations. The curved LV septum bulges into the RV cavity. The larger part of the LV has a muscular component, whereas the upper part is thin and consists of fibrous tissue (the so-called membranous ventricular septum or septum membranaceum) that is situated just beneath the aortic valve. After an individual reaches 60 years of age, the basal part of the muscular septum increases in size, giving it a sigmoid appearance that mimics HCM on echocardiography (13-15). Normally, the LV wall thins at the apex and gradually thickens toward its base. Even in hypertrophied ventricles, the myocardium is only 1–2 mm thick at its tip. The heart wall consists of a thin subepicardial layer and a thicker trabeculated subendocardial layer at a ratio of approximately 1:2. The papillary muscles supporting the mitral valve are essential structural components of the LV wall. In the parasternal short-axis

view, two distinct portions of papillary muscles are visible and are named, according to their positions, the anterolateral and posteromedial groups. The anterior muscular band is slightly larger than the posterior one, and each pillar consists of a major trunk with one or multiple heads from which chordae tendinae extend.

The apical and basal parts of the LV rotate in two opposite directions. The band in the subendocardium is a right-handed or counterclockwise helix that descends from the basal loop to the apex, while the band in the subendocardium is a left-handed or clockwise helix that ascends from the apex to the basal loop. The helix angle changes continuously from the subendocardium to the subepicardium and varies by 60 degrees. The initial contractile motion of the basal loop causes a stiffer shell muscle to form, constricting the LV. This motion causes the isovolumic phase of systole. The next motion is the contraction of the descending band, which leads to clockwise and counterclockwise twisting extending downward from the base to the apex. This torsion causes the myocardial fibers to shorten and thicken, resulting in ejection. Shortly after the activation of the inner band, the ascending loop starts contracting, and this phase lasts beyond the contraction of the descending loop. This results in twisting and thickening motions that occur in opposite directions, partially contributing to ejection. When the contraction of the descending bands stops, the contracting ascending band becomes more longitudinal, lengthening the LV and creating an avenue for suction. The last motion is a response that allows LV filling during the remaining part of diastole.

In summary, during the abovementioned complex myocardial mechanics, two major deformation directions are initiated: shortening along the long axis of the chamber (longitudinal deformation) and shortening of the myofibers along the short axis (circumferential deformation). These two mechanics result in radial thickening and subsequent ejection. Different deformation directions can be quantified by measuring myocardial strain. Strain indicates the deviation of a certain myocardial segment from its original length throughout the cardiac cycle and is measured as a percentage (16, 17). At the preclinical level, strain is considered the most sensitive parameter for identifying myocardial disease in numerous cardiac diseases. It has proven value for finding early signs and predicting outcomes in some conditions, such as ischemic heart disease, heart failure,

non-ischemic cardiomyopathies and arterial hypertension (18). In sports cardiology, strain is a parameter that is used to quantify LV systolic function and differentiate physiological, exercise-induced remodeling from asymptomatic HCM or hypertrophy induced by chronic arterial hypertension (18, 19). Longitudinal and circumferential shortenings are the main contributors to myocardial performance and ejection fraction (EF). Global longitudinal strain (GLS) is defined as the average peak regional systolic strain measured in all LV segments from the apical view (20). It is considered the most sensitive and accurate measurement and has important prognostic implications.

2.1.2 Right ventricle

The importance of RV function was first described in 1616 by Sir William Harvey in his thesis, De Motu Cordis: "Thus, the RV may be said to be made for the sake of transmitting blood through the lungs, not for nourishing them" (21, 22).

Under normal physiological conditions, the RV is the most anteriorly situated heart chamber. It is positioned directly behind the sternum and wraps around the LV. In contrast to the cone-shaped LV, the RV has a triangular or semilunar shape, depending on the projection (lateral or vertical) being observed. Its sharp right edge forms the acute margin of the heart. Because it has thin walls and a crescentic shape, the RV is more compliant and better able to adjust to augmentations in volume and pressure. The RV has a greater end-diastolic volume than does the LV. Thus, assuming similar stroke volumes, the RV EF is somewhat lower than that of the LV. The RV sections are separated into those with anterior, inferior and lateral walls as well as basal, mid, and apical sections (23). Morphologically, RV includes three components (1) the inlet: tricuspid valve, chordae tendineae, and papillary muscles; (2) the heavily trabeculated myocardium of the apex; and (3) the outlet or the RV outflow tract (RVOT) (24). The anatomical features of the RV are the following: 1) the presence of prominent trabeculations and muscular bands (the parietal, septomarginal and moderator bands), 2) the trileaflet configuration of the atrioventricular valve with the septal attachment of the papillary muscles, 3) more than 3 layers of papillary

muscles, and 4) a more apically positioned tricuspid valve (25). Two layers of RV myocardium are present. In the subepicardial layer of the RV, the myocytes are oriented predominantly circumferentially and parallel to the atrioventricular groove. In contrast, the subendocardial muscle fibers of the RV are predominantly arranged longitudinally (these longitudinal fibers are found in the endocardial layer, while oblique fibers in the superficial layer) (26). Echocardiography reveals that there are dissimilarities between LV and RV wall thickness. The RV has a relatively thinner wall (3-4 mm) as it supports low-pressure pulmonary circulation. Conversely, the LV wall is thicker (6-11 mm) and is responsible for providing the systemic blood supply (27).

There are three main mechanisms contributing to RV systolic function: 1) inward movement of RV free wall ("bellows effect") 2) longitudinal shortening of RV with traction of tricuspid annulus towards the apex 3) bulging of the interventricular septum towards the RV cavity secondary to LV contraction (28, 29). The RV contracts in a "peristaltic" pattern that proceeds from the sinus, where fibers are predominantly oriented obliquely and have an average major radius of curvature of nearly 4 cm, to the infundibulum, where the fibers are circumconal and have a small radius of curvature of 0.8 cm (30, 31). During the isovolumic contraction phase, the subepicardial myocytes of the inflow tract displace the RV circumferentially. The subendocardial fibers are responsible for the longitudinal contraction of the RV during the ejection phase. Traditionally, this longitudinal contraction is considered a major contributor to RV performance. The circumferential contraction of the outflow tract is crucial to the maintenance of high tension during systole, which results in infundibular subvalvular support of the pulmonary valve unidirectional function. The interventricular septum also supports LV and RV functions. These twists and rotations do not substantially contribute to RV pump functions (32, 33). An overview of the differences between LV and RV structures and functions is represented in Table 1.

Table 1. Comparison of Normal RV and LV Structure and Function (adapted based on Haddad et al) (22).

Characteristics	RV	LV
Structure	Inflow region, trabeculated myocardium, infundibulum	Inflow region and myocardium, no infundibulum
Shape	From the side: triangular cross-section: crescentic	Elliptic
End-diastolic volume, mL/m^2	75±13 (49–101)	66±12 (44–89)
Mass, g/m^2	26±5 (17–34)	87±12 (64–109)
Thickness of ventricular wall, mm	2 to 5	7 to 11
Ventricular pressures, mm Hg	25/4 [(15–30)/(1–7)]	130/8 [(90–140)/(5–12)]
EF, %	61±7 (47–76) >40–45*	67±5 (57–78) >50*
Ventricular elastance (Emax), mm Hg/mL	1.30±0.84	5.48±1.23
Compliance at end diastole, mm Hg^{-1}	Higher compliance than LV**	5.0±0.52×10^{-2}
Filling profiles	Starts earlier and finishes later increase lower filling velocities	Starts later and finishes earlier, higher filling velocities
PVR vs SVR, dyne •s•cm^{-5}	70 (20–130)	1100 (700–1600)
Stroke work index, g/m2 per beat	8±2 (1/6 of LV stroke work)	50±20
Exercise reserve	↑RVEF≥5%	↑LVEF≥5%
Resistance to ischemia	Greater resistance to ischemia	More susceptible to ischemia
Adaptation to disease state	Better adaptation to volume overload states	Better adaptation to pressure overload states

PVR - pulmonary vascular resistance; SVR - systemic vascular resistance; *- Lower range of normal RV function used in clinical practice; lower value of normal described with radionuclide angiography; **- Based on sarcomere length–pressure curve relationship, limited data on end-diastolic passive compliance in humans; ↑-increase.

2.2 The impact of intense exercise of strength or endurance types of training: Morganroth theory.

Since the 20th century, sports have broadly been categorized into three groups based on the intensity and type of exercise they require: dynamic (aerobic, isotonic), static (anaerobic, isometric) and combined (34, 35). The terms "dynamic" and "static exersice" are based on the mechanical action of muscles and are the most commonly applied in clinical practice. According to the muscle metabolism type, the terms "aerobic" and "anaerobic" are used by specialists. The 3rd, so-called "combined type of exercise" group refers to the types of sports (such as football, basketball), where both aerobic and anaerobic activity is present. Some of high resistance dynamic types of exercise (e.g., throwing (field events)), resistance band exercises, gymnastics) are classified as high-intensity static exercise due to the excessive cardiovascular demands.

Basically, aerobic exercise (e.g., kickboxing, walking, hiking, and aquaerobics) increases the heart rate (HR) and the oxygen supply to muscle tissues to sustain a certain level of training, resulting in increased cardiac output. In contrast, anaerobic exercise is the high-intensity exercise performed during short exertion sports (e.g., weightlifting and bodybuilding), which results in a high blood pressure load. Aerobic exercise can turn into anaerobic exercise when the work load is too high for a certain individual. However, several types of exercises considered to be isotonic (e.g., sprinting, cycling, and jumping) are performed primarily anaerobically (36).

Table 2. Classification of sports (adapted based on Mitcel et al) (36).

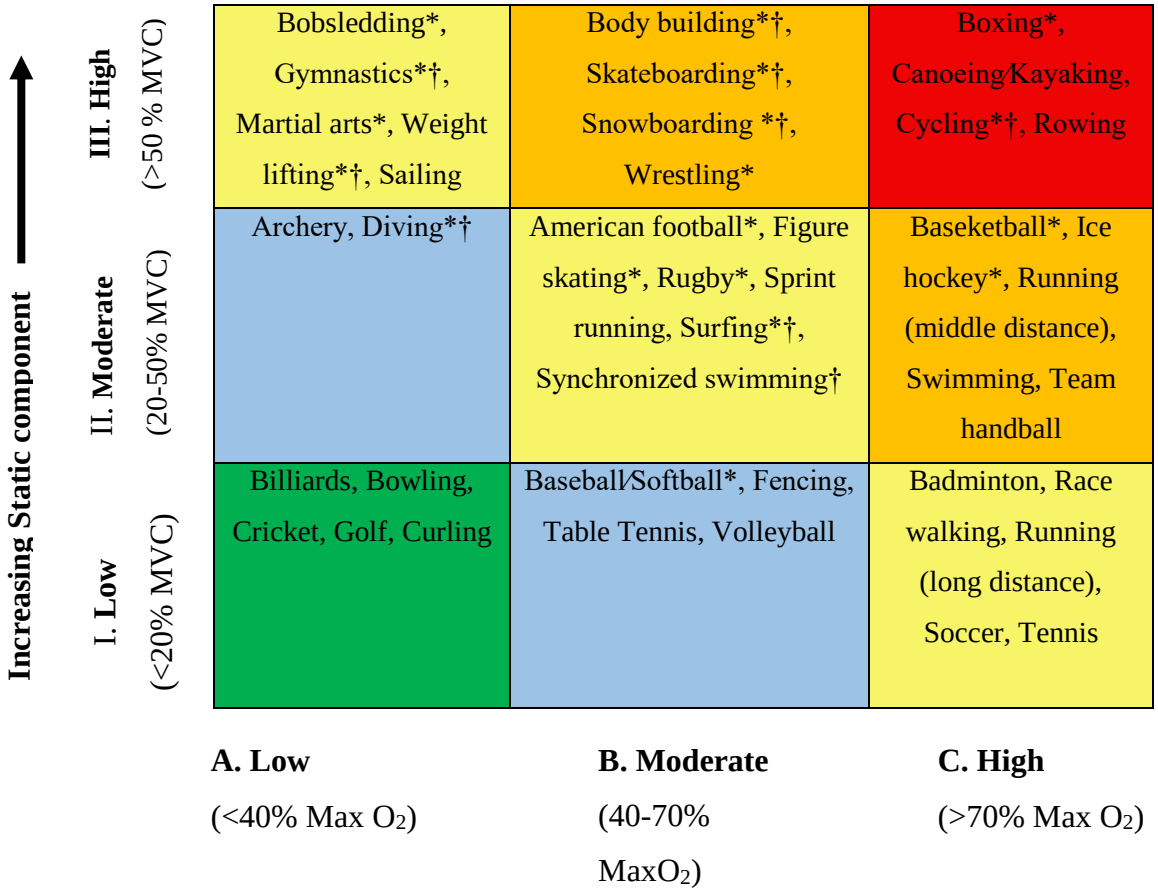

This classification is based on the peak static and dynamic components achieved during competition. The intensity of exercise is indicated by color: Green indicates the types of sports with the lowest total cardiovascular demand (cardiac output and blood pressure), while those with the highest are shown in red. Blue, yellow, and orange indicate those with low-moderate, moderate, and high-moderate total cardiovascular demand. MaxO2 indicates the maximum oxygen uptake, and MVC indicates the maximal voluntary contraction. * Danger of collision, † Increased risk in the presence of syncope.

Physiological changes in cardiac morphology and function occur if an athlete trains over 10 hours per week, and their development depends on the type of exercise (37). Endurance exercise results in eccentric cardiac remodeling during which cardiac adaptations are induced by a high "volume" load: increased ventricular volumes, moderate wall thickening, and a low resting HR. In strength-trained athletes, the cardiac phenotype is determined by the increased "pressure" load and results in concentric remodeling: increased wall thickness, relatively small ventricular volumes and a minimally changed HR. This notion was initially presented in 1975 by Morganroth et al. and subsequently called the "Morganroth hypothesis" (38). This hypothesis is largely accepted and is currently used in sports cardiology. However, the theory has also been extensively criticized due to its oversimplification of the processes it describes and because its supporting data have become more controversial with progress in imaging modalities (e.g., echocardiography and cardiac resonance imaging, CMR). Some authors have provided questionable data about the inability of resistance athletes to have concentric remodeling. Resistance-trained athletes often perform a Valsalva maneuver that equalizes transmural pressures and afterload during exertion (39). A longitudinal study performed in football athletes at an American college confirmed the Morganroth hypothesis by showing that resistance-trained athletes exhibit concentric heart remodeling in response to prolonged athletic performance (40).

2.3 Cardiac adaptation to intense exercise

2.3.1 Left ventricular adaptation to intense exercise.

A large body of literature is devoted to the LV adaptations that occur in response to intense training. Regular intense exercise is traditionally associated with an enlargement in LV dimensions and mass compared to the parameters observed in sedentary controls. Physiological sport-induced LV hypertrophy (LVH) is largely determined by demographic

factors: age, ethnicity, sex, body size, and type of sport discipline. Black athletes represent a large proportion of the athletes competing at the national level in the U.S. and United Kingdom. In black athletes, if LVWT ≤15 mm in an individual with an absence of cardiac symptoms and no family history of HCM, LVH is considered to be in the normal range, and no further investigation is needed (41). Although several studies have reported LVH of up to 19 mm in some ultra-endurance athletes, a maximal LVWT >16 mm can indicate pathology, and in these cases, HCM should be suspected (42, 43). In a study of 700 adolescent (16 years old) British endurance athletes, LVWT did not exceed 11 mm (44). Subsequent studies performed in a large cohort of highly trained athletes have shown that only a small percentage of these athletes present an LVWT of more than 12 mm. A recent study that included 3500 intensively trained British athletes showed in that 1.5% of the athletes exhibited an LVWT >12 mm (45).

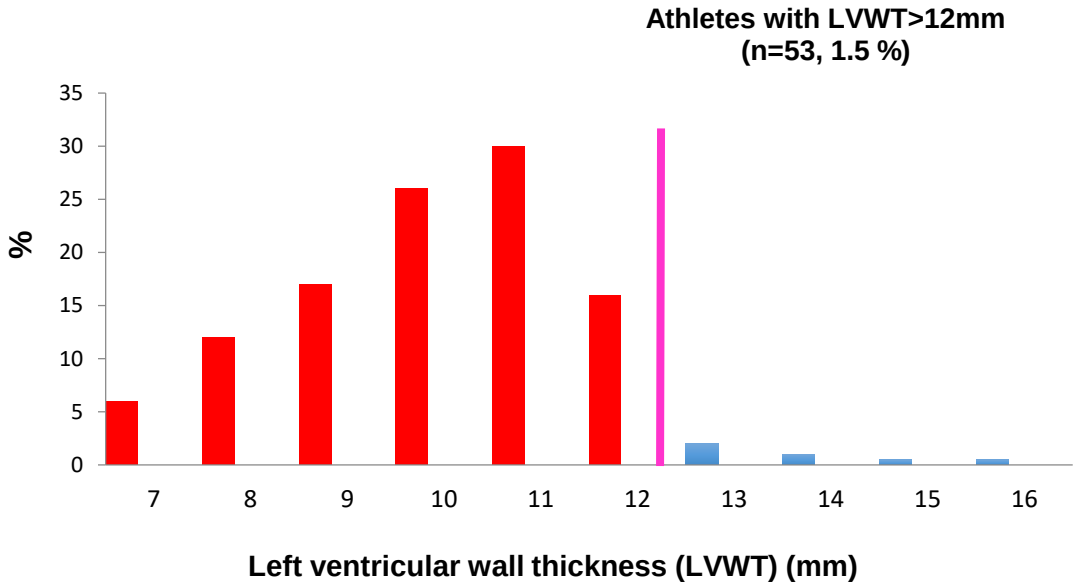

Figure 1. Diagram showing the distribution of LVWT in 3500 highly trained athletes. The results indicate that ~2% of the athletes exhibited a LVWT >12 mm (45).

The type of exercise and body surface area (BSA) are two essential determinants of LVH in athletes. Athletes performing ultra-endurance combined types of sport (e.g., cycling,

swimming, canoeing and ultra-endurance running) exhibit the greatest increases in LVWT. Conversely, there is the generally accepted concept that athletes performing pure isometric sports, such as weightlifting and wrestling, rarely exhibit an LVWT >12 mm. A BSA>2.0 m2 increases the probability of identifying LVH (46, 47). The LV and RV response to intense endurance exercise varies: the LV primarily presents with concentric hypertrophy during the first 6 to 9 months after the initiation of endurance training, with the degree depending on the intensity and duration of the exercise. Subsequently, LV dilation occurs, resulting in eccentric remodeling. In contrast, the RV presents with eccentric remodeling at all levels of training (48). LVH and a lower HR are characteristically observed in young and adult athletes, but they are less marked in older athletes (49).

2.3.2 Right ventricular adaptation to intense exercise. Right ventricular exercise-induced dysfunction.

Intensive exercise results in RV enlargement and wall thickening. However, more significant changes are promoted by endurance exercise than strength training (50). This "physiologic phenomenon" should be taken into consideration when evaluating athletes for sports eligibility (50). Regarding the RV, an athlete's heart phenotype mainly develops after two years of regular physical training (49). Similar to the LV, racial differences are also observed in the RV. In a study of athletes in the Scandinavian football league, athletes with an African ancestry had significantly more concentric remodeling in the RV than was observed in the Caucasian athletes (51). In some athletes, the RV undergoes structural and electrical remodeling that may create a substrate for life-threatening arrhythmias, although SCD remains a rare event in young athletes (52). Intense exercise increases RV wall stress, and the RV is disproportionately affected (53). The increases in pulmonary artery pressures caused by intense training can be higher than the contractile reserve of the RV, an effect that can result in reduced cardiac output and exercise intolerance (54). Due to the lack of elasticity of the pulmonary artery and the reduced ability of the pulmonary circulation to dilate, RV afterload can become considerably augmented. In rodents, intense endurance

training can result in fibrosis of the RV myocardium (55). In humans, research performed in veteran endurance athletes confirmed the results of animal-model studies and demonstrated the presence of myocardial fibrosis in veteran competitive endurance athletes (>50 years old) (56). Research has also demonstrated that myocardial damage and a significant depletion in RV function are observed after intensive bouts of ultra-endurance training. Almost all such abnormalities resolve within 1 week (57). In humans, RVEF but not LVEF was lower in athletes with complex ventricular arrhythmias than in healthy athletes and sedentary volunteers without arrhythmias. During a short duration of maximal exercise, the RV experiences greater hemodynamic stress than does the LV, resulting in transient RV injury with possible long-term structural consequences (53, 58). Acute RV dysfunction with impaired RV systolic function was registered immediately after a prolonged endurance race. Regional differences in RV longitudinal function have been detected: while RV apical wall strain increased, RV basal wall strain did not significantly decrease during the season (59). This phenomenon can possibly be explained by the sequential activation of the RV myocardium and the influence of moderator band contraction on the wall motions of the apical and basal free walls. The irreversible RV structural and functional changes that occur as a consequence of long-term intensive endurance exercise training are now called "exercise-induced RV dysfunction" (60-62). Kirchhof et al. were the first to suggest that exercise could modify the expression of AC in mice with a heterozygous deficiency in plakoglobin. In "athlete" mice, early functional changes resulted in RV dysfunction and arrhythmias (63). These findings were further supported by studies performed in human populations. The initial such investigation is described in Sen-Chowdhry et al., who registered that RV volumes were higher and RV function was lower in 11 endurance athletes than in a larger group of sedentary volunteers, and the reported diagnosis in these athletes was AC (64). These observations were confirmed in further studies in which athletes were at a higher risk of meeting the Task Force diagnostic criteria for AC (65, 66). The "threshold theory" of phenotypic expression was first proposed in 2003 before there was any clear evidence of a correlation between intense exercise and the AC-like phenotype (67). Although it remains controversial, The "Heidbuchel syndrome" theory of exercise-induced AC was supported by the 'marathon

rat' studies (55). Further investigations conducted among professional cyclists who presented with palpitations showed that these athletes showed clinical evidence of RV arrhythmias and mild RV dysfunction, although in the vast majority of cases there was no family history of AC (68).

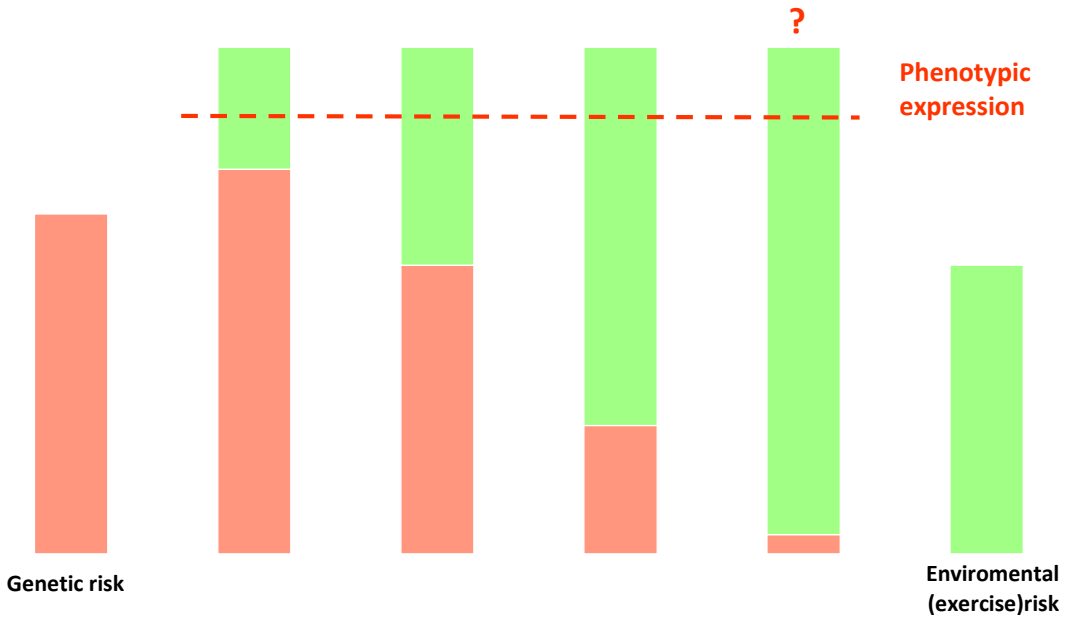

Figure 2. Threshold for phenotypic expression for AC as a spectrum of genetic and environmental risk (adapted based on La Gerche et al) (69).

The present diagram (Figure 2) demonstrates the interdependence of genetic and environmental factors (e.g., exercise), which combine to reach a threshold at which the AC phenotype is expressed. A vast genetic risk can cause clinical AC with little aggravation from exercise. However, a low genetic risk may require a significant additional contribution from exercise stress to trigger AC. It remains controversial whether extreme exercise can cause an AC phenotype when there is little or no genetic risk.

Further investigation is needed to explore the interconnection between intense exercise (as an environmental risk factor) and AC development (as a genetic risk factor) or to determine whether any other factors (e.g., dietary, lifestyle, or co-morbidities) may influence AC disease expression. Further studies aimed at finding other causes of SCD (e.g., channelopathies) is also required. Although the use of ICDs in clinical practice can prevent the development of exercise-triggered arrhythmias, we are now entering a world in which we will need to establish the effect of exercise on the disease substrate for each of these conditions (69).

Investigations of the RV in endurance athletes are justified by the need for a more complete understanding of athletic physiology and the clinical need for better risk stratification of athletes who present with any symptoms or arrhythmias.

2.4 Female athlete's heart

Despite the large amount of data available about male athlete's heart, female athlete's heart has rarely been investigated in the literature. Research has shown that long-term endurance training induced very similar bi-ventricular remodeling in male and female athletes. Independent of training load, however, RV size was larger and bi-ventricular resting function was lower in males (70). Female athletes have lower LV mass (LVM) than male sportsmen (71). There was a significant difference between the two aforementioned groups in LVMi (left ventricular mass index), indicating that gender differences in LVM are not be explained by the fact that body size is different between males and females. One possible mechanism for this finding is that the increase in absolute blood pressure with peak exercise is smaller in female athletes (72, 73). Additionally, estimated mean arterial blood pressure values are also lower in female than in male athletes (71). It has been suggested that androgenic hormone levels and genetic factors may play a role in the sex-related difference observed in athletes. Testosterone and estrogen-sensitive receptors are present in myocytes, but as myocardial mass increased, their protective effects against cardiac hypertrophy were diminished (74). However, the upper limits of LVWT did not exceed 11

mm in female athletes (44, 71, 75). The largest LVWT reported was 12 mm among 1000 female Italian athletes (76). When LVWT is greater than 12 in a female athlete, there is a high probability that HCM will be diagnosed. Endurance-trained female athletes had lower LV SV than were observed in male athletes. This can be explained by the fact that female athletes tend to have smaller body mass and smaller LV end-diastolic volumes (EDV) and therefore smaller SV. (44, 47, 76). SV was lower in females than in male controls, but there was no difference body mass relative to gender (77). Some racial differences are associated with female athlete's heart. In Western countries, black female athletes form an increasing proportion of world class international competitors. In black female athletes, intensive physical exercise promotes higher LVH values and repolarization changes than are observed in age-matched and similar body size white female athletes competing in a similar sport. However, a maximal LVWT >13 mm or deep T-wave inversions in the inferior and lateral leads are rarely presented and require further investigation (78). Insulin-like growth factor (IGF) is considered an essential regulator of cell proliferation. Recent research has indicated that IGF mediates physiological LVH. The presence of race-related polymorphisms that affect IGF1 function within the African population may explain the greater prevalence of LVH in black athletes (79).

Generally, atrial volumes are significantly larger in athletes. However, only a small difference was found between female controls and female athletes, suggesting that atrial adjustment to training is more modest in women than in men (80).

2.5 Basic principles and importance in SCD of athletes

SCD is one of the most important causes of death worldwide. This disorder accounts for 5% to 10% of all sudden deaths resulting from unexplained reasons in individuals >65 years of age. It occurs in young adults and has a male to female ratio of 2.7:1. SCD accounts for an estimated 450,000 deaths or 15% of all annual deaths in the United States (81). Athletes are at greater risk of SCD than are their non-athletic matched groups due to the increased risks associated with vigorous exercise (8). When SCD occurs in an athlete, it

is viewed as a rare but dramatic tragedy and will generate significant media attention and discussion among medical specialists, sports communities, and laypersons alike. The incidence of SCD is higher in males than in females. The data provided for high school and college athletes indicates that the incidence of SCD is 5-fold higher in male than in female athletes (82). SCD appears to be more common in African (black) athletes, with a reported incidence rate of 5.6/100,000 per year in the U. S. (83).

2.5.1 Etiology of SCD in athletes

The most common causes of exercise-related SCD in young (<35 years old) athletes are cardiomyopathies, such as ARVC and HCM (9). Black athletes exhibit higher death rates from HCM than their white counterparts (20% vs. 10%, respectively) based on the U.S. autopsy data (84). In older athletes (>35 years old), in 80% of cases SCD occurs due to coronary artery disease. The basic causes of SCD in young athletes are presented in Fig. 3.

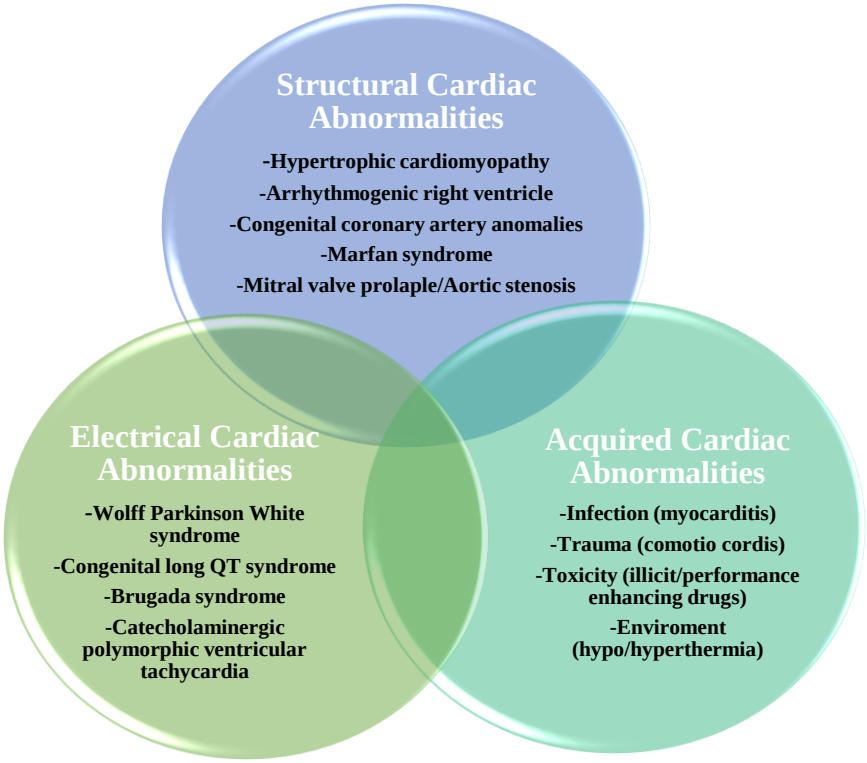

Figure 3. Groups of causes of SCD in Young Athletes (adapted based on Chandra N. et al) (8, 85). The common causes of SCD in young athletes can be divided into structural, electrical, and acquired cardiac abnormalities. In the top circle the most frequently observed causes are depicted.

Sudden death occurs more frequently in certain types of sports. In the U. S. basketball and football have the largest prevalence, whereas in Europe, soccer predominates (86).

2.6 Hypertrophic cardiomyopathy

HCM is a primary myocardial disease with an autosomal dominant pattern of inheritance. It is characterized by LVH in the absence of another functional or structural cardiac abnormality (87). The reported prevalence of HCM is 0.2% in the general population and 0.07% to 0.08% in athletes (88). It is a genetic cardiac disorder caused by mutations in one of twelve sarcomeric genes.

The modern view of HCM was first introduced by Teare in 1958, who described it as an asymmetric hypertrophy in young adults (89). The generally accepted definition of HCM is a disease state characterized by unexplained LVH associated with nondilated ventricular chambers in the absence of another cardiac or systemic disease that itself would cause myocardial hypertrophy. The crucial role in diagnosis is played by echocardiographic examination where maximal LVWT≥15 mm (LVWT of 13 to 14 mm referred as borderline), in the presence of family history (reported HCM in first-line relatives) (87).

The differential diagnosis between athlete's heart and HCM represents a vital clinical dilemma because at least 10% of adolescent patients with HCM may be at high risk for SCD (90). Nowadays the therapeutic strategies available for SCD prevention are: the ICD, disqualification of athletes with HCM from intense competitive sports (91).

SCD is caused by ventricular tachyarrhythmias (ventricular tachycardia/ventricular fibrillation) and usually occur in the presence of ≥1 the major risk factors (appropriate ICD interventions of 4% per year in patients implanted for primary prevention). However, some of patients (0.6% per year in non-ICD populations) with diagnosis of HCM may inexpectedly die in the absence of all conventional risk factors. Late gadolinium enhancement on CMR helps to determine scar tissue as a potential substrate of fatal arrhythmias (92, 93). A risk-stratification algorithm has been largely effective in identifying patients at highest risk who are eligible for primary prevention of sudden death with an ICD, thereby markedly reducing HCM-related mortality to 0.5% per year (94).

2.7 Arrhythmogenic cardiomyopathy

AC is a chronic, progressive, heritable myocardial disorder and is one of the leading causes of SCD in young, apparently healthy individuals (95). Three subtypes have been proposed:

- right-dominant – generally referred to as AC,
- biventricular forms with early biventricular involvement
- left-dominant with predominant LV involvement.

First clinical signs reveal during adolescence and are exercise-related. They include (pre)syncope, dyspnea, palpitations, arrhythmic (pre)syncope and sudden cardiac arrest due to ventricular arrhythmias, which is typical for athletes. At later stages, heart failure may develop (96).

AC is a poorly understood and often underdiagnosed disorder of the RV. AC classified as 1 of the 5 primary cardiomyopathies in 1995. The prevalence of AC was estimated to be 1 in 5000 people and to account for up to 20% of all SCDs in people younger than 35 years old. (97, 98). In a series of 86 cases of sudden death, AC was identified in 10.3% of the cases and found to be the second leading cause of SCD. AC can occur in both sexes at any age, but sudden deaths tend to occur in adults between 15 and 45 years old (mean age, approximately 30 years old) (99, 100). The strongest predictor of SCD during exertion is AC. Athletes with AC are 6 times more likely to die during exertion than are those with other cardiac pathologies (92% of SCD experienced on the athletic field) (101). In recent years, great advances have been made in the understanding of the pathogenesis of AC. The exact pathogenesis of AC is still unclear, but this involves a genetic factor: approximately 50% of patients with AC have one or more mutations in genes that encode desmosomal proteins (desmoglein-2, desmocollin-2, plakoglobin, plakophilin and desmoplakin). AC is considered to be “a disease of the desmosome” (102, 103). Currently, the genetic mutations known to be associated with AC include those in PG, PKP2, DSP, DSC2, DSG2, TGFb3, TMEM43, RYR2, TTN, and JUP (104).

Table 3. Revised 2010 Task Force Criteria for AC (adapted based on Marcus F.) (105).

Revised 2010 Task Force Criteria for AC	
1. Global or regional dysfunction and structural alterations	
Major	Minor
2D Echo Criteria **Regional RV akinesia, dyskinesia, or aneurysm AND 1 of the following measured at end-diastole:** **- PLAX RVOT≥32 mm (PLAX/BSA ≥19 mm/m^2), or** **- PSAX RVOT≥36 mm (PSAX/BSA ≥ 21 mm/m^2), or** **- Fractional area change ≤ 33%**	*2D Echo Criteria* Regional RV akinesia or dyskinesia or dyssynchronous RV contraction AND 1 of the following measured at end-diastole: - PLAX RVOT≥29 to <32 mm (PLAX/BSA ≥16 to <19 mm/m^2), or - PSAX RVOT≥32 to <36 mm (PSAX/BSA ≥18 to <21 mm/m^2), or - Fractional area change>33% ≤40% *CMR criteria* Regional RV akinesia or dyskinesia or dyssynchronous RV contraction AND 1 of the following: - RV EDV/BSA ≥100 to 110 mL/m^2 (male) or ≥90 to 100 mL/m^2 (female) - RV EF>40 to ≤ 45%
2. Tissue characterization of wall	
Major	Minor
Residual myocytes <60% by morphometric analysis (or <50% if estimated), with fibrous replacement of the RV free wall	Residual myocytes 60% to 75% by morphometric analysis (or 50%to 65% if estimated), with fibrous replacement of the RV

myocardium in ≥1 sample, with or without fatty replacement of tissue on endomyocardial biopsy	free wall myocardium in ≥1 sample with or without fatty replacement of tissue on endomyocardial biopsy
3. Repolarization abnormalities	
Major	Minor
Inverted T waves in right precordial leads (V1, V2, and V3) or beyond in individuals >14 years of age (in the absence of complete RBBB QRS ≥120 ms)	Inverted T waves in V1 and V2 in individuals >14 years of age (in the absence of complete RBBB) or in V4, V5, and V6 Inverted T waves in leads V1, V2, V3, and V4 in individuals >14 years of age in the presence of a complete RBBB
4. Depolarization/conduction abnormalities	
Major	Minor
Epsilon wave (reproducible low-amplitude signals between end of QRS complex to onset of T wave) in the right precordial leads (V1 - V3)	Late potentials by SAECG in ≥1 of 3 parameters in the absence of a QRSd of ≥110 msec on standard ECG: - Filtered QRS duration (fQRS)≥114 msec - Duration of terminal QRS<40 microV≥ 38 ms - Root-mean-square voltage of terminal 40 ms≤20 micro V Terminal activation duration≥55 ms measured from the nadir of the S-wave until the end of all depolarization deflections (including R') inV1, V2, or V3
5. Arrhythmias	
Major	Minor
Nonsustained or sustained VT of LBBB morphology with superior axis	Nonsustained or sustained VT of RVOT configuration, LBBB morphology with inferior axis or of unknown axis>500 PVCs per 24 hours on Holter monitoring

6. Family History	
Major	Minor
AC in first degree relative who meets Task Force Criteria **AC confirmed pathologically at autopsy or surgery in first degree relative** **Identification of pathogenic mutation categorized as associated or probably associated with AC in the patient under evaluation**	History of AC in first degree relative in whom it is not possible to determine whether the family member meets Task Force Criteria Premature sudden death (<35 years of age) due to suspected AC in a first degree relative AC confirmed pathologically or by current Task Force Criteriain second-degree relative

The diagnosis of AC is based on a combination of major and minor criteria. To make a diagnosis of AC requires either 2 major criteria or 1 major and 2 minor criteria or 4 minor criteria.

The risk factors for SCD in AC are not as well-defined as those for HCM. Frequent endurance exercise increases the risk of ventricular tachycardia/ventricular fibrillation and heart failure. The most important prognostic markers are syncope, a prior history of SCD or sustained ventricular tachycardia, which define many high-risk patients who are most appropriate for treatment with the primary prevention, ICD (106).

2.8 Pre-participation screening

Pre-participation screening is the medical systematic practice of evaluating athletes before competition for abnormalities that could cause of SCD or disease progression. Adequate cardiac screening is able to prevent the majority of cardiac events in athletes. To prevent SCD, high-risk individuals are excluded from competitive sport. Two major screening programs are used in the world today: American and Italian. In the U.S., the mandatory screening protocol includes a family and personal history and a physical examination. In Italy, screening consists of a resting electrocardiogram to detect cardiac and rhythm abnormalities (107). The question of whether the U.S. or Italian screening protocol is the best for identifying athletes at risk is the subject of considerable debate. Data obtained in Italy have shown that the risk of adverse cardiac events was decreased by almost 90% in young competitive athletes after a questionnaire and physical examination were performed and a 12-lead resting ECG was applied as part of a routine screening protocol (108).

ECG is a non-invasive technique that allows the continuous monitoring of HR, enabling the detection of life-threatening arrhythmias. However, its cost-efficiency and feasibility have been an issue of debate. In the U.S., ECG was not included in the athlete screening protocol because it has a high rate of false-positive results and is not cost-effective (109). Even if ECG is considered the method of choice for diagnosing cardiomyopathies and ionic channel-related diseases, many asymptomatic cardiac abnormalities, such as mitral valve prolapse and bicuspid aortic valve, which are considered the most frequent congenital disorders in adults, could go unrecognized (107).

Recently, echocardiography has become a valuable addition to the protocols used to obtain diagnoses and prognoses and to monitor structural heart diseases. It permits the practitioner to characterize cardiac anatomy and ventricular function and visualize valvular structure and function. The advantages of echocardiography include its non-invasiveness, availability, relatively low cost, and myocardial responsiveness to potentially ischemic stimuli (stress-echo). Moreover, echocardiography enables the clinician to image myocardial perfusion along with wall motion and wall thickening (110). Unfortunately,

despite previous attempts to introduce echocardiography into the protocol for pre-participation screening of athletes, this technique has also been found to be cost-ineffective (109). However, introducing the use of an ECG during pre-competition screening could be reasonable because despite the fact that ECG is regarded as a sensitive method, ECG is the best method for diagnosing a range of cardiac pathologies. Moreover, the added value provided by novel, advanced ECG techniques, such as speckle tracking or 3D echocardiography, has not yet been evaluated.

2.9 Ultrasound

2.9.1 Basic principles and conventional parameters

M-mode: Although M-mode has been largely replaced by 2D echocardiography, it is still an important part of the echocardiographic study nowadays. It allowes the visualization of even the most thin or fast moving cardiac structures such heart valves or endocardium. In sports cardiology it can be applied in the evaluation of cardiac dimensions such as wall thickness, chamber size and subsequent estimation of ventricular function. A single beam in an ultrasound scan produces the one-dimensional M-mode picture, where movement of a certain structure (e.g., heart valve) can be depicted in a wave-like manner. That allows an unequalled high sample of rating of more than 2000 frames per second, compared to 2D echo where there are only 40-80 frames per second. This is linked to high special and temporal resolution.

The initial attempts at the quantification of LV function were based on one-dimensional, M-mode linear measurements of the LV internal dimension in diastole and systole, using Teichholz method. This modality is no longer recommended for the estimation of the LV systolic function and volumes (111). General limitations remain: dependence on the image quality, nonperpendicular axes, poor definition of the borders. This should be taken into consideration during the interpretation of the measurements.

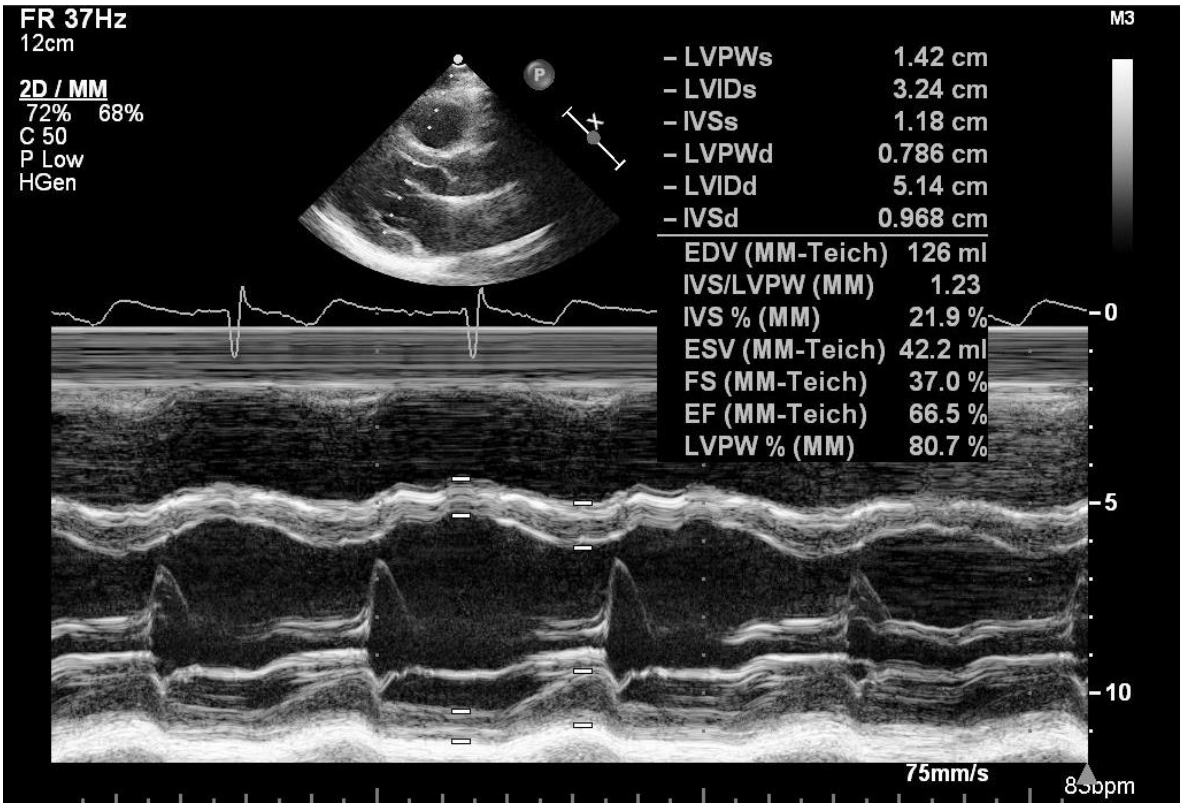

Figure 4. One-dimensional, M-mode linear measurements of the LV internal dimension in diastole and systole using Teichholz method. LV internal dimensions were measured in parasternal long axis view at the level of the LV minor axis, approximately at the level of the mitral valve leaflet tips.

The first and most commonly used echocardiographic method of LVM estimation is the linear method, which uses end-diastolic linear measurements of the interventricular septum (IVSd), LV inferolateral wall thickness, and LV internal diameter derived from M-mode orby 2D-guided M-mode approach. This method utilizes the Devereux and Reichek "cube" formula, which assumes a prolate ellipsoid shape of the LV with a ratio of 1:2 minor- to major-axis (112).

The Devereux formula for calculation of LVM is in wide clinical use.The formula, usually stated as (113)

$$LVMASS = 0.8 \times (1.04[(LVIDd + LVPWd + IVSd)^3 - (LVIDd)^3]) + 0.6 \text{ g}$$

LVIDd: LV internal diameter in end-diastole, LVPWd: LV posterior wall diameter in end-diastole, IVSd: interventricular septum in end-diastole.

However, any error in linear measurements can result in significant inaccuracies because all measurements are cubed in the LVM formula. This formula is also not accurate in asymmetric LVH, dilated cardiomyopathy, and other conditions with regional differences in LVWT (111). The major limitation of M-mode is its one dimensional nature such that only the structures transected by the M-mode cursor are displayed. Only the perpendicular orientation of the ultrasound beam to the structure of interest determines of the accuracy of the ultrasound study and the image quality. If the orientation of the beam to the structure of interest is not perpendicular, it will link to a slight deformation of the structure and incorrect measurements.

TAPSE (tricuspid annular plane systolic excursion) represents the distance of excursion of the lateral part of the tricuspid annulus towards the apex during systole. It is obtained in a four-chamber view, using an M-mode cursor passed through the tricuspid lateral annulus and measuring the amount of longitudinal displacement of the annulus at peak-systole. Normal value is above 16 mm. Despite its simplicity and several limitations, TAPSE is a powerful measure of RV function and still widely used in clinical practice.

B-mode: 2D echo is the basis of the echocardiographic examination, representing the initial imaging mode by allowing the overall evaluation of structures of interest. And also, it is used to guide such imaging modes as M-mode or spectral Doppler. 2D echo provides real-time and relatively high-resolution tomographic views of the heart useful to obtain anatomical and functional information.

Measurement of LVEF. The most frequently used technique for LV volume estimation in 2D echocardiography is the *biplane method of discs (modified Simpson`s rule).* This methodology is based on the principle of calculation of total LV volume as the summation of a series of elliptical discs of equal height, equally spaced along the long axis of the LV (114). LV end-diastolic and end-systolic volumes (LVEDV and LVESV, respectively) are measured by contouring the LV endocardial surface on both apical four-chamber (A4C) and apical two-chamber (A2C) views.

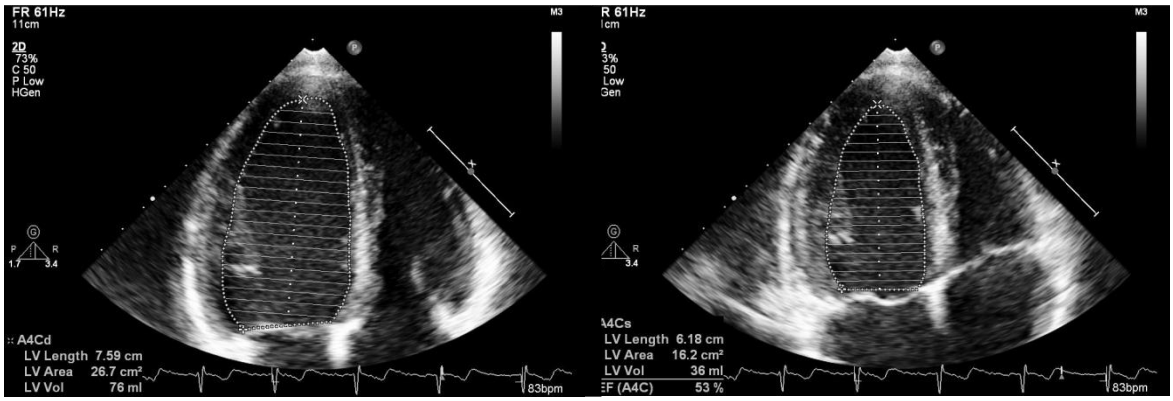

Figure 5. Simpson`s method. The endocardium is traced in end-systole and end-diastole in A4C view.

The Modified Quinones Equation for the EF estimation is widely used in clinical echocardiographic routine:

$$EF\ (\%) = (SV/EDV) \times 100$$

The main limitations of this method are the foreshortening of the ventricular apex and the possible tangentially A2C view acquisition. The former may result in inaccurate assessment of the LVEF, and most frequently on its overestimation. Conversely, the tangentially A2C view acquisition causes underestimation of the true volume. The current gold standard method for LV volumes and function evaluation is CMR imaging (115). LV evaluation by

3DE appears to be the closest method regarding accuracy and reproducibility. (116, 117) LV volumes calculated by Simpson`s method tend to be smaller than those obtained by 3D full-volume echocardiography and CMR (118).

Most regularly, RV can be obtained from the A4C RV focused view and its size should be measured at end-diastole. If the RV is larger than the LV in this view, it is more likely to be severly enlarged (2). The following RV diameters need to be obtained:

- the basal diameter-maximal short-axis diameter in the basal part of the RV.
- the mid-cavity diameter– measured at the middle part of the RV halfway between basal diameter and RV apex.
- The length – from the tricuspid annulus towards the RV apex (2).

The fractional area change (FAC) estimates RV function from the A4C view. It calculates the fraction of the end-diastolic and end-systolic RV area along the cardiac cycle. Normal value for RV FAC is above 35% (119).

RV FAC (%) = (RV EDA – RV ESA)/RV EDA x 100

2.9.2 2D deformation imaging

Speckle-tracking echocardiography is a special 2D non-Doppler technique, which measures myocardial deformation (120). It detects multiple unique patterns and natural acoustic reflections described as “speckles”. These can interfere with the ultrasound beam in the myocardium and be tracked throughout the cardiac cycle. Each region of the myocardium has a unique speckle pattern (like the fingerprint) that allows the region to be traced from frame to frame during the post processing analysis. This algorhythm provides quantitative analysis of the tissue motion and deformation (strains).

Strain is the percentage of change from original length of a distinct region of interest. Strain rate is defined as the rate of deformation (e.g., how fast the deformation occurs). The strain can be either Langrangian or natural. Lagrangian strain is defined as the as follows:

$$S_{L(t)}=\frac{L-L0}{Lo}=\frac{\Delta L}{Lo},$$

where L(t) is the length at a given point in time and L_0 is the reference length at the reference to $t_{0,}$ usually taken at end-diastole (121).
Natural strain is defined relative to previous time instance but not original length: (121)

$$S_{N(t)}= ln\left(\frac{L1}{L0}\right)$$

2D strain based on speckle tracking is an emerging innovative method providing information about the functional status of all cardiac chambers (122). Three perpendicular axes orienting the global geometry of LV define the local cardiac coordinate system: longitudinal, radial and circumferencial. Shortening and thickening can be quantified on segmental level or globally. Although GLS has been shown to be reproducible and accurate, 2D global circumferential strain (GCS) and 2D global radial strain (GRS) are less reliable, with measurement variability of >10% and 15%, respectively, which limits their

use in the evaluation of LV systolic function in clinical practice (123). The example of speckle-tracking technique is presented in Figure 6.

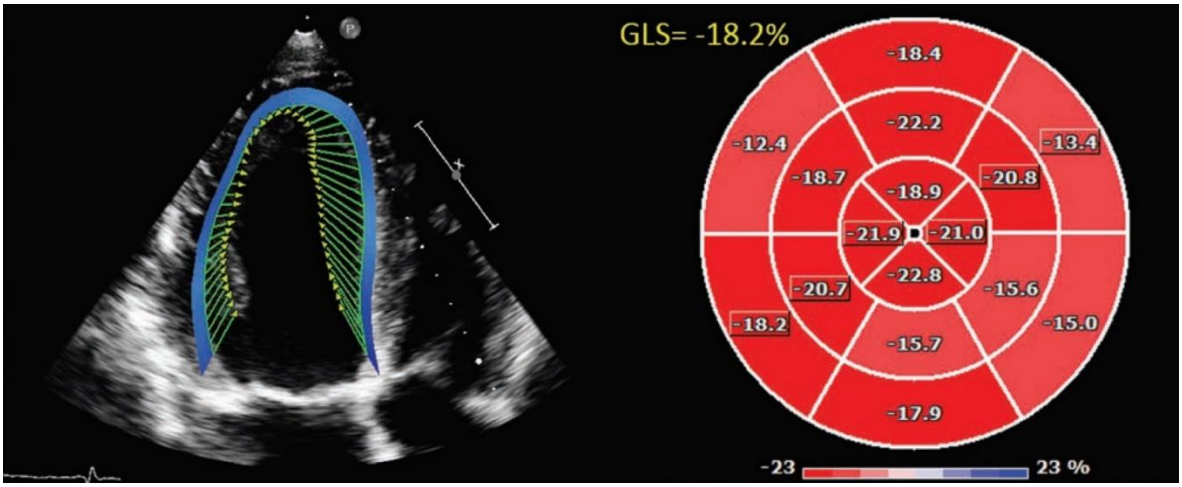

Figure 6. 2D speckle-tracking analysis for global longitudinal strain. The graphical representation (bull's eye) of peak strain values in a 16-segment model of the LV. GLS is the average of all segments.

GLS has been proposed in numerous studies to be superior to LVEF for detecting subtle alterations in myocardial function and predicting cardiac events. Evidence also suggests its feasibility and usefulness for evaluating the RV. Because RV myofibers also run longitudinally, longitudinal shortening accounts for a major portion of RV systolic function and can also be quantified by speckle tracking echocardiography. Despite the fact that TAPSE also refers to longitudinal shortening, it represents only one aspect of complex RV functions and is strongly influenced by overall heart motions and loading conditions as well as technical challenges (124). Hence, 2D imaging is less capable of measuring the other two motion components of the RV.

2.9.3 Three-dimensional echocardiography: basic principles

3DE represents a major innovation in echocardiography. The milestone in the advancement of present 3D technology has been the development of fully sampled matrix array trasthoracic transducers which have enabled advanced digital processing and improved image formation algorithms. The backbone of the 3DE technology is a transducer. In contrast with the 2D phased-array transducer which is composed of 128 electrically isolated piezoelectric elements arranged in a single row, 3DE matrix array transducers are composed of around 3000 individually connected and simultaneously active (fully sampled) piezoelectric elements with operating frequencies ranging from 2 to 4 MHz for transthoracic transducer. Piezoelectric elements are arranged in rows and columns to forming a rectangular grid (matrix configuration) within the transducer. The electronically controlled phasic firing of the elements within the matrix generates a scan line that propagates radially (y or axis direction), laterally (x or azimutal direction) and in elevation (z direction) in order to aquire a volumetric pyramid of data. Importantly, the last generation of matrix tranducers contain advanced crystal materials what allow to reduce heating production by increasing the efficiency of the transduction process by improving the conversion of transmit power into ultrasound energy and of received ultrasound energy into electrical power.

Currently, there are three different methods for 3DE data acquisition: (125)

> ***real-time (or "live") 3D imaging***– pyramidal 3D volumetric data set is obtained each cardiac cycle and visualized live, beat after beat similar to 2D scanning.
>
> ***multiplane imaging –*** simultaneous 2D views can be obtained at high frame rate using predefined or user-selected plane orientations and displayed using the split screen option

multibeat ECG-triggered 3D imaging **–** multibeat acquisition is accomplished by sequential aquisitions of narrow smaller volumes obtained from several ECG-gated consecutive heart cycles (2-6 cardiac cycles) that are subsequently stitched together to create a single volumetric data set. Once acquired, the data set cannot be changed by manipulating the probe as in live 3D imaging and analysis requires offline slicing, rotation and cropping of the acquired data set.

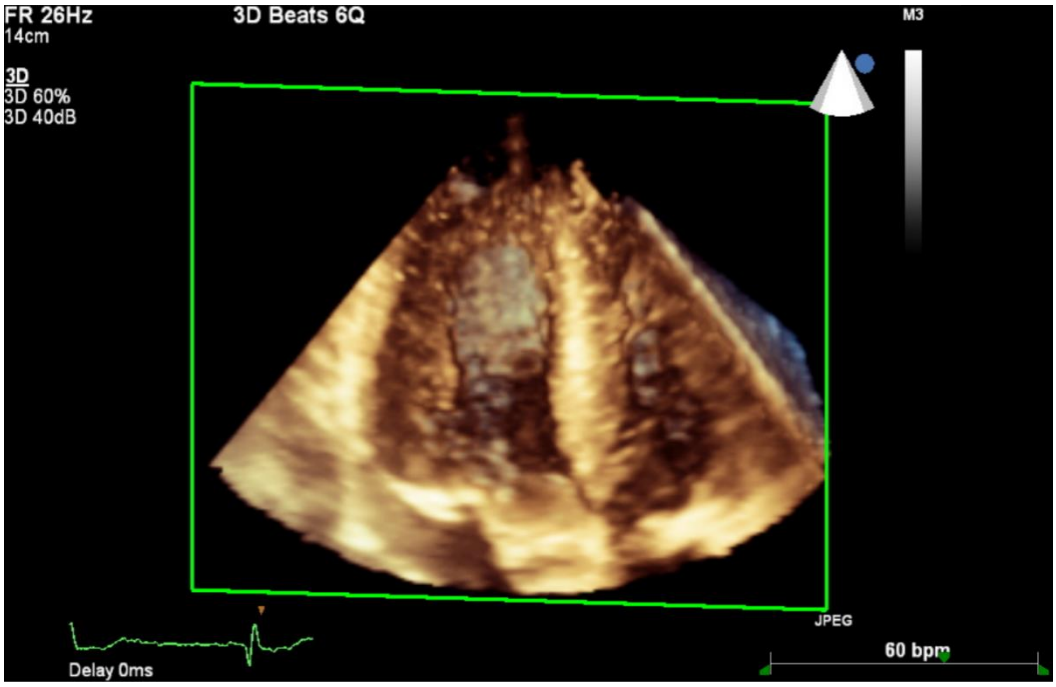

Figure 7. 3D full-volume acquisition, reconstructed from 6 cardiac cycles of LV and RV, obtained from the A4C view.

There are several fields where 3DE is applied nowadays in the current clinical practice: 1) the evaluation of cardiac chamber volumes and mass, without their shape assumptions; (125, 126) 2) presentation of realistic views of the anatomy and pathology of heart valves; (127, 128) 3) the assessment of regional LV wall motion and quantification of systolic dyssynchrony; (129) 4) volumetric quantification of regurgitant lesions and shunts with

3DE color Doppler imaging; (130) 5) monitoring and guiding interventional procedures in the catheterization laboratory, in the operating room and during hybrid operations as well (111) and 6) stress imaging (131). However, to be implemented more broadly in routine clinical practice, a full understanding of its technical principles and a systematic approach to image acquisition and analysis are required (125).

One of the main purposes of 3D imaging of LV is to provide more accurate volume and EF measurements independent of geometric assumptions regarding LV shape.

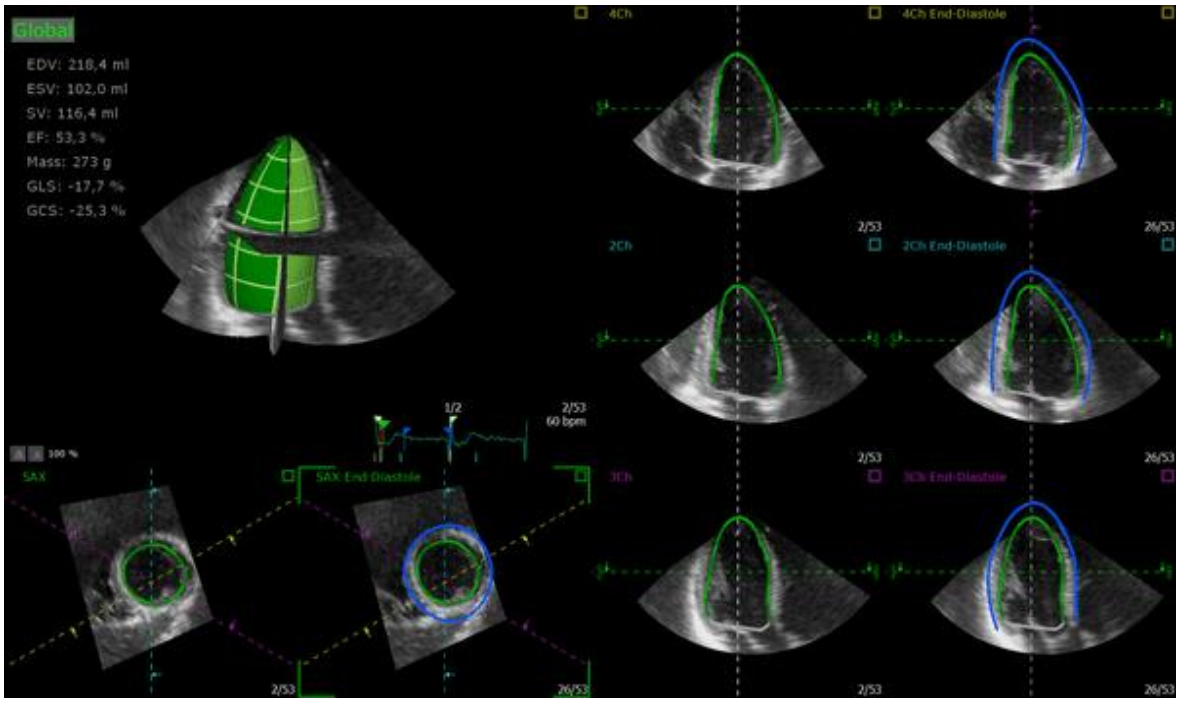

Figure 8. Volumes can be obtained from 3DE data set using semi-automated software. The software uses automated border-detection to create 3D endocardial shell of the entire ventricle from which volumes are calculated. The user manually adapts endocarial borders. 3DE data sets are viewed using surface rendering.

The accuracy of echocardiographically measured LV volumes is critically important for improving risk stratification. Studies have shown that LV volumes and LV EF predict

future cardiovascular outcomes in patients with various cardiac conditions. The strengths of an LV assessment obtained with 3DE is that no geometric assumption is necessary and it is unaffected by foreshortening (111).

With full-volume mode and multiple beat acquisitions, the LV volume and function can be more accurately determined by 3D than by 2D echocardiography (132). 2D echocardiography derived LV chamber sizes have been consistently underestimated compared to the gold standard CMR. To the contrary, 3DE has the advantages of established accuracy and reproducibility, and has been shown to be better correlated with CMR measured volumes with less underestimation (116, 133-135). In 3DE, the LV EDV and ESV are measured by semi-automatic border delineation in 3D space with manual adjustment when required. In cases where border delineation is still difficult owing to trabeculae or poorly defined with 3DE imaging, contrast agents maybe infused to enhance LV opacification. The 3DE eliminates geometric assumption or circumvents foreshortened views that are the common source of errors in 2DE.

Additionally, real-time 3D estimations of LVM are in better agreement with CMR measurements than are those acquired via 2D direct and M-mode echocardiography (136, 137). Real-time 3D assessment of LVM demonstrated excellent correlation with CMR data with a Pearson's correlation coefficient (r) of 0.99, in comparison to the 2D method versus CMR, which had an r of 0.84 (136). Similarly, the interobserver and intraobserver variability of real-time 3D measurements were 7% and 8%, respectively, which were significantly better than the interobserver and intraobserver variability of the 2D method (37% and 19%, respectively) (137). In addition, LVM values by real-time 3D reportedly were similar to CMR values with only a minimal bias of 4 grams (137). Therefore, the real-time 3D technique improves the accuracy and reproducibility of echocardiography estimation of LVM but is highly dependent on the equipment used and the quality of the images obtained. ASE and European Association of Cardiovascular Imaging Chamber Quantification Guidelines did not provide normal reference values for real-time-3D-derived LVM because of limited published data (111).

Global assessment of the RV is even more challenging by 2D echocardiography. 3DE gated wide-angled acquisition can overcome the limitations of 2D echocardiography, which enables to display the surfaces of the entire RV and to thoroughly assess its geometry and function, volumes, EF. For experienced echocardiographers with access to special software, it is recommended to use 3D-derived RV EF (111).

Studies have shown that 3DE determined RV volumes and function correlated well with CMR, with good reproducibility (138-143). The main limitations are the need for special software and imagequality. RV outflow wall is in close proximity to the sternum and dropout of the wall precludes accurate estimation of RV volumes. In addition, 3DE may not image the entire RV in patients with severely dilated RV.

2.9.4 ReVISION method

Estimation of the RV function represents a challenge due to complexity of RV geometry and its mechanics. Just like regarding the LV, global functional assessment may not be sensitive enough to notice subtle alterations and characterize myocardial mechanics. As mentioned already, there are three major mechanisms which contribute to RV pump function: (i) longitudinal shortening by traction of the tricuspid annular plane towards the apex; (ii) the inward (radial) motion of the RV free wall referred as the bellows effect; and (iii) the bulging of the interventricular septum during the LV contraction along with stretching the free wall over the septum. The majority of the conventional parameters obtained by 2D transthoracic echocardiography refer only to the longitudinal contraction of the chamber. The ReVISION method (Right VentrIcular Separate wall motion quantificatiON) is a custom method aimed to decompose the motion of the exported RV beutel along three orthogonal axes and calculate the respective volume at each time frame (28). It separately quantifies the extent of longitudinal, radial and anteroposterior displacement of the RV walls and assesses their relative contribution to the global RV EF, using 3D data sets of the RV.

Dedicated software (4D RV-Function 2, TomTec Imaging GmbH, Unterschleissheim, Germany) is commercially available to generate a 3D surface rendering model (beutel) of the RV by a semi-automated algorithm. The Euclidean axes in the dedicated software's output correspond to the anatomically relevant ones (longitudinal, radial and anteroposterior). The movement of the RV wall can be decomposed in a vertex-based manner (e.g. for the longitudinal motion we took into account only the movement of the vertices along the Y axis).

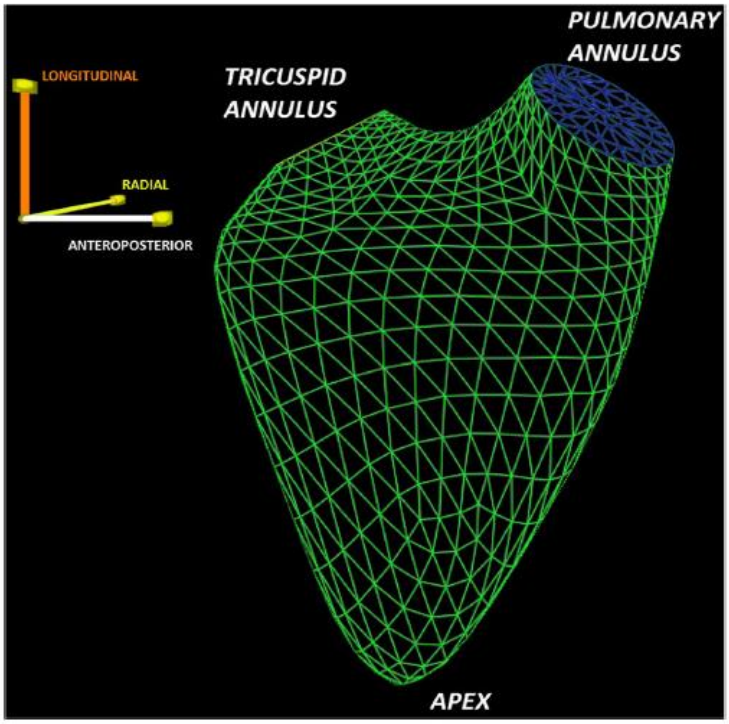

Figure 9. Example of the exported mesh (RV beutel) using the wireframe surface rendering display method. The model is positioned to correspond to the three anatomically relevant axes (longitudinal, radial and anteroposterior).

The volumes of the beutels corresponding to the RV wall motion in only one direction (either longitudinal, radial, or anteroposterior) were calculated at each time frame using the signed tetrahedron method.

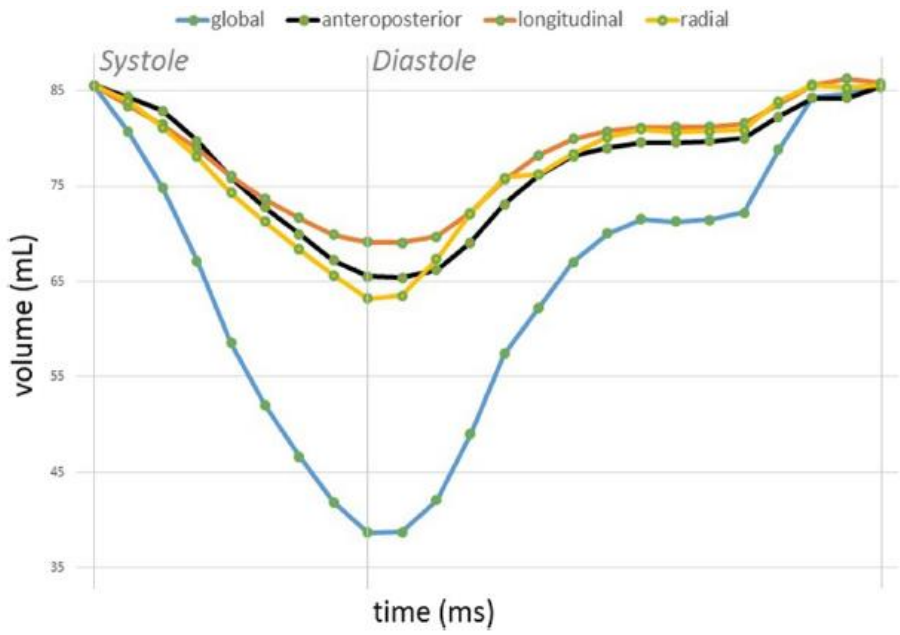

Figure 10. One beat global (blue line) and decomposed volume-time curves of the RV in a healthy volunteer

EF is the most common measure of RV pump function in a routine echocardiographic examination. It is defined as the ratio of stroke volume to EDV. Using the ReVISION method, volume changes due to the RV wall motion along the three directions can be separately quantified and the corresponding EF value can be calculated (i.e. radial EF). The relative contribution of the RV wall motion along the three different directions to global RV EF can be expressed by the ratio of the given direction's EF to global EF. It is important to note, that these parameters are measured in a completely automated way, therefore, the ReVISION method implies no added intra- or interobserver variability.

2.9.5 3D echocardiography in clinical routine and in assessing physiological and pathological RV remodeling

3DE is a major innovation in cardiovascular ultrasound. In contrast with 2DE, 3D is able to reconstruct the cardiac structures from any spatial point of view, to provide thorough information about volumes, structures and function of the cardiac chambers and valves. New generation of matrix-array transducers, recently introduced to clinical practice, made possible to visualize 3D cardiac structures in real time and to overcome the previous limitations.

Innovative postprocessing programs to analyse 3D datasets regarding the LV have provided higher accuracy in the analysis of LV morphology and function both on global and regional levels (144). Moreover, for the diagnostics of valvular heart diseases, this new method has proven to be robust for understanding the complicated anatomy of the valves and theirfunction, primarily in the mitral valve. It has proven its value in nonsurgical mitral procedures such as edge to edge mitral repair and transcatheter closure of paravaluvular leaks (157). Color Doppler 3DE is enable to depict the exact location of the regurgitant orifice, severity and character of mitral regurgitation. 3DE is also used in evaluating the aortic annulus for transcatheter aortic valve implantations (145, 146). 3DE is valuable method for diagnostics of congenital heart disease, as well as for the accurate assessment of morphology, size and exact location of cardiac masses (e.g., vegetations, thrombi and tumours) (147, 148).

3DE combined with deformation analysis has the ability to establish a connection between the mechanics of cardiac contraction, the underlying structure of cardiac fiber arrangement and global geometry, which is especially important in the initial phases of disease progression (149, 150). GLS by 2D speckle tracking has already an established prognostic value compared to LV EF regarding major adverse cardiac events (151). The novel and even more advanced 3D parameters are promising in this regard as well. And while the more we know about the LV, the more questions arise regarding the RV.

RV function is impaired in a range of clinical conditions: congenital heart diseases, pulmonary hypertension, myocardial infarction, cardiomyopathies, etc. Despite the growing interest towards the RV, its myocardial mechanics is still not thoroughly understood either in physiological or pathological conditions. 2D strain of the LV is a reliable and powerful measurement to estimate LV mechanics. However, 2D strain may be insufficient regarding the RV due to its complex shape and motion pattern (152). There are several 3DE software solutions available to reconstruct the surface model of the RV and subsequently, to measure its volume and EF. Although this is a breakthrough, global function assessment (by measuring EF) may still not be sensitive enough to detect subclinical pathological conditions, as it is also not regarding the LV.

Further analysis of the 3D models enables to separately quantify the different wall motion directions and evaluate the relative contribution of each component. The investigation of RV myocardial mechanics is a promising new field in echocardiographic research. However, still little is known not just about pathological conditions, but also about physiology (healthy people or even athletes). A better understanding of RV physiology and physiological remodeling seen in athlete's heart may help in a more sensitive diagnosis of pathological conditions affecting the RV inclusive of underlying pathological processes with athlete's heart.

3. OBJECTIVES

3.1 Investigation of cardiac remodeling in female athletes induced by different types of exercise training

The vast majority of the literature describes male athlete's heart, and detailed information about physiological cardiac remodeling in female athletes is lacking. We aimed to shed more light on the dichotomous cardiac adaptations observed among elite female competitors who participate in either a more static or a more dynamic sport discipline and to compare them to the results obtained in healthy, sedentary volunteers. Using 3DE, we aimed to characterize both LV and RV remodeling in these populations.

3.2 Investigation of physiologic cardiac remodeling in elite male kayak and canoe athletes

The high-level, mixed-type exercise performed in nature sport disciplines induces distinct alterations in cardiac morphology and function. We have aimed to characterize the cardiac remodeling that occurs in elite kayak and canoe athletes and to compare these results with those obtained in healthy, sedentary volunteers. Using 3DE, we aimed to produce a detailed investigation of both LV and RV remodeling in these populations.

3.3 Determination of RV mechanical pattern in pathological RV remodeling

The complex RV mechanical pattern may undergo a shift due to several reasons. We aimed to investigate a distinct population with functional remodeling but still maintained global function of the RV to show the phenomenon of the change between the relative importance of longitudinal and radial wall motions. Heart transplant (HTX) patients can serve as an example of pathological remodeling of RV with preserved EF.

4. METHODS

4.1 Study populations

4.1.1 Female athlete's heart

In a single-center study we have performed the current investigation in three distinct cohorts to evaluate the athlete`s heart in different athlete`s populations. Fifteen elite female athletes competing in International Federation Bodybuilding and Fitness (IFBB) BikiniFitness category were enrolled in the study. Furthermore, 15 elite age-matched female waterpolo athletes (all capped in the national team of the corresponding age category) were invited to this voluntary screening between 2016 and 2017. For comparison, 15 age-matched healthy, non-trained (no previous participation in intensive training, <3 hours of exercise/week) women were investigated. Study participants gave a prior written informed consent to the examinations. All of the measurements were performed at least 12 hours after last athletic training of the athletes. The protocol included detailed medical history and training regime along with standard physical examination, blood pressure measurement and 12-lead ECG, echocardiography and body composition. Subjects with uncommon echocardiographic and/or ECG changes, suboptimal echocardiographic image quality or athletes who suspended regular training in the last 6 months were excluded (n=3).

4.1.2 Elite male kayak or canoe athletes

We investigated 11 male kayak or canoe athletes, competing in Olympic, World and⁄or National Team. We registered the medical history and antropomentic data, physical examination, blood pressure measurement and 12-lead ECG. Exclusion criterias were any of previously known cardiac diseases (except for treated hypertonia), presence of moderate

or severe grade of valvular diseases diagnosed during physical examination by ECG or by echocardiography and at previous magnetic resonance imaging (MRI) examination. For the control group we invited 10 age-matched healthy non-trained volunteers.

4.1.3 HTX recipients

In the time frame of December 2014 to January 2017, we have retrospectively collected those echocardiograms of HTX recipients followed-up by our Center, where transthoracic 3D datasets were acquired suitable for further analysis (n=66). Those patients were included, who were already discharged from intensive care unit after HTX or arrived to regular follow-up visit. Exclusion criteria were (i) hemodynamic instability and/or need for inotropic agents; (ii) previous rejection ≥ ISHLT grade 2R or ≥ pAMR2; (iii) postoperative need for ventricular assist device; (iv) severe tricuspid insufficiency or any severe valvular disease; (v) non-sinus rhythm on ECG; (vi) diagnosis of chronic allograft vasculopathy; (vii) suboptimal 3DE image quality (inadequate visualization of the entire RV endocardial surface inclusive of RV outflow tract—confirmed also on short-axis planes—and/or the presence of stitching artifacts). Finally, 51 patients have been entered into current analysis. An age-and gender-matched control population (n=30) was selected with a normal echocardiographic report and without any known cardiovascular or other diseases and free from any medication using our existing database of healthy volunteers.

To create a relevant database, medical history, preoperative, intraoperative, and follow-up data of each patient were collected using the in-hospital electronic medical records. Anthropometric, blood pressure, and heart rate values were determined at time-point of the analyzed echocardiogram in both groups.

4.2 Methodology

4.2.1 Body composition measurement

Weight and height were measured using validated standard equipment. All participants wore light clothing and were barefoot. Body mass index (BMI) was calculated by dividing the body weight by the squared height. BSA was calculated using the Mosteller formula.

$$BSA\ (m^2) = (height\ (cm) \times weight\ (kg)/3600)^{1/2}$$

Body composition assessment was performed by a Bodystat 1500MDD machine (Bodystat Ltd., Douglas, UK). Participants removed all metal and other objects that could interfere with the scan and were instructed to empty their bladder before the assessment. Each participant was in supine position in the center of the table with palms down and arms beside the body. Age, height, weight and gender were entered into the machine for performing the automatic calculations. Fat free mass index (FFMI) was calculated as the fat free mass (kg), divided by the square of height (m^2).

4.2.2 Conventional echocardiography

Tranthoracic echocardiographic examination was performed with patient in the left lateral decubitus position with continuously registered ECG. Echocardiographic examinations were performed on commercially available ultrasound systems (Philips iE33 or EPIQ 7G, X5-1 and S5-1 transducers, Best, The Netherlands). Standard acquisition protocol consisting of loops from parasternal, apical and subxyphoid views were used according to current guidelines. For post-processing, acquisitions were stored on TomTecImageArena platform (TomTec Imaging GmbH, Unterschleissheim, Germany). In parasternal long-axis view, IVSd, LV internal (LVIDd) and LVPWd thickness diameters were measured on end-diastolic frame using 2D-guided M-mode technique. Relative wall thickness was calculated by 2xLVPWd/LVIDd. We calculated LV mass using the Devereux-formula. In A4C view,

early (E) and late (A) waves of mitral inflow and deceleration time of E wave were measured using pulsed wave spectral Doppler. Mitral annular lateral, septal and tricuspid annular systolic (s'), early diastolic (e') and late diastolic (a') velocities were measured by pulsed wave Doppler on tissue Doppler imaging. LA and RA volumes were measured by monoplane Simpson's method and indexed to BSA. In RV-focused A4C views, basal and mid RV diameter and RV length were measured. TAPSE was assessed on M-mode recording. Valvular diseases were quantified according to current guidelines. Beyond the conventional echocardiographic examination, ECG-gated full-volume 3D datasets reconstructed from 4 or 6 cardiac cycles optimized for the LV or the RV were obtained for further analysis on an off-line workstation. BSA was calculated using Mosteller equation.

4.2.3 3D echocardiography

3D datasets focused on the LV were processed by a single experienced operator using semi-automated, commercially available software (4D LV-Analysis 3, TomTec Imaging GmbH, Unterschleissheim, Germany). We determined end-diastolic (EDVi), end-systolic (ESVi), stroke volumes (SVi) and mass (LVMi) indices. Parameters were normalized to BSA. To characterize LV function, EF and deformation parameters such as GLS and GCS were also assessed. Off-line analysis of the datasets focused on the RV were performed by the same operator using commercially available software (4D RV-Function 2, TomTec). The algorithm automatically generates RV endocardial contour which was manually corrected on multiple short- and long-axis planes throughout the entire cardiac cycle. We quantified RV EDVi, ESVi, SVi normalized to BSA and EF. Furthermore, the software automatically measures FAC and free wall longitudinal strain derived from the 3D dataset. The created 3D model was exported volume-by-volume throughout the cardiac cycle and analyzed further by our custom-made ReVISION method. In brief, the wall movements of the exported RV model are decomposed in a vertex-based manner. The volumes of the models accounting for only one direction were calculated at each time frame using the signed tetrahedron method. By the decomposition of the 3D model's motion along the three

orthogonal, anatomically relevant axes, volume loss attributable to either longitudinal, radial or anteroposterior wall motions could be separately quantified. Thus, longitudinal (LEF), radial (REF), and anteroposterior (AEF) ejection fraction and their ratio to TEF (LEF/ TEF, REF/TEF, AEF/TEF, respectively) could be expressed as a measure of the relative contribution of the given wall motion direction.

4.3 Statistical analyses

Statistical analysis was performed using dedicated software (StatSoft STATISTICA v12, Tulsa, OK, USA). Data are presented as mean±standard deviation or medians with interquartile range as appropriate depending on the distribution of the values, whereas categorical variables were expressed as percentage. Shapiro-Wilk test was used to test normal distribution. Based on that, unpaired Student's *t*-test or Mann-Whitney *U*-test was used to compare two distinct groups. To compare categorical variables, Chi-square test was applied. One-way ANOVA followed by Fisher post-hoc test was used to compare three distinct groups, and Pearson or Spearman test was performed for correlation analysis as appropriate. The intraobserver and interobserver reproducibility were evaluated using Lin's concordance correlation coefficient.

A non-echocardiographer investigator randomly selected 10 HTX patients and further five healthy controls and exported these studies anonymized. The main operator reconstructed the 3D RV models again to assess intraobserver variability compared to the original measurements, while a second experienced operator also performed the measurements to assess interobserver variability. Then, the fully automated ReVISION method was applied on the three subset of 3D models, and reproducibility of ESV values with either only longitudinal or only radial motion component enabled was calculated. p values<0.05 were considered statistically significant.

5. RESULTS

5.1 Investigation of cardiac remodeling in female athletes induced by different types of exercise training

Basic characteristics of the study groups are presented in Table 4.

Table 4. Basic demographic and anthropometric characteristics of the study groups.

	Fitness athletes	Waterpolo athletes	Healthy controls	ANOVA p
n	15	15	15	
Age (years)	24±3	24±4	23±2	0.357
Height (m)	1.63±0.05*	1.75±0.06$^{\#\S}$	1.66±0.06*	<0.0001
Weight (kg)	57.0±7.1*	65.7±5.4$^{\#\S}$	56.6±8.3*	<0.001
BMI (kg/m^2)	21.3±1.9	21.4±1.2	20.5±2.8	0.399
BSA (m^2)	1.6±0.1*	1.8±0.1$^{\#\S}$	1.6±0.1*	<0.0001
FFMI (kg/m^2)	18.2±1.8*§	17.1±1.1$^{\#\S}$	14.9±1.4*$^{\#}$	0.001
Systolic blood pressure (mmHg)	115±14*	135±12$^{\#\S}$	122±10*	<0.0001
Diastolic blood pressure (mmHg)	74±9	76±6	76±2	0.684
Heart rate (/min)	63±9§	69±14§	82±7*$^{\#}$	0.003

BMI: body mass index, BSA: body surface area, FFMI: fat-free mass index; * significant versus waterpolo athletes, $^{\#}$ significant versus fitness athletes, § significant versus controls

The athlete groups and the healthy, sedentary volunteers were age-matched. Fitness athletes started professional activity since an average of 3.4±1.6 years and trained 12±2 hours a week. Waterpolo athletes started their career since 12.1±4.6 years and trained 24±8 hours a week. Waterpolo athletes had higher height, weight and correspondingly, BSA. BMI was similar among groups. FFMI was higher in waterpolo athletes compared to controls and even higher in fitness athletes compared to both other groups. Systolic blood pressure of waterpolo athletes was higher. Heart rate was lower in athlete groups compared to controls. Interventricular septal thickness, posterior wall thickness and LV internal diameter were higher in waterpolo athletes compared to both fitness athletes and controls. RWT did not differ between groups. E and A waves of mitral inflow, E/A ratio, deceleration time and mitral annular septal and lateral diastolic velocities, as well as E/e' ratio were comparable among the groups referring to similar diastolic function. LA volume and LA volume index were higher in waterpolo athletes, while comparable between fitness athletes and controls. Conventional linear measurements of RV geometry and function showed no significant difference among groups. TAPSE and tricuspid annular systolic and diastolic velocities were also similar. RA volume and RA volume index were higher only in waterpolo athletes compared to the sedentary volunteer group (Table 5).

Table 5. Comparison of conventional echocardiographic measurements among the groups.

	Fitness athletes (n=15)	Waterpolo athletes (n=15)	Healthy controls (n=15)	ANOVA p
IVSd (mm)	7.5±0.9*	9.5±1.5#§	7.0±0.9*	<0.0001
LVPWd (mm)	7.2±1.5*	8.3±0.8#§	6.6±1.1*	0.006
LVIDd (mm)	45.6±4.6*	49.0±2.9#§	43.6±3.3*	0.005
RWT	0.32±0.07	0.34±0.04	0.31±0.06	0.416
E wave (cm/s)	78.4±21.4	78.9±7.9	93.1±16.4	0.115
A wave (cm/s)	54.1±13.5	49.6±14.9	58.8±13.9	0.359
E/A ratio	1.64±0.34	1.73±0.57	1.67±0.50	0.890
DCT (cm/s)	164.1±49.5	190.1±41.2	171.8±25.9	0.261
mitral lateral annulus s' (m/s)	0.10±0.03	0.11±0.01	0.12±0.03	0.058
mitral lateral annulus e' (m/s)	0.17±0.04	0.18±0.03	0.18±0.06	0.686
mitral lateral annulus a' (m/s)	0.08±0.03	0.08±0.02	0.08±0.01	0.896
mitral medial annulus s' (m/s)	0.09±0.02	0.09±0.01	0.10±0.03	0.160
mitral medial annulus e' (m/s)	0.13±0.03	0.13±0.01	0.15±0.04	0.205
mitral medial annulus a' (m/s)	0.08±0.02	0.07±0.01	0.08±0.02	0.078
E/e' average	4.76±1.25	4.43±0.85	5.90±3.02	0.147
LA volume (ml)	30.1±11.2*	47.9±10.6#§	28.6±6.0*	0.007
LA volume index (ml/m^2)	17.4±8.0*	27.4±7.2#§	18.1±3.7*	0.026
RVID base (mm)	38.1±4.7	41.1±5.7	36.2±5.1	0.241
RVID mid (mm)	32.5±3.9	36.1±4.2	29.3±4.2	0.076

RV length (mm)	81.6±10.5	88.4±12.1	76.2±14.0	0.107
TAPSE (mm)	22.6±6.2	24.9±3.1	24.8±3.8	0.362
tricuspid annulus s' (m/s)	0.14±0.03	0.12±0.02	0.14±0.03	0.054
tricuspid annulus e' (m/s)	0.15±0.02	0.15±0.04	0.18±0.04	0.099
tricuspid annulus a' (m/s)	0.10±0.02	0.08±0.02	0.09±0.02	0.162
RA volume (ml)	36.9±11.9	46.2±8.7§	28.7±11.9*	0.001
RA volume index (ml/m^2)	21.5±8.9	25.8±7.6§	17.7±6.4*	0.011

IVSd: interventricular septal thickness in end-diastole, LVPWd: left ventricular posterior wall thickess in end-diastole, LVIDd: left ventricular internal diameter in end-diastole, RWT: relative wall thickness, DCT: deceleration time, LA: left atrium, RVID: right ventricular internal diameter, TAPSE: tricuspid annular plane systolic excursion, RA: right atrium; * significant versus waterpolo athletes, # significant versus fitness athletes, § significant versus controls

Fitness athletes presented similar LV EDV, ESV and stroke volumes compared to healthy, sedentary volunteers (Table 6).

Table 6. Comparison of 3DE measurements among the groups.

	Fitness athletes (n=15)	Waterpolo athletes (n=15)	Healthy controls (n=15)	ANOVA p
LV EDV (ml)	121±18*	149±15#§	115±11*	<0.0001
LV EDVi (ml/m^2)	76±13*	84±8#§	73±8*	0.045
LV ESV (ml)	45±12*	65±10#§	40±8*	<0.0001
LV ESVi (ml/m^2)	28±8*	36±5#§	25±4*	0.002
LV EF (%)	63±6*	57±5#§	65±6*	0.006
LV SV (ml)	76±12	85±12	75±10	0.102
LV SVi (ml/m^2)	48±7	48±7	48±8	1.000
LVM (g)	125±20*§	163±23#§	90±15*#	0.006
LVMi (g/m^2)	78±13*§	91±10#§	57±10*#	<0.0001
GLS (%)	-22.2±3.2*	-18.8±1.6#§	-23.1±1.7*	<0.0001
GCS (%)	-30.6±4.5	-27.2±4.2§	-34.4±4.9*	0.006
RV EDV (ml)	99±21*	154±26#§	88±17*	<0.0001
RV EDVi (ml/m^2)	61±12*	86±14#§	55±9*	<0.0001
RV ESV (ml)	40±9*	69±16#§	35±8*	<0.0001
RV ESVi (ml/m^2)	25±6*	39±9#§	22±4*	<0.0001
RV EF (%)	59±6	56±5	60±4	0.129
RV SV (ml)	58±15*	85±12#§	52±10*	<0.0001
RV SVi (ml/m^2)	36±9*	48±7#§	33±6*	<0.0001
FAC (%)	50±7	49±7	54±4	0.312
Free wall longitudinal strain (%)	-31.1±5.0	-33.5±4.4	-30.7±4.7	0.325

LV: left ventricular, EDVi: end-diastolic volume index, ESVi: end-systolic volume index, EF: ejection fraction, SVi: stroke volume index, LVMi: left ventricular mass index, GLS: global longitudinal strain, GCS: global circumferential strain, RV: right ventricular, FAC: fractional area

change; * significant versus waterpolo athletes, # significant versus fitness athletes, § significant versus controls

Waterpolo athletes, however, had higher LV EDV and ESV even after indexing to BSA. Correspondingly, LV EF was similar in fitness athletes compared to controls, while it was lower in waterpolo athletes. LV stroke volume and stroke volume index did not differ between groups. LVM and LVMi were significantly higher in the athlete groups, the hypertrophy however, was even more prominent in waterpolo athletes. Referring to the geometrical changes, global longitudinal and circumferential strains were lower in waterpolo athletes. Systolic deformation parameters were similar between fitness athletes and controls. Similarly, RV EDV, ESV and stroke volumes were all similar in fitness athletes and controls, while they were higher in waterpolo athletes. RVEF showed no difference between the groups. Neither did FAC and free wall longitudinal strain, referring to similar systolic function of the RV.

Table 7. Comparison of the relative contribution of the different motion directions of the RV among the three study groups.

	Fitness athletes (n=15)	Waterpolo athletes (n=15)	Healthy controls (n=15)	ANOVA p
LEF (%)	25.9±5.3	28.1±3.7	25.3±6.3	0.267
LEF/TEF	0.46±0.07	0.52±0.06§	0.42±0.08*	<0.001
REF (%)	26.3±5.6	19.9±7.4§	32.4±8.6*	<0.001
REF/TEF	0.47±0.09*	0.36±0.10#§	0.53±0.09*	<0.001
AEF (%)	25.1±5.2	22.5±3.9	26.0±6.5	0.213
AEF/TEF	0.44±0.07	0.42±0.07	0.43±0.07	0.633

LEF: longitudinal ejection fraction, REF: radial ejection fraction, AEF: anteroposterior ejection fractions, TEF: total ejection fraction; * significant versus waterpolo athletes, # significant versus fitness athletes, § significant versus controls

Regarding the relative contribution of different RV motion directions, we have found no difference between fitness athletes and healthy controls (Table 7). However, waterpolo athletes had significantly higher longitudinal contribution to total EF compared to controls along with significantly lower radial contribution compared to the two other groups (Table 7).

In fitness athletes, FFMI correlated with RV EDV ($r=0.607$, $p<0.05$), RV SV ($r=0.647$, $p<0.05$) and RV length ($r=0.575$, $p<0.05$), in waterpolo athletes weekly training time correlated with LVM ($r=0.527$, $p<0.05$), while training years with LVMi ($r=0.567$, $p<0.05$).

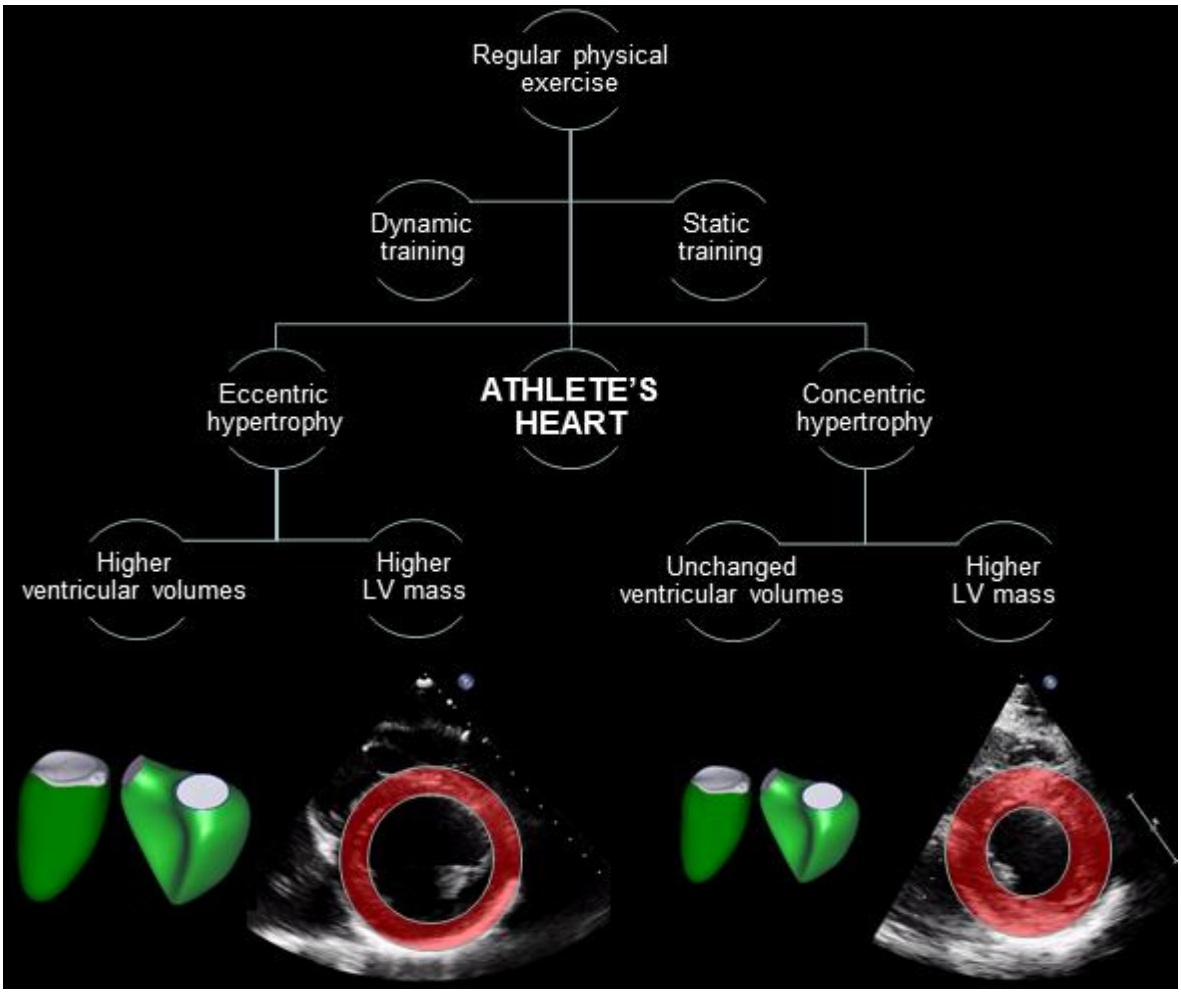

Figure 11. Schematic representation cardiac adaptation to intense exercise. Mainly dynamic exercise training induced eccentric hypertrophy in female waterpolo athletes, with higher left and right ventricular volumes (3DE derived models, respectively) and also higher LVM (parasternal short axis view of the LV showing dilation and higher mass). On the other hand, mainly static exercise training induced concentric hypertrophy in female fitness athletes, with unchanged ventricular volumes, however, higher LVM (parasternal short axis view of the LV showing higher mass without dilation).

5.2 Investigation of physiologic cardiac remodeling in elite male kayak and canoe athletes

Based on the inclusion criteria, the athletes and the control group did not differ significantly in their age (Table 8). Their height, body weight and BSA were similar. Systolic and diastolic blood pressure was significantly higher in athletes. However, their heart rate was lower than expected. The athletes have been professionally active since 19±4 and trained 19±4 a week (Table 8).

Table 8. Basic demographical and hemodynamic parameters in athletes and controls

	Athlete	Control	p
n	11	10	
Age (years)	29±5	27±4	0.429
Body height (cm)	182±10	176±10	0.154
Body weight (kg)	80±8	86±17	0.295
BSA (m^2)	2.02±0.13	2.02±0.25	0.930
Systolic blood pressure (Hgmm)	140±10	118±10	0.001
Diastolic blood pressure (Hgmm)	76±9	66±4	0.018
Heart rate (/min)	54±7	64±13	0.033
Training hours (/week)	19±4		
Competition years	19±4		

According to conventional echocardiographic parameters, both the septal and posterior wall thickness in end-diastole was significantly higher in athletes (Table 9). LVM calculated with the Devereux formula showed significantly increased values for athletes. Relative RWT in the athlete group showed concentric type of LVH.

Table 9. Conventional echocardiographic parameters in athletes and control group

	Athletes (n=11)	Control (n=10)	p
IVSd (mm)	13.4±2.0	10.5±1.8	0.002
LVPWd (mm)	11.9±1.2	8.8±1.9	<0.001
LVIDd (mm)	52.7±3.7	48.6±4.6	0.039
LVIDs (mm)	34.5±3.1	32.3±7.0	0.348
LV mass Devereux (g)	340±58	207±49	<0.001
Relative wall thickness	0.48±0.07	0.40±0.09	0.030
RV basal diameter (mm)	46.5±3.8	39.1±2.5	<0.001
RV mid diameter (mm)	40.4±2.5	30.9±3.6	<0.001
RV length(mm)	89±6	79±8	0.002
TAPSE (mm)	25.5±4.3	24.8±2.6	0.668
LA volume (ml)	85±20	58±14	0.002
LA volume index (ml/m^2)	39±16	28±6	0.043
RA volume (ml)	82±22	47±13	<0.001
RA volume index (ml/m^2)	41±10	23±6	<0.001
Mitral E wave (m/s)	0.8±0.2	0.9±0.1	0.201
Mitral A wave (m/s)	0.5±0.1	0.6±0.1	0.083
Mitral E/A ratio	1.8±0.4	1.7±0.4	0.570
Deceleration time (ms)	187±29	181±41	0.682
Mitral lateral anulus s' (m/s)	0.11±0.01	0.1±0.02	0.507
Mitral lateral anulus e'(m/s)	0.16±0.03	0.18±0.04	0.406
Mitral lateral anulus a' (m/s)	0.13±0.19	0.08±0.01	0.493
Mitral septal anulus s'(m/s)	0.09±0.02	0.09±0.02	0.983
Mitral septal anulus e'(m/s)	0.12±0.04	0.13±0.03	0.577
Mitral septal anulus a'(m/s)	0.07±0.02	0.08±0.02	0.076
Mean E/e' ratio	5.2±1.2	5.4±1.2	0.778
Tricuspid anulus s' (m/s)	0.14±0.02	0.13±0.03	0.392
Tricuspid anulus e' (m/s)	0.14±0.03	0.15±0.03	0.770
Tricuspid anulus a' (m/s)	0.10±0.02	0.10±0.03	0.760

LV: left ventricle, RV: right ventricle, LA: left atrium, RA: right ventricle, „d”: end-diastolic, „s”: end-systolic, IVS: interventricular septum, PW: posterior wall, ID: internal diameter, TAPSE: tricuspid annular plane systolic excursion

Regarding the RV linear parameters, similar differences can be observed (Table 9). Basal, mid and RV longitudinal diameters were significantly higher in athletes. The TAPSE values determined by M-mode showed no difference between the two groups. Both the LA and RA were significantly higher in athletes, (as well as indexed to BSA). No difference in the diastolic function was observed, neither E and A waves of mitral inflow, nor E/A ratio and deceleration time. We found no difference in either lateral or medial mitral anulus Tissue Doppler Imaging (TDI) E/e'. The RV PW TDI values also did not differ between the two groups (Table 9).

The parameters obtained with 3DE are presented in Table 10. LV EDV, ESV and stroke volumes were significantly higher in the athletes compared to control group as well as after indexing the values to BSA. LV EF was significantly lower in athletes, however, its values remained within normal range. LVM, determined by 3DE, also showed elevated values in top athletes (indexed to BSA), but it was significantly lower if compared to the values obtained with the Devereux formula. GLS and GCS were significantly lower in athletes (Figure 12).

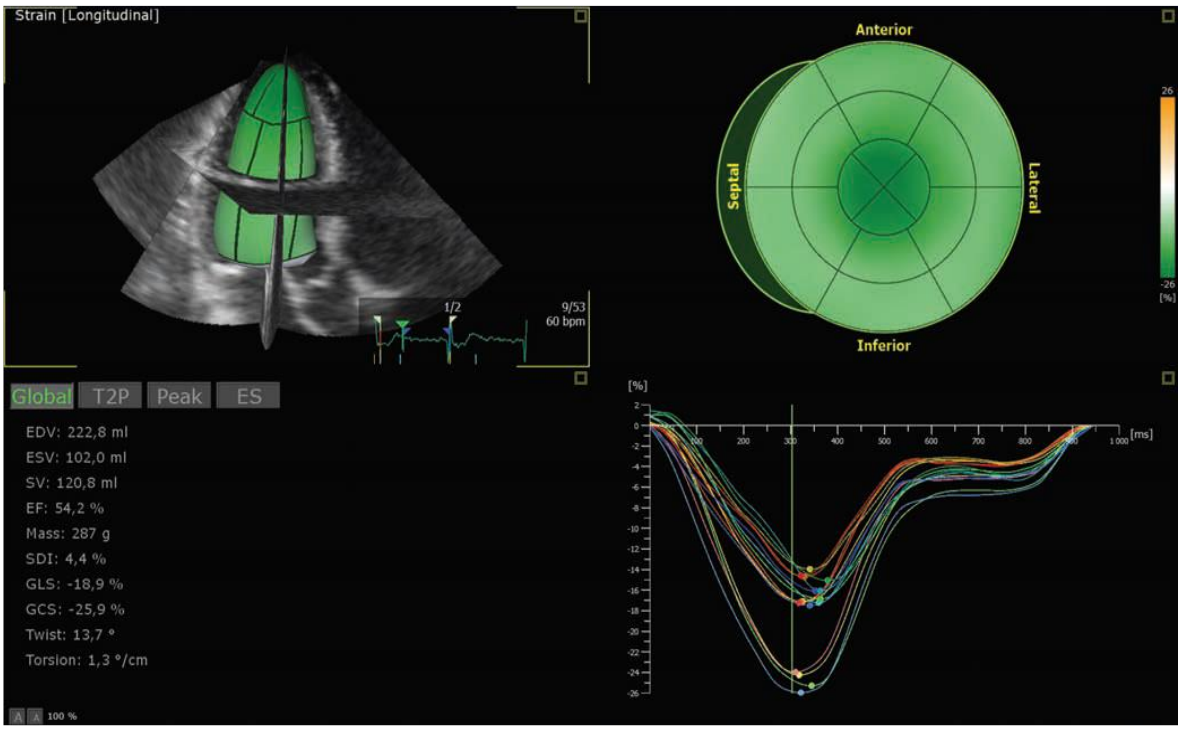

Figure 12. Example of LV 3D volume and strain analysis in an athlete. On the left side the values of the left ventricular "beutel" model and the derived volumetric and deformation parameters can be observed. On the right side, the 16 LV segments, so- called "bull's eyes" and time-strain (longitudinal strain) curves.

Similarly to LV, RV EDV, ESV and EF evaluated by 3DE was also significantly higher in athletes (Table 10). In athletes, the RV EF was lower than in controls, remaining, however the low-normal range (Figure 13). The FAC calculated using 3DE did not differ between the two groups. Both the septal and the free wall longitudinal strains were lower in athletes (Table 10).

Table 10. 3DE parameters in athletes and control group

	Athletes (n=11)	Control (n=10)	p
LVEDV (ml)	197±31	135±26	<0.001
LVEDVi (ml/m^2)	98±16	66±6	<0.001
LVESV (ml)	89±16	51±16	<0.001
LVESVi (ml/m^2)	44±8	25±5	<0.001
LVSV (ml)	108±17	84±14	0.003
LVSVi (ml/m^2)	54±9	41±4	<0.001
LVEF (%)	55±4	63±5	<0.001
LVM (g)	240±45	140±23	<0.001
LVMi (g/m^2)	119±24	69±8	<0.001
LVGLS (%)	-17.9±1.6	-22.1±3.0	<0.001
LVGCS (%)	-25.9±2.6	-29.6±3.5	0.012
RVEDV (ml)	207±41	131±20	<0.001
RVEDVi (ml/m^2)	103±19	65±9	<0.001
RVESV (ml)	102±24	54±11	<0.001
RVESVi (ml/m^2)	50±11	27±4	<0.001
RVSV (ml)	106±19	78±14	<0.001
RVSVi (ml/m^2)	53±10	39±7	0.001
RVEF (%)	51±3.1	59±5	<0.001
FAC (%)	50.8±6.5	55.3±10.9	0.281
RV septal LS (%)	-19.7±3.7	-25.4±4.0	0.005
RV free wall LS (%)	-29.6±3.3	-33.2±3.7	0.039

LV: left ventricular, RV: right ventricular, „i": body surface area index, EDV: end-diastolic volume, ESV: end-systolic volume, SV: stroke volume, EF: ejection fraction, „M": muscle mass, LS: longitudinális strain, „C": circumferencial, „G": global, FAC: fractional area change

Regarding the relative contribution of different RV wall motion directions, we have found no difference between the male athletes and corresponding controls (Table 11).

Table 11. **Comparison of the different motion directions of the RV between the study groups.**

	Athletes (n=11)	Control (n=10)	p
LEF (%)	21.9±4.9	26.4±3.3	0.100
LEF/TEF	0.42±0.09	0.47±0.06	0.136
REF (%)	21.5±3.7	24.4±4.5	0.134
REF/TEF	0.45±0.09	0.43±0.06	0.556
AEF (%)	20.9±4.8	26.3±3.6	0.052
AEF/TEF	0.43±0.09	0.46±0.08	0.414

LEF: longitudinal ejection fraction, REF: radial ejection fraction, AEF: anteroposterior ejection fractions, TEF: total ejection fraction

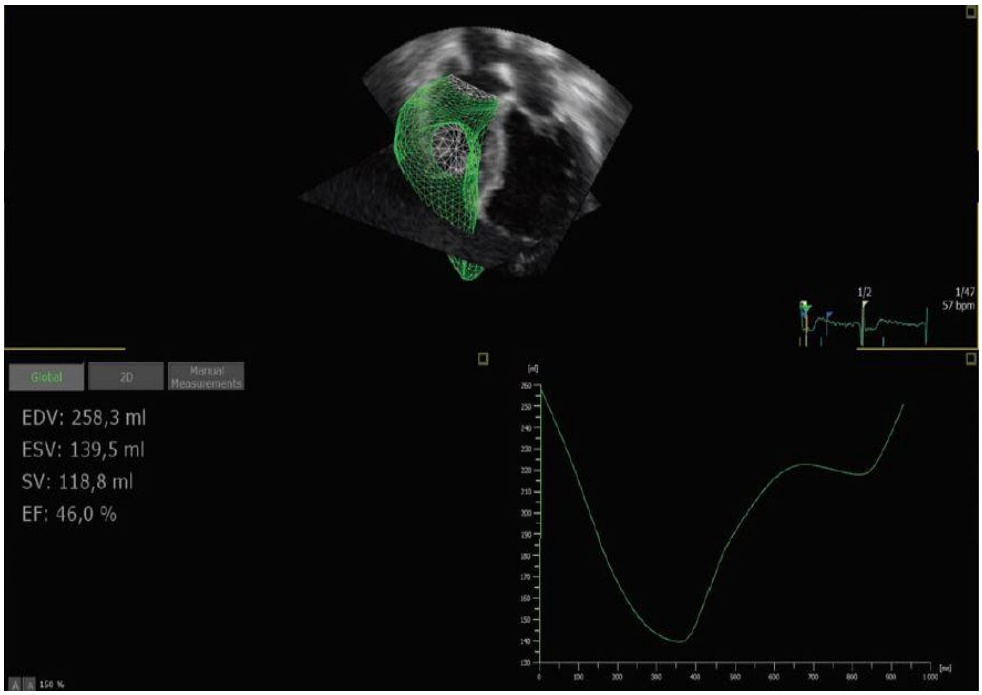

Figure 13. Example of RV 3D analysis in an athlete. The RV "mesh" model is represented above, volumetric values and the RV time-volume curve can be observed.

5.3 Determination of RV mechanical pattern in pathological RV remodelling

Demographic characteristics of the study groups are shown in Table 12. The mean age of the predominantly male HTX patients was 52 years. The age-and gender-matched control group did not show any statistically significant difference in terms of height, weight, BMI, BSA, systolic, and diastolic blood pressure compared to the HTX group (Table 12). HTX patients had significantly higher heart rate attributable to the denervation of the heart. The bicaval surgical technique was used in every patient.

LV end-diastolic-, end-systolic volumes, and stroke volume along with their BSA-indexed values showed no difference between the study groups (Table 12). LVEF and GLS were also similar, excluding the presence of LV systolic dysfunction. There was a trend toward significance in terms of higher LVM in HTX patients (Table 12).

Table 12. Baseline characteristics and left ventricular echocardiographic data of HTX and controls

	HTX (n=51)	Control (n=30)	p value
Age, y	52.3±10.8	50.1±13.0	0.60
Female, n (%)	11 (22)	11(36)	0.14
Height, cm	173.3±9.4	170.1±11.7	0.19
Weight, kg	74.0± 2.9	70.0±11.0	0.16
BMI, kg/m²	24.6 ± 4.0	24.1±2.8	0.56
BSA, m²	1.9±0.2	1.8±0.2	0.11
SBP, mm Hg	122.4±14.0	124.2±13.1	0.53
DBP, mm Hg	79.4±8.1	74.7±8.4	0.41
HR, 1/min	86.5±13.1	65.8±10.4	<0.0001
LV EDV, mL	100.5±24.8	95.4±24.2	0.46
LV EDVi, mL/m²	53.6±12.0	52.4±10.4	0.66
LV ESV, mL	38.5±13.3	35.1±9.7	0.31
LV ESVi, mL/m²	20.5±6.7	19.2±4.4	0.71

LV SV, mL	62.1±13.5	58.3±19.0	0.53
LV SVi, mL/m²	33.1±6.6	33.1±6.7	0.99
LV EF, %	62.4±5.8	63.2±3.4	0.44
LV GLS, %	−19.3±1.8	−19.1±2.0	0.57
LVM, g	131.6±22.2	122.5±20.0	0.14
LVMi, g/m²	71.0±14.0	67.8±9.2	0.85

BMI, body mass index; BSA, body surface area; DBP, diastolic blood pressure; EDV, end-diastolic volume; EF, ejection fraction; ESV, end-systolic volume; GLS, global longitudinal strain; HR, heart rate; i, indexed to BSA; LV, left ventricle; LVM, left ventricular mass; SBP, systolic blood pressure; SV, stroke volume.

Basic clinical characteristics of HTX patients are presented in Table 13. About 51% of patients were transplanted due to end-stage heart failure with nonischemic etiology and the operation was performed at a mean age of 51 years. To investigate the potential effects of perioperative circumstances, several hemodynamic and procedural parameters were collected. The median time elapsed after HTX was 226 days, ranging from 8 days to 18 years.

Table 13. Indications for HTX, peri- and postoperative parameters

	HTX (n=51)
Etiology	
Nonischemic DCM, n (%)	26 (51)
Ischemic DCM, n (%)	21 (41)
AC, n (%)	1 (2)
Other, nonspecified, n (%)	3 (6)
Age at HTX, y	50.5±11.1
Peri- andpostoperative parameters	
Preoperative PVR, Wood	2.73±1.1
Cold ischemic time, min	216.3±44.3
Aortic cross-clamping time, min	106.0±23.1
Cardiopulmonary bypass time, min	197.3±35.5
Age of donors, y	41.3±11.6
Gender of donors, female, n (%)	8 (16)
Length of ICU stay, d	16.7±17.0
Postoperative sildenafil use, n (%)	44 (86)
Sildenafil use at time-point of echocardiography, n (%)	5 (10)
Elapsed time after HTX at time-point of echocardiography, d[a]	226 (95-827)

AC, arrhythmogenic right ventricular dysplasia/cardiomyopathy; DCM, dilated cardiomyopathy; ICU, intensive care unit; PVR, pulmonary vascular resistance. [a]Median interquartile range.

Conventional and 3DE parameters of the RV are summarized in Table 14. In terms of conventional linear measurements, RV mid diameter and length were similar, the basal diameter showed enlargement of the RV in HTX patients. Measurements referring to longitudinal shortening showed consequently lower values compared to the control group (TAPSE, s′ by tissue Doppler imaging, free wall and septal longitudinal strain). Nevertheless, FAC, which partly incorporates radial function as assessed on a 2D A4C view, was normal and similar to healthy volunteers in HTX patients (44%, Table 14).

Table 14. Conventional parameters of the right heart in HTX vs controls

	HTX (n = 51)	Control (n = 30)	p value
RV basal diameter, mm	34.7 ± 7.6	27.6 ± 5.1	<0.0001
RV mid diameter, mm	32.1 ± 7.6	29.1 ± 5.2	0.07
RV length, mm	73.4 ± 8.1	74.2 ± 6.6	0.65
TAPSE, mm	10.8 ± 5.2	21.1 ± 3.7	<0.0001
FAC, %	44.2 ± 8.8	44.1 ± 4.8	0.99
PW TDI s′, cm/s	10.3 ± 2.3	13.9 ± 2.0	<0.0001
RV Tei Index	0.5 ± 0.13	0.36 ± 0.08	<0.0001
RV Free wall LS, %	20.1 ± 5.3	29.5 ± 3.7	<0.0001
RV Septal LS, %	11.9 ± 4.9	19.5 ± 4.0	<0.0001
RV EDV, mL	96.3 ± 27.2	97.3 ± 23.6	0.87
RV EDVi, mL/m²	50.8 ± 12.3	53.9 ± 11.8	0.28
RV ESV, mL	51.2 ± 15.1	44.9 ± 12.5	0.06
RV ESVi, mL/m²	27.2 ± 7.0	24.8 ± 6.2	0.13
RV SV, mL	45.1 ± 15.3	52.4 ± 12.5	0.03
RV SVi, mL/m²	23.6 ± 7.1	29.1 ± 4.0	0.0001
RV TEF, %	46.7 ± 7.2	54.1 ± 4.0	<0.0001
Moderate TR, n (%)	4 (8)	0 (0)	<0.0001
PASP, mm Hg	34.2 ± 7.2	16.1 ± 5.4	<0.0001
IVC at expiration, mm	16.2 ± 4.4	14.2 ± 5.6	0.16

EDV, end-diastolic volume; ESV, end-systolic volume; FAC, fractional area change; i, indexed to body surface area; IVC, inferior vena cava; LS, longitudinal strain; PASP, pulmonary arterial systolic pressure; PW TDI s′, pulsed-wave tissue Doppler imaging systolic velocity; RV, right ventricular; SV, stroke volume; TAPSE, tricuspid annular plane systolic excursion; TEF, total ejection fraction; TR, tricuspid regurgitation.

There was no statistically significant difference in terms of end-diastolic and end-systolic RV volumes. RV EF was lower in HTX patients; however, it remained within the lower

limits of normal range (153). Correspondingly, stroke volume and stroke volume index were lower in HTX patients. There were only four patients with moderate tricuspid regurgitation in our HTX group (severe regurgitation was exclusion criterion). Pulmonary arterial systolic pressure was higher in the transplanted cohort than in controls (Table 14). Figure 14 depicts our results regarding the relative contribution of longitudinal, radial, and anteroposterior wall motions to global RV function.

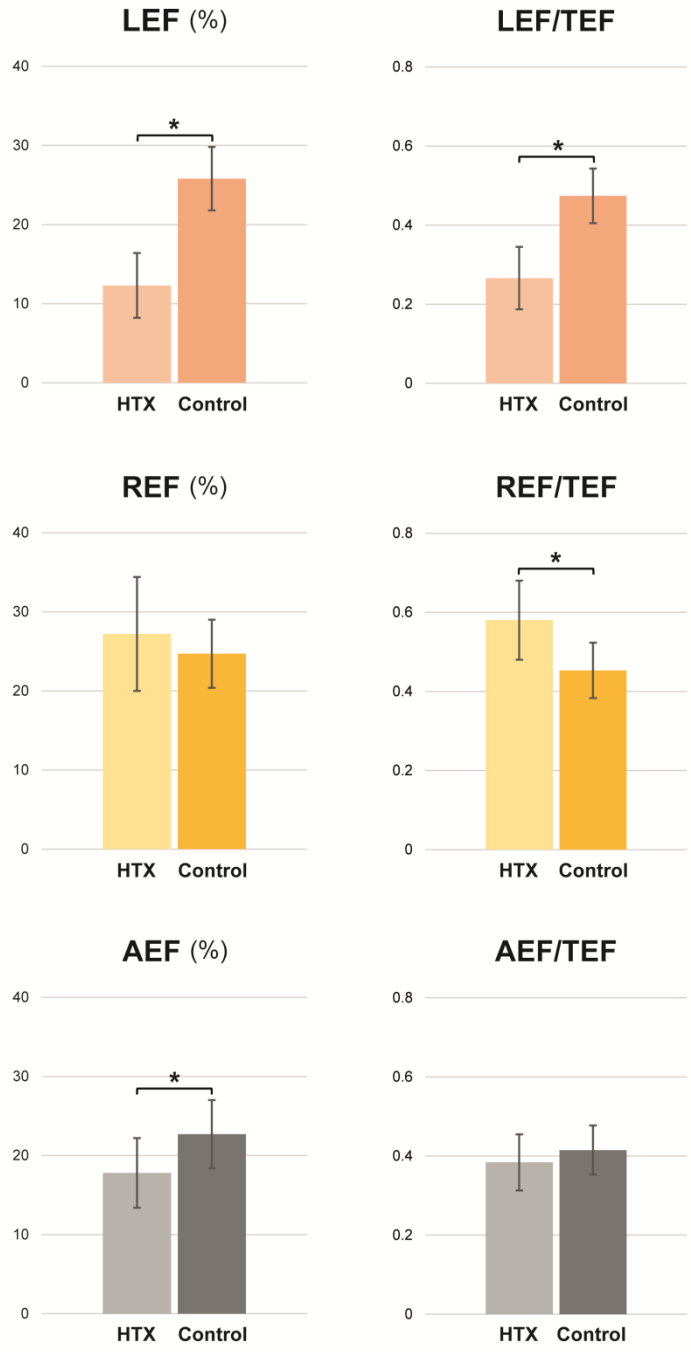

Figure 14. Relative contribution of the different wall motion components to RV EF in heart transplant recipients vs controls. Longitudinal—LEF, radial—REF, anteroposterior—AEF ejection fraction, total right ventricular ejection fraction TEF, transplant recipients (HTX). *p<0.05

In line with conventional echocardiographic parameters, longitudinal EF and its ratio to TEF was significantly lower in HTX patients compared to healthy controls. However, REF/TEF ratio was significantly higher in HTX patients compared to controls. AEF value alone was lower in HTX patients, and its ratio to TEF was not significantly different from healthy volunteers (Figure 14). In HTX patients, REF/TEF was significantly higher compared to both LEF/TEF and AEF/ TEF (LEF/TEF vs REF/TEF vs AEF/TEF: 0.27± 0.08 vs 0.5±0.10 vs 0.38±0.07, ANOVA, $p<0.0001$), which confirmed the radial wall motion to be dominant determining global RV function after HTX (Figure 15). On the contrary, in healthy volunteers only AEF/TEF ratio was smaller than LEF/TEF, while REF/TEF and LEF/TEF were similar (LEF/TEF vs REF/TEF vs AEF/TEF: 0.47±0.07 vs 0.45±0.07 vs 0.41±0.06, ANOVA, $p=0.0034$). In HTX patients, RV TEF assessed by 3DE correlated with FAC ($r=0.762$, $p<0 .0001$), free wall LS ($r=0.394$, $p=0.018$) and septal LS ($r=0.430$, $p=0.032$); however, TAPSE did not. LEF correlated moderately ($r=0.421$, $p= 0.0023$), while REF strongly with TEF ($r=0.767$, $p<0.0001$) in HTX recipients. We found no association between the perioperative hemodynamic or procedural parameters and the RV functional measurements at follow-up. Similarly, no correlation was established between postoperative sildenafil usage and RV morphology and function. The time elapsed after HTX showed correlation with RV longitudinal function (time vs TAPSE: $r=0.577$, $p<0.0001$; vs free wall LS: $r=0.483$, $p=0.0003$; vs septal LS: $r=0.492$, $p=0.0002$; vs LEF/TEF, $r=0.289$, $p=0.0039$), on the other hand, it had a negative correlation with the dominance of radial contribution (REF/TEF: $r=-0.285$, $p=0.042$). There was no association between anteroposterior shortening of the RV and time after HTX. We have also compared our HTX patients within 1 year and over 1 year after transplantation (29 vs 22 patients, respectively). There was no difference between the two groups in terms of 3D volumetric RV parameters (HTX within vs over 1 year; RV EDVi: 51.7±13.5 vs 49.7±11.0 mL/m2, $p= 0.57$; RV ESVi: 27.4±7.8 vs 26.9±6.1 mL/m2, $p=0.80$; RV SVi: 24.2±7.2 vs 22.7±7.1 mL/m2, $p=0.45$; RV TEF: 47.1±6.5 vs 46.3±8.3%, $p=0.72$).

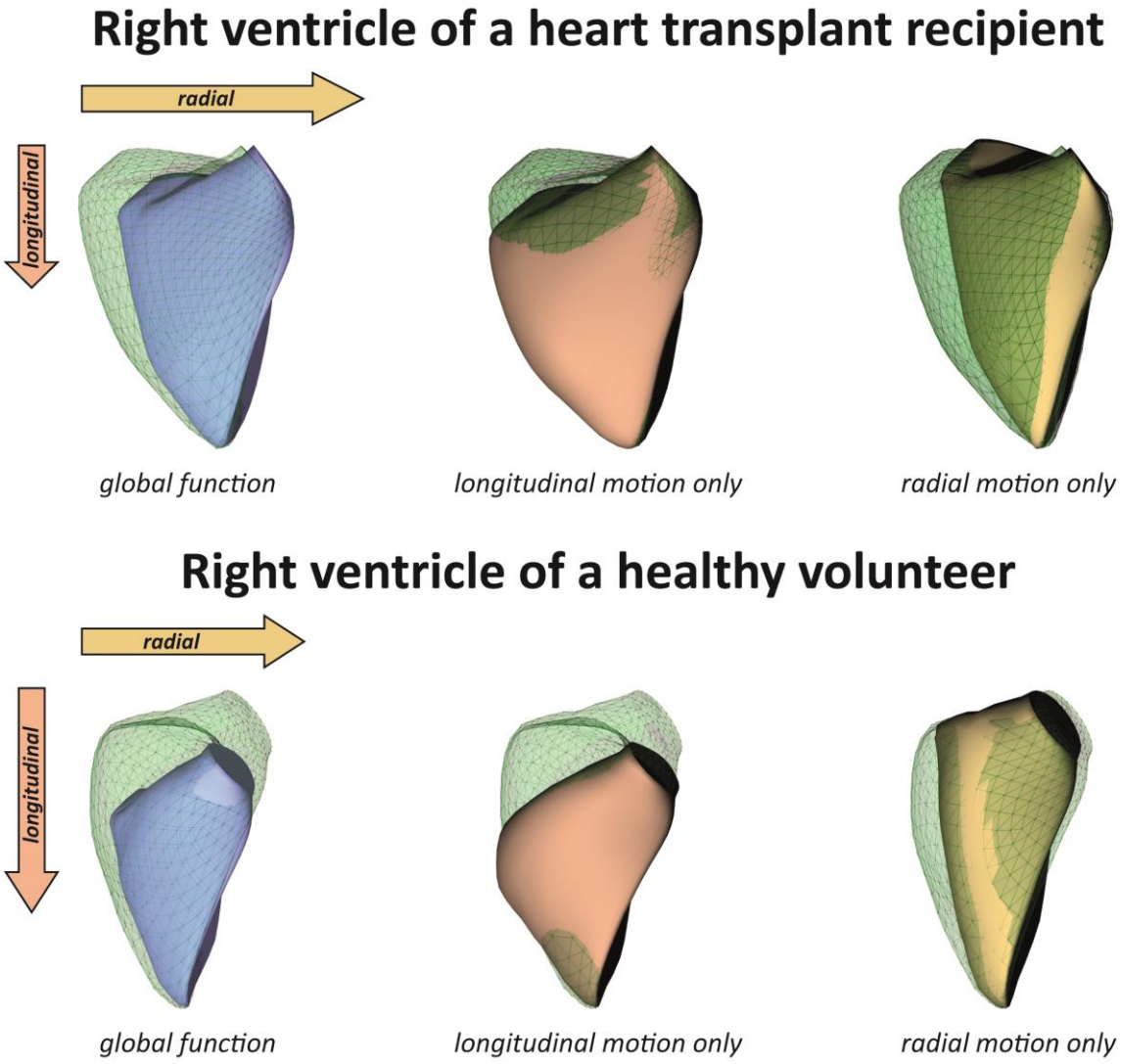

Figure 15. Representative examples of RV motion pattern in a heart transplant recipient vs a healthy volunteer. Green mesh represents EDV, and the blue surface is the ESV with all motion directions enabled. By decomposing the motion of the 3D RV model, the different anatomically relevant wall motion directions can be separately quantified. The radial motion is supernormal, and the longitudinal is decreased in the HTX patient compared to the healthy volunteer. Orange surface represents the volume loss at end-systole generated by only the longitudinal motion. Yellow surface represents the volume loss at end-systole generated by only the radial motion.

While FAC remained unchanged (42.3±7.8 vs 46.9±9.7, p=0.075), parameters referring to longitudinal shortening showed significant increase in time (TAPSE: 9.0±3.8 vs 13.3±6.1 mm; p=0.04, free wall LS: −18.2±3.9 vs −22.4±6.2%, p=0.0047; septal LS: −10.6±3.8 vs 13.5±5.9%, p=0.037). The relative contribution of longitudinal and radial wall motions to global RV function was different: The LEF/TEF ratio was significantly higher (0.23 ± 0.08 vs 0.31±0.06, p=0.0002), the REF/TEF ratio was significantly lower (0.6±0.09 vs 0.54±0.10, p=0.0039) in patients transplanted over 1 year. On the other hand, there was no significant difference in terms of AEF/ TEF between the groups (0.37±0.07 vs 0.40±0.07, p=0.12). We found no correlations between perioperative parameters and RV functional measurements in either subgroup.

Intraobserver and interobserver variability for RV volumes are summarized in Table 15. Intraobserver concordance correlation coefficient values ranged from 0.921 to 0.948, while interobserver values were lower in some degree.

Table 15. Intra-and interobserver variability of RV 3DE derived volumes. Lin's concordance correlation coefficient values.

	Intraobserver variability (95% CI)	Interobserver variability (95% CI)
RV EDV	0.921 (0.821-0.966)	0.901 (0.792-0.954)
RV ESV	0.948 (0.876-0.979)	0.925 (0.831-0.967)
ESV (longitudinal only)	0.923 (0.827-0.967)	0.887 (0.747-0.952)
ESV (radial only)	0.934 (0.845-0.973)	0.913 (0.838-0.954)

RV, right ventricle; EDV, end-diastolic volume; ESV, end-systolic volume.

6. DISCUSSION

6.1. Investigation of cardiac remodeling in female athletes induced by different types of exercise training

In our first study, we aimed at comparing two different sport disciplines in the context of female athlete's heart using 3DE. In IFBB BikiniFitness athletes, a mild, concentric-type of LVH is present, while in waterpolo athletes eccentric LVH develops (Figure 12). To the best of our knowledge, our study is the first to characterize athlete's heart of BikiniFitness competitors and also to suggest the applicability of Morganroth's hypothesis in women.

Athlete's heart is first and foremost characterized by a physiological increase in LVM (46, 154). Morganroth's classical hypothesis suggests that sports with mainly endurance exercise nature result in eccentric LVH, while power sports induce concentric hypertrophy (38). However, the spectrum of athlete's heart is very broad and substantive investigation of the adaptation induced by mostly endurance or power training is difficult, especially among women (49, 155). Therefore, we selected our study population to address this issue. Waterpolo is a good example of mixed exercise training with mainly dynamic components and a very high training load (>20 hours/week) with international anti-doping protocols in effect. The goal of IFBB BikiniFitness athletes however, is completely different: to sculpt a muscular, defined and toned, healthy looking physique with a reasonable amount of muscle mass (36). Training regime of these fitness athletes comprises mainly of relatively short duration but markedly high intensity static exercises, with dynamic components and overall training time being limited to avoid unwanted muscle mass loss. The use of performance and muscle enhancing doping is also strictly audited by the IFBB and is also counterproductive in this category. To date, no study has investigated this increasingly popular sport. We have found that female athlete's heart of fitness competitors is characterized by mild, concentric-type LVH compared to the significantly higher amount of LVM and eccentric hypertrophy presented by female waterpolo athletes. LV and RV

systolic or diastolic function was found to be unchanged in fitness athletes compared to healthy, sedentary volunteers.

Nevertheless, selection of imaging modality to delineate even subtle alterations in cardiac morphology and function is of pivotal importance. 3DE was shown to have better correlation with gold standard cardiac MRI compared to conventional M-mode and 2D echocardiographic measurements (153, 156, 157). The technical setup is essential in this regard since for example, LVWT values did not show difference between fitness athletes and controls in our study. 3DE, however, was able to show LVH of fitness athletes. The same applies to LV and RV volumetric measurements. I.e. simple linear RV parameters failed to indicate difference even between waterpolo athletes and healthy controls, however, 3DE showed a marked dilation of the RV in waterpolo athletes which corresponds to previous literature and their nature of exercise (158). This highlights the usefulness of 3DE in measuring chamber volumes and LVM in the athlete's heart. In waterpolo athletes furthermore, we were able to show the correlation between the time of training and gain of LVM.

Exercise-induced dilation of the ventricles often leads to low-normal resting values regarding functional parameters (159, 160). In our cohort, waterpolo athletes had lower LV EF along with decreased longitudinal and circumferential systolic deformation compared to both healthy volunteers and fitness athletes. The increased LV contractility of athlete's heart is a well-known phenomenon, however, resting echocardiographic parameters are not able to explore this and this is true for advanced imaging markers as well, like strains (161). Despite the lower values of systolic function parameters in waterpolo athletes, LV stroke volume and stroke volume index were similar among groups. Regarding the RV, EF and free wall longitudinal strain remained comparable in both athlete groups to sedentary volunteers, resulting in a higher SV and SVi in waterpolo athletes (along with the dilation of the RV). It has been recently shown in female athletes, that exercise-induced cardiac remodeling appears in a balanced manner both at the interventricular and atrioventricular levels, yet correlating with the intensity of dynamic exercise (162). Our results are in line with these observations. Moreover, we found that in waterpolo athletes a unique functional shift is present regarding the relative contribution of the different RV motion directions.

Longitudinal contribution to RV EF was supernormal, however, radial contribution was lower compared to sedentary controls, however, these results require further verification by a higher case number.

Diastolic function of athlete's heart may be also an important feature, as even resting measures may be capable to indicate the supernormal function of athletes and moreover, to differentiate between physiological and pathological hypertrophies (163). In our current study, the three investigated groups were similar in terms of all diastolic function parameters. Similar to the dilation of the ventricles, LA and RA were also significantly larger in waterpolo athletes, while were comparable between fitness athletes and controls. Bi-atrial dilation of endurance athletes is also an established phenomenon along with known gender differences in it (164).

We have also assessed body composition to characterize muscle gain of fitness athletes. Fat free mass index (FFMI) is a popular parameter among bodybuilders because reflects better muscle mass gain than BMI (165, 166). Moreover, high values may also refer to anabolic steroid abuse and could be used for screening purposes (165). Our results of athletes are typical for healthy, non-user athletes and the values of control subjects also correspond well to previous normative studies (166). Despite the waterpolo athletes had higher height and weight, fitness athletes presented with even higher FFMI showing the remarkable muscle mass gain related to this sport discipline. Interestingly, we have found significant correlations between FFMI and RV, but not LV remodelling, which may suggest potential effects of static exercise training to RV morphology and function (167).

6.2 Investigation of physiologic cardiac remodeling in elite male kayak and canoe athletes

The echocardiographic examination of the athletes still represents a challenge due to the lack of data about this topic. There are no guidelines about what to consider as normal values in the athlete`s heart. This happens due to several reasons: it`s problematic to find a large number of athletes of the same sex, of the same age and of the same type of exercise performed. In the present study (the second of ours) we have provided a detailed description of the left and right ventricular morphology and function in male kayak and canoe World-class athletes using 3DE. It can be stated that significantly larger volumes for both the LV and RV can be evaluated. At the same time, the EF of both chambers is lower compared to healthy, sedentary volunteers, which is also applicable to the longitudinal strain of the chambers. The majority of studies on sports cardiology are determined to examine the changes in the LV in response to exercise. This is partialy due to the fact that this part of the heart is directly responsible for the load-related circulatory demand and serves as a motor of the systemic circulation. Prominent changes in the structure and function of LV are compared to the sedentary population. The previously mentioned theory that correlates between the quality of the load and the morphological changes has been proven by several large studies, but the presence of exercise-induced LVH and dilatation is not fully established, since both the static and the dynamic load groups can present each other's characteristics (38, 46, 168-170).

In most types of sports, the degree of static and dynamic component varies, so a wide range of the morphological and functional changes can be observed in the heart (171). The ranging of sports by load characteristics is a widely accepted method and can provide a rough estimate of the specific physiological remodeling expected for a particular athlete.

Although kayak and kanoe belong to the dynamic type of sport–the results of our study showed concentric LVH. The functional changes of the LV with regular physical exercise have also been investigated in a number of studies. Taking that into consideration, it can be stated in general that athletes have a preserved EF at rest, however, by a considerable number of athletes slightly lower values of EF can be evaluated (172).

Novel methods of evaluation of myocardial function such as 2D speckle-tracking analysis show that decreased longitudinal strain is determined as compared to controls (173). This is primarily due to the changes in the LV geometry, as the increased EDV allows the heart to provide an adequate peripheral perfusion even at lower resting heart rate, which is also demonstrated by a substantial increase in resting volume as compared to the normal population (170). The animal model of the athlete`s heart shows a close correlation between strain parameters and the increased contractility measured by invasive pressure-volume analysis (161).

All of these stimulate a superior, multi-component examination of myocardial mechanics in the athlete's heart, which may allow a better recognition of pathological cases (155, 163).

However, RV remodeling occurs also during exercise training: in the case of dynamic type of sports, dilation of both LV and RV is present (174, 175). These results are also confirmed by our current investigation. Results in case of static exercise remain controversial, however, in strength training, where LV as a systemic pressure generator is the key element of performance, the role of RV may be inferior. Global and regional systolic functions show similar changes regarding the RV: EF is mildly reduced and also, lower resting longitudinal strain is present as compared to sedentary healthy controls (176, 177).

Our advanced 3DE approach also confirmed this, since not only the RV EF was decreased compared to the healthy controls, but both septal and longitudinal strain also showed lower values. All of these changes, similarly to the LV, can be attributed to geometric changes (28, 177, 178).

6.3 Determination of RV mechanical pattern in pathological RV remodelling

The main results of our third study are that (i) the longitudinal shortening of the RV is significantly decreased in HTX patients without relevant differences in RV geometry and global function; (ii) this phenomenon is attributable to the supernormal radial motion of the RV free wall, which maintains RV ejection fraction; (iii) in time, there is a tendency toward the recovery of RV longitudinal shortening in HTX recipients. About 50% of cardiac complications and 20% of mortality are related to RV failure in the early postoperative period after HTX (179, 180). RV systolic dysfunction, as assessed by conventional echocardiography, is a common finding in HTX patients. However, the decrease in RV function defined by routine measurements is poorly associated with the clinically manifested right heart failure. The possible cause is that conventional measurements, which refer mainly to the longitudinal shortening of the chamber (TAPSE, s′ by tissue Doppler imaging), are not accurate to evaluate global RV function in HTX recipients (181). Echocardiographic data of our cohort of patients showed the same characteristics: Parameters of longitudinal function were decreased not only in the early postoperative period, but also during long-term follow-up. Nevertheless, global function, as assessed by 3DE, was maintained, which corresponds to previous observations using 3D imaging modalities (182, 183). TAPSE, the most widely used parameter of RV function, failed to show correlation with 3D derived EF. There are also several technical issues; however, the altered motion pattern of the structurally complex RV may play a pivotal role in this underestimation. Therefore, to achieve a comprehensive characterization of RV function, other motion directions have to be also taken into consideration. There are three major mechanisms which contribute to RV pump function: (i) longitudinal shortening by traction of the tricuspid annular plane towards the apex; (ii) the inward (radial) motion of the RV free wall referred as the bellows effect; and (iii) the bulging of the interventricular septum during the LV contraction along with stretching the free wall over the septum (139). The relative significance of the aforementioned mechanisms may be different in certain cardiovascular conditions. According to our and others' experience by visual estimation,

we hypothesized that the radial motion is dominant determining global RV function in HTX patients.

Several previous works suggested the importance of the radial free wall motion; however, 2D imaging modalities failed to robustly delineate this motion direction due to the complex 3D structure of the RV (181, 182, 184, 185). FAC represents an important 2D parameter, because it partly incorporates the radial direction by being calculated from the end-diastolic and end-systolic areas of the RV on an A4C view or even during transesophageal echocardiography. In our study, FAC was similar in HTX patients and healthy subjects, while correlating well with EF. However, FAC suffers from the inherent 2D nature of its calculation, referring to a single plane of the large RV free wall surface. 3DE provides precise geometric information on the RV and also permits the measurement of global function (i.e., EF), which was only achievable by cardiac MRI (186). It has been shown that 3DE-derived EF is a useful marker of functional status after HTX (187). Moreover, further analysis of the 3D models enables to separately quantify the different wall motion directions and evaluate the relative contribution of each component. Using this approach, our results confirmed the dominance of radial wall motion in HTX patients. REF/TEF ratio was supernormal, while LEF/TEF was decreased similarly to other parameters of longitudinal function (Figure 15). In the control group, the relative contribution of longitudinal and radial wall motions was nearly the same. Furthermore, the results of our cohort correspond to previous literature that RV longitudinal shortening remains decreased throughout long-term follow-up (182, 187). Patients transplanted over 1 year still presented with decreased longitudinal function. However, a slow recovery is suggested to be present, while global function and geometry remain unchanged. We found correlations between TAPSE, longitudinal strain, LEF/TEF, and the time elapsed after HTX. Therefore, the instantaneous dominance of the radial wall motion after transplantation may be shifted back toward longitudinal shortening in time. The anteroposterior motion of the RV may mainly reflect the ventricular interdependence: LV contraction stretches the RV free wall insertion points resulting in a considerable contribution to RV function. The relative contribution of

anteroposterior shortening to global function was unaffected by time, which may be related to the maintained LV function.

There are several underlying mechanisms which may be the causes of this functional change. First and foremost, the elevated pulmonary pressure of the recipient may be a factor. Beyond the preexistent pulmonary hypertension, cardiopulmonary bypass also results in a transient pulmonary vasoconstriction (188). It is also known that pulmonary hypertension is a significant risk factor of acute right-sided failure and also a predictor of long-term survival (180, 189). In the early postoperative period, increased afterload results in dilation of the RV (190). However, pulmonary vascular resistance decreases after the procedure and only slightly elevated pressures are expected later, even in cases of severe preoperative pulmonary hypertension (190-192). Therefore, we should be cautious highlighting only pulmonary pressures regarding RV functional shift on a long-term follow-up. In primary pulmonary hypertension patients, a close relationship can be observed between pulmonary vascular resistance and various RV functional parameters (193). Moreover, these patients show maintained longitudinal RV shortening for a long time and the loss of radial function is suggested to be an early marker of the disease (194, 195). These findings are not concordant with what is seen in HTX patients.

Beside hemodynamics, (patho)physiological changes associated with brain death of the donor and also organ preservation may contribute to the functional shift (196, 197). It has been shown that the loss of pericardial constraint due to the incomplete closure of the pericardial sac and mismatch in the donor-recipient heart size has significant impact on cardiac mechanics (198). According to experimental simulations, the intact pericardial sac may reduce radial contraction of the ventricles with a concomitant increase in the longitudinal function (199). Clinical studies also support that the deterioration of RV longitudinal function is concurrent with the pericardial incision (200). RV longitudinal shortening measured by TAPSE is reported to be reduced in cardiac surgery patients as well, despite normal EF, therefore, the same phenomenon partly coexists after every cardiac surgery (184, 201).

However, the magnitude of longitudinal functional loss seems to be smaller and the recovery appears much faster in these patient populations (202-204). Previous studies

reported the similar nature and extent of RV functional shift in cardiac surgery patients with or without pericardial repair, suggesting that the loss of pericardial constraint may not be solely responsible for the altered RV mechanics (205). We should also mention the potential detrimental effects of immunosuppressive regimens in this regard (206). Beyond the aforementioned potential causes, loss of the substantial innervation of the RV myocardium may be an other important factor resulting in complex functional changes of the RV (207). However, it has been suggested that the transplanted heart can be reinnervated by both sympathetic and parasympathetic fibers (208, 209). Hypothetically, the slow recovery of longitudinal function can be a result of reinnervation as well. Of note, we may expect differences between the surgical techniques applied during HTX, which can result in different geometry and function of the right heart (210).

6.4 Limitations

There are some limitations regarding the listed studies that have to be acknowledged. The low number of investigated athletes represents a limitation. However, our approach was to select distinct populations from different sport disciplines representing the highest level possible. Waterpolo athletes had a longer training history and more extensive weekly training sessions compared to fitness athletes and their exercise nature is rather mixed than clearly dynamic. These factors may bias our comparison. Only resting echocardiographic measurements were performed in our studies. Further investigations are warranted to characterize cardiac function of female fitness athletes during exercise. Our studies have a cross-sectional design, while the temporal changes in LV and RV volumes and mass, such as throughout a training season or dynamics of deconditioning remain unknown. Despite 3DE solutions are commercially available, LA and RA volumes were calculated by a 2D method in our studies. Despite the clear advantages of 3DE, still cardiac MRI is the gold standard method for the quantification of LV and RV volumes and mass. Our future goal is to investigate the changes in the parameters at the time of exercise performance.

Regarding the assessment of RV function among HTX patients, an evident limitation of our study is its retrospective, cross-sectional approach. The patient population is broad in terms of time elapsed after transplantation, and therefore, the correlations of functional parameters vs time could be demonstrated. On the other hand, we were unable to show the potential significance of the perioperative hemodynamic and procedural parameters. We have initialized our prospective study to better characterize the timing and causes of this functional shift mechanism. Complete exclusion of higher grade rejection episodes and chronic allograft vasculopathy (which can deteriorate biventricular myocardial mechanics) is difficult, especially in patients transplanted for a longer time (211-213). Regular biopsies are discontinued after 1 year according to our institutional protocol, while chronic allograft vasculopathy is assessed on a yearly basis using invasive or CT coronary angiography. Of note, the reported TAPSE values are calculated by the dedicated 3D software, which results in lower absolute values compared to the M-mode method. This may limit comparability to previous publications, but fits better to our retrospective study design gaining better generalizability.

7. CONCLUSIONS

To the best of our knowledge, our study is the first to characterize female athlete's heart of IFBB BikiniFitness competitors. In our study we demonstrated that predominantly static exercise regime induced a mild, concentric-type hypertrophy, while in waterpolo athletes higher ventricular volumes and eccentric LV hypertrophy develop. Fitness athletes presented unchanged LV and RV systolic and diastolic function compared to sedentary volunteers. These findings highlight the applicability of Morganroth's classical hypothesis in the context of female athlete's heart.

Furthermore, kayak and canoe top-level male athletes have significant LV and RV dilation. LVM is also significantly increased, resulting in concentric LVH. Resting LV and RV function remains lower (EF and LS) compared to healthy volunteers. Further studies are needed to better understand the morphological and functional changes induced by regular, vigorous exercise, however, 3DE can provide valuable assistance.

We have found that after HTX, the radial motion of RV free wall compensates the decreased longitudinal shortening to maintain RV EF. In time, longitudinal function may recover. 3DE may be a useful method in everyday clinical practice to accurately measure global RV function. If 3D analysis is not available, a detailed 2D echocardiographic assessment is necessary involving such measurements, which also refer to the radial motion of the RV. Prospective studies are needed to better characterize the underlying causes of RV functional shift and to determine the potential predictive value of the novel RV parameters.

8. SUMMARY

Characterizations of RV morphology and function are an important step in cardiovascular investigations. We showed that 3DE is an effective and promising method for the evaluation of RV morphology and function, overcoming numerous limitations of 2D echocardiography. Athlete's heart attracts significant scientific interest, not just because of evaluating exercise-induced alterations and a potentially better recognising underlying pathological processes in athletes, but also for a deeper understanding of cardiac physiology. Our research included a scientifically underrepresented, but clinically important subgroup of athletes: females and also females with dominantly static type of exercise. We found that the classical hypothesis of Morganroth is applicable to this group of athletes, as a mild, concentric type of LV hypertrophy developed. Regarding the RV, there were no geometrical and functional alterations when they were compared to healthy controls, however, waterpolo female athletes (a mixed type of exercise training) had significantly higher RV volumes and low-normal resting function. Moreover, we have found a unique functional shift in the relative contribution of different RV motion direction, which warrants further investigation. We have also investigated a male, elite athlete population competing in kayaking or canoeing showing concentric LVH, in spite the fact that they performed a dynamic type of sport. Using 3DE approach, RV EF was decreased compared to the healthy controls, and both septal and longitudinal strain also showed lower values along with a prominent dilation of the chamber. There is no clear definition for what should be considered a normal value in athlete's heart. This is due to inability of recruiting a higher number of athletes in different ethnical, age groups (e.g., adolescents and master athletes), sport disciplines and importantly, females. Our current studies shed some light on the above-mentioned issues. Notably, athletes with known underlying diseases should be also investigated to draw a final conclusion in this topic. In the future it may enable a better diagnostic performance and SCD risk stratification in athletes. Moreover, we have also demonstrated the dominance of radial wall motion in HTX patients. Further, prospective studies are needed in several patient populations to investigate the presence of such changes in RV functional pattern and its diagnostic and prognostic power.

9. ÖSSZEFOGLALÁS

A jobb kamra morfológiájának és funkciójának pontos megítélése fontos lépés a kardiovaszkuláris kivizsgálások sorozatában. Vizsgálataink rámutattak, hogy a hagyományos paraméterekkel szemben a 3D echokardiográfia ígéretes és hatékony módszer a jobb kamra vizsgálatában. A sportszív vizsgálata jelentős tudományos érdeklődést generál, nem csupán az edzés indukálta kardiális változások és a potenciálisan mellette jelen lévő kórállapotok kimutatása miatt, hanem globálisan a kardiális élettan mélyebb megértése okán is. Vizsgálatainkban egy, az irodalmi adatokból alig ismert populációt jellemeztünk: női, döntően statikus edzésmunkát végző sportolókat. Kimutattuk, hogy Morganroth klasszikus hipotézise igaz rájuk nézve is: enyhe, koncentrikus típusú bal kamra hipertrófia fejlődik ki ezen sportolókban. A jobb kamrai morfológia és funkció tekintetében nem találtunk különbséget a kontroll csoporttal összevetve. Mindazonáltal egy kevert, statikus és dinamikus edzettségű vízilabdás populációban egy egyedi funkcionális változást találtunk: a jobb kamra longitudinális kontrakciója szuperdomináns volt a radiálissal szemben. Ennek a jelenségnek az igazolása és jelentőségének megítélése további, nagyobb esetszámú kutatómunkát igényel. Szintén vizsgáltunk szűk világelitbe tartozó férfi kajakos és kenus élsportolókat. Ugyan ezek elsősorban dinamikus sportágként ismeretesek, mégis koncentrikus típusú bal kamrai hipertrófiát találtunk sportolóinknál. 3D echokardiográfia segítségével a kontroll csoporthoz képest kissé alacsonyabb jobb kamrai ejekciós frakció és szeptális, illetve szabad fali longitudinális strain volt mérhető, a markáns dilatáció mellett. Sportolói echokardiográfiás normálértékek továbbra sem ismeretesek, mely elsősorban a különböző speciális alcsoportok (etnikum, korosztály, sportág, nem szerint, stb.) gyér irodalmi adatainak „köszönhető”. Jelen vizsgálatainkkal némileg ezen az úton szándékoztunk elindulni. Reményeink szerint a közeljövőben a kardiológia még inkább képessé válik a sportolói hirtelen szívhalál megelőzésére. A jobb kamrai komplex mechanikai funkció megítélése azonban további érdekességeket tartogat: szívtranszplantált betegekben a mintázat teljesen megváltozik és a radiális mozgáskomponens válik a meghatározóvá. További prospektív vizsgálatok szükségesek ezen funkcionális mintázatváltások diagnosztikus és prognosztikus erejének megítélésére.

10. ACKNOWLEDGEMENTS

I would firstly like to express my gratitude to my supervisor, Prof. Dr. Bela Merkely, for giving me the opportunity to study in Hungary, for helping me in regard of any financial, and professional aspect I had difficulties with.

I would also like to thank my other supervisor Dr. Attila Kovacs to show me all tips and tricks of echocardiography, teaching me the pitfalls of scientific writing and how to make my PhD thesis successful.

I am very grateful to Dr. Violetta Kekesi, without who all the administrative processes starting with my admission and ending with the termination of my studies will not be possible.

I would also like to thank Dr. Balint Lakatos and Dr. Edes Istvan Ferenc, Dr. Pal Abraham for their contribution, collaboration, helpful advice and suggestions.

I would always remain grateful to Dr. Elektra Bartha, Dr. Astrid Apor, Dr. Csilla Liptai, Dr. Andrea Szucs for showing me interesting clinical cases in every day echocardiographical practice.

I would thank my dear friends and colleagues from Russia Dr. Nika Nozsina, Dr. Leila Velieva for their constant support and love, their advice always helped me any time despite the distance between us.

A very special word of thanks goes to my Russian and Hungarian family and to my husband Gergely Farkas, who did their best to make me keep going through all the challenges I faced and who made my life better.

11. BIBLIOGRAPHY

1. Voelkel NF, Quaife RA, Leinwand LA, Barst RJ, McGoon MD, Meldrum DR, Dupuis J, Long CS, Rubin LJ, Smart FW, Suzuki YJ, Gladwin M, Denholm EM, Gail DB. (2006) Right ventricular function and failure: report of a National Heart, Lung, and Blood Institute working group on cellular and molecular mechanisms of right heart failure. Circulation, 114: 1883-1891.
2. Rudski LG, Lai WW, Afilalo J, Hua L, Handschumacher MD, Chandrasekaran K, Solomon SD, Louie EK, Schiller NB. (2010) Guidelines for the echocardiographic assessment of the right heart in adults: a report from the American Society of Echocardiography endorsed by the European Association of Echocardiography, a registered branch of the European Society of Cardiology, and the Canadian Society of Echocardiography. J Am Soc Echocardiogr, 23: 685-713.
3. Haddad F, Doyle R, Murphy DJ, Hunt SA. (2008) Right ventricular function in cardiovascular disease, part II: pathophysiology, clinical importance, and management of right ventricular failure. Circulation, 117: 1717-1731.
4. D'Andrea A, Morello A, Iacono AM, Scarafile R, Cocchia R, Riegler L, Pezzullo E, Golia E, Bossone E, Calabro R, Russo MG. (2015) Right Ventricular Changes in Highly Trained Athletes: Between Physiology and Pathophysiology. J Cardiovasc Echogr, 25: 97-102.
5. Henschen S. (1899) Skidlauf und skidwettlauf: Eine medizinische Sportstudie. Mitt Med Klin Upsala, 2.
6. Darling EA. (1899) The effects of training: a study of the Harvard University crews. Boston Med Surg J, 141: 205-209.
7. White PD. (1918) The pulse after a marathon race. J Am Med Assoc, 71: 1047-1048.
8. Chandra N, Bastiaenen R, Papadakis M, Sharma S. (2013) Sudden cardiac death in young athletes: practical challenges and diagnostic dilemmas. J Am Coll Cardiol, 61: 1027-1040.

9. Chandra N, Papadakis M, Sharma S. (2010) Preparticipation screening of young competitive athletes for cardiovascular disorders. Phys Sportsmed, 38: 54-63.

10. Elmaghawry M, Alhashemi M, Zorzi A, Yacoub MH. (2012) A global perspective of arrhythmogenic right ventricular cardiomyopathy. Glob Cardiol Sci Pract, 2012: 81-92.

11. Kushwaha SS, Grupper A. (2015) Suspected ARVC in the Athlete: Do T-Wave Findings Really Help in Diagnosis? J Am Coll Cardiol, 65: 2712-2713.

12. Bogaert J, Rademakers FE. (2001) Regional nonuniformity of normal adult human left ventricle. Am J Physiol Heart Circ Physiol, 280: H610-620.

13. Kitzman DW, Scholz DG, Hagen PT, Ilstrup DM, Edwards WD. (1988) Age-related changes in normal human hearts during the first 10 decades of life. Part II (Maturity): A quantitative anatomic study of 765 specimens from subjects 20 to 99 years old. Mayo Clin Proc, 63: 137-146.

14. Kitzman DW, Edwards WD. (1990) Age-related changes in the anatomy of the normal human heart. J Gerontol, 45: M33-39.

15. Ho SY. (2009) Anatomy and myoarchitecture of the left ventricular wall in normal and in disease. Eur J Echocardiogr, 10: 3-7.

16. Sengupta PP, Tajik AJ, Chandrasekaran K, Khandheria BK. (2008) Twist mechanics of the left ventricle: principles and application. JACC Cardiovasc Imaging, 1: 366-376.

17. Sengupta PP, Korinek J, Belohlavek M, Narula J, Vannan MA, Jahangir A, Khandheria BK. (2006) Left ventricular structure and function: basic science for cardiac imaging. J Am Coll Cardiol, 48: 1988-2001.

18. Dandel M, Lehmkuhl H, Knosalla C, Suramelashvili N, Hetzer R. (2009) Strain and strain rate imaging by echocardiography - basic concepts and clinical applicability. Curr Cardiol Rev, 5: 133-148.

19. Saghir M, Areces M, Makan M. (2007) Strain rate imaging differentiates hypertensive cardiac hypertrophy from physiologic cardiac hypertrophy (athlete's heart). J Am Soc Echocardiogr, 20: 151-157.

20. Sjoli B, Orn S, Grenne B, Vartdal T, Smiseth OA, Edvardsen T, Brunvand H. (2009) Comparison of left ventricular ejection fraction and left ventricular global strain as

determinants of infarct size in patients with acute myocardial infarction. J Am Soc Echocardiogr, 22: 1232-1238.

21. Harvey W. (1628) Exercitatio Anatomica de Motu Cordis et Sanguinis in Animalibus.

22. Haddad F, Hunt SA, Rosenthal DN, Murphy DJ. (2008) Right ventricular function in cardiovascular disease, part I: Anatomy, physiology, aging, and functional assessment of the right ventricle. Circulation, 117: 1436-1448.

23. Jiang L, Levine RA, Weyman AE. (1997) Echocardiographic Assessment of Right Ventricular Volume and Function. Echocardiography, 14: 189-206.

24. Hayrapetyan H. (2015) Anatomical and physiological patterns of right ventricle. J Cardiol Curr Res, 2: 49.

25. Farb A, Burke AP, Virmani R. (1992) Anatomy and pathology of the right ventricle (including acquired tricuspid and pulmonic valve disease). Cardiol Clin, 10: 1-21.

26. Ho SY, Nihoyannopoulos P. (2006) Anatomy, echocardiography, and normal right ventricular dimensions. Heart, 92: 2-13.

27. Foale R, Nihoyannopoulos P, McKenna W, Kleinebenne A, Nadazdin A, Rowland E, Smith G. (1986) Echocardiographic measurement of the normal adult right ventricle. Br Heart J, 56: 33-44.

28. Lakatos B, Toser Z, Tokodi M, Doronina A, Kosztin A, Muraru D, Badano LP, Kovacs A, Merkely B. (2017) Quantification of the relative contribution of the different right ventricular wall motion components to right ventricular ejection fraction: the ReVISION method. Cardiovasc Ultrasound, 15: 8.

29. Buckberg G, Hoffman JI. (2014) Right ventricular architecture responsible for mechanical performance: unifying role of ventricular septum. J Thorac Cardiovasc Surg, 148: 3166-3171.

30. Dell'Italia LJ. (1991) The right ventricle: anatomy, physiology, and clinical importance. Curr Probl Cardiol, 16: 653-720.

31. Geva T, Powell AJ, Crawford EC, Chung T, Colan SD. (1998) Evaluation of regional differences in right ventricular systolic function by acoustic quantification echocardiography and cine magnetic resonance imaging. Circulation, 98: 339-345.

32. Kukulski T, Hubbert L, Arnold M, Wranne B, Hatle L, Sutherland GR. (2000) Normal regional right ventricular function and its change with age: a Doppler myocardial imaging study. J Am Soc Echocardiogr, 13: 194-204.

33. Jiang L. Right ventricle. In: Weyman AE (ed), Principles and Practice of Echocardiography. Lippincott Williams & Wilkins, Philadelphia, 1994: 901-921.

34. Asmussen E. (1981) Similarities and dissimilarities between static and dynamic exercise. Circ Res, 48: I3-10.

35. Mitchell JH, Wildenthal K. (1974) Static (isometric) exercise and the heart: physiological and clinical considerations. Annu Rev Med, 25: 369-381.

36. Mitchell JH, Haskell W, Snell P, Van Camp SP. (2005) Task Force 8: classification of sports. J Am Coll Cardiol, 45: 1364-1367.

37. La Gerche A, Heidbuchel H. (2015) Response to Letters Regarding Article, "Can Intensive Exercise Harm the Heart? You Can Get Too Much of a Good Thing". Circulation, 131: e526.

38. Morganroth J, Maron BJ, Henry WL, Epstein SE. (1975) Comparative left ventricular dimensions in trained athletes. Ann Intern Med, 82: 521-524.

39. Haykowsky M, Taylor D, Teo K, Quinney A, Humen D. (2001) Left ventricular wall stress during leg-press exercise performed with a brief Valsalva maneuver. Chest, 119: 150-154.

40. Weiner RB, Wang F, Isaacs SK, Malhotra R, Berkstresser B, Kim JH, Hutter AM, Jr., Picard MH, Wang TJ, Baggish AL. (2013) Blood pressure and left ventricular hypertrophy during American-style football participation. Circulation, 128: 524-531.

41. Basavarajaiah S, Boraita A, Whyte G, Wilson M, Carby L, Shah A, Sharma S. (2008) Ethnic differences in left ventricular remodeling in highly-trained athletes relevance to differentiating physiologic left ventricular hypertrophy from hypertrophic cardiomyopathy. J Am Coll Cardiol, 51: 2256-2262.

42. Nagashima J, Musha H, Takada H, Murayama M. (2006) Left ventricular chamber size predicts the race time of Japanese participants in a 100 km ultramarathon. Br J Sports Med, 40: 331-333.

43. Rodriguez Reguero JJ, Iglesias Cubero G, Lopez de la Iglesia J, Terrados N, Gonzalez V, Cortina R, Cortina A. (1995) Prevalence and upper limit of cardiac hypertrophy in professional cyclists. Eur J Appl Physiol Occup Physiol, 70: 375-378.

44. Sharma S, Maron BJ, Whyte G, Firoozi S, Elliott PM, McKenna WJ. (2002) Physiologic limits of left ventricular hypertrophy in elite junior athletes: relevance to differential diagnosis of athlete's heart and hypertrophic cardiomyopathy. J Am Coll Cardiol, 40: 1431-1436.

45. Basavarajaiah S, Wilson M, Whyte G, Shah A, McKenna W, Sharma S. (2008) Prevalence of hypertrophic cardiomyopathy in highly trained athletes: relevance to pre-participation screening. J Am Coll Cardiol, 51: 1033-1039.

46. Pluim BM, Zwinderman AH, van der Laarse A, van der Wall EE. (2000) The athlete's heart. A meta-analysis of cardiac structure and function. Circulation, 101: 336-344.

47. Pelliccia A, Maron BJ, Spataro A, Proschan MA, Spirito P. (1991) The upper limit of physiologic cardiac hypertrophy in highly trained elite athletes. N Engl J Med, 324: 295-301.

48. Arbab-Zadeh A, Perhonen M, Howden E, Peshock RM, Zhang R, Adams-Huet B, Haykowsky MJ, Levine BD. (2014) Cardiac remodeling in response to 1 year of intensive endurance training. Circulation, 130: 2152-2161.

49. Pavlik G, Major Z, Csajagi E, Jeserich M, Kneffel Z. (2013) The athlete's heart. Part II: influencing factors on the athlete's heart: types of sports and age (review). Acta Physiol Hung, 100: 1-27.

50. D'Andrea A, Riegler L, Golia E, Cocchia R, Scarafile R, Salerno G, Pezzullo E, Nunziata L, Citro R, Cuomo S, Caso P, Di Salvo G, Cittadini A, Russo MG, Calabro R, Bossone E. (2013) Range of right heart measurements in top-level athletes: the training impact. Int J Cardiol, 164: 48-57.

51. Gjerdalen GF, Hisdal J, Solberg EE, Andersen TE, Radunovic Z, Steine K. (2014) The Scandinavian athlete's heart; echocardiographic characteristics of male professional football players. Scand J Med Sci Sports, 24: e372-380.

52. La Gerche A, Baggish AL, Knuuti J, Prior DL, Sharma S, Heidbuchel H, Thompson PD. (2013) Cardiac imaging and stress testing asymptomatic athletes to identify those at risk of sudden cardiac death. JACC Cardiovasc Imaging, 6: 993-1007.

53. La Gerche A, Heidbuchel H, Burns AT, Mooney DJ, Taylor AJ, Pfluger HB, Inder WJ, Macisaac AI, Prior DL. (2011) Disproportionate exercise load and remodeling of the athlete's right ventricle. Med Sci Sports Exerc, 43: 974-981.

54. La Gerche A, Claessen G. (2015) Is exercise good for the right ventricle? Concepts for health and disease. Can J Cardiol, 31: 502-508.

55. Benito B, Gay-Jordi G, Serrano-Mollar A, Guasch E, Shi Y, Tardif JC, Brugada J, Nattel S, Mont L. (2011) Cardiac arrhythmogenic remodeling in a rat model of long-term intensive exercise training. Circulation, 123: 13-22.

56. Wilson M, O'Hanlon R, Prasad S, Deighan A, Macmillan P, Oxborough D, Godfrey R, Smith G, Maceira A, Sharma S, George K, Whyte G. (2011) Diverse patterns of myocardial fibrosis in lifelong, veteran endurance athletes. J Appl Physiol (1985), 110: 1622-1626.

57. La Gerche A, Connelly KA, Mooney DJ, MacIsaac AI, Prior DL. (2008) Biochemical and functional abnormalities of left and right ventricular function after ultra-endurance exercise. Heart, 94: 860-866.

58. Ector J, Ganame J, van der Merwe N, Adriaenssens B, Pison L, Willems R, Gewillig M, Heidbuchel H. (2007) Reduced right ventricular ejection fraction in endurance athletes presenting with ventricular arrhythmias: a quantitative angiographic assessment. Eur Heart J, 28: 345-353.

59. La Gerche A, Burns AT, Mooney DJ, Inder WJ, Taylor AJ, Bogaert J, Macisaac AI, Heidbuchel H, Prior DL. (2012) Exercise-induced right ventricular dysfunction and structural remodelling in endurance athletes. Eur Heart J, 33: 998-1006.

60. D'Ascenzi F, Pelliccia A, Corrado D, Cameli M, Curci V, Alvino F, Natali BM, Focardi M, Bonifazi M, Mondillo S. (2016) Right ventricular remodelling induced by exercise training in competitive athletes. Eur Heart J Cardiovasc Imaging, 17: 301-307.

61. Heidbuchel H, La Gerche A. (2012) The right heart in athletes. Evidence for exercise-induced arrhythmogenic right ventricular cardiomyopathy. Herzschrittmacherther Elektrophysiol, 23: 82-86.

62. Bohm P, Schneider G, Linneweber L, Rentzsch A, Kramer N, Abdul-Khaliq H, Kindermann W, Meyer T, Scharhag J. (2016) Right and Left Ventricular Function and Mass in Male Elite Master Athletes: A Controlled Contrast-Enhanced Cardiovascular Magnetic Resonance Study. Circulation, 133: 1927-1935.

63. Kirchhof P, Fabritz L, Zwiener M, Witt H, Schafers M, Zellerhoff S, Paul M, Athai T, Hiller KH, Baba HA, Breithardt G, Ruiz P, Wichter T, Levkau B. (2006) Age- and training-dependent development of arrhythmogenic right ventricular cardiomyopathy in heterozygous plakoglobin-deficient mice. Circulation, 114: 1799-1806.

64. Sen-Chowdhry S, Syrris P, Ward D, Asimaki A, Sevdalis E, McKenna WJ. (2007) Clinical and genetic characterization of families with arrhythmogenic right ventricular dysplasia/cardiomyopathy provides novel insights into patterns of disease expression. Circulation, 115: 1710-1720.

65. James CA, Bhonsale A, Tichnell C, Murray B, Russell SD, Tandri H, Tedford RJ, Judge DP, Calkins H. (2013) Exercise increases age-related penetrance and arrhythmic risk in arrhythmogenic right ventricular dysplasia/cardiomyopathy-associated desmosomal mutation carriers. J Am Coll Cardiol, 62: 1290-1297.

66. Saberniak J, Hasselberg NE, Borgquist R, Platonov PG, Sarvari SI, Smith HJ, Ribe M, Holst AG, Edvardsen T, Haugaa KH. (2014) Vigorous physical activity impairs myocardial function in patients with arrhythmogenic right ventricular cardiomyopathy and in mutation positive family members. Eur J Heart Fail, 16: 1337-1344.

67. Heidbuchel H, Hoogsteen J, Fagard R, Vanhees L, Ector H, Willems R, Van Lierde J. (2003) High prevalence of right ventricular involvement in endurance athletes with ventricular arrhythmias. Role of an electrophysiologic study in risk stratification. Eur Heart J, 24: 1473-1480.

68. La Gerche A, Robberecht C, Kuiperi C, Nuyens D, Willems R, de Ravel T, Matthijs G, Heidbuchel H. (2010) Lower than expected desmosomal gene mutation prevalence in

endurance athletes with complex ventricular arrhythmias of right ventricular origin. Heart, 96: 1268-1274.

69. La Gerche A. (2015) Defining the interaction between exercise and arrhythmogenic right ventricular cardiomyopathy. Eur J Heart Fail, 17: 128-131.

70. Sanz-de la Garza M, Giraldeau G, Marin J, Grazioli G, Esteve M, Gabrielli L, Brambila C, Sanchis L, Bijnens B, Sitges M. (2017) Influence of gender on right ventricle adaptation to endurance exercise: an ultrasound two-dimensional speckle-tracking stress study. Eur J Appl Physiol, 117: 389-396.

71. Yilmaz DC, Buyukakilli B, Gurgul S, Rencuzogullari I. (2013) Adaptation of heart to training: a comparative study using echocardiography & impedance cardiography in male & female athletes. Indian J Med Res, 137: 1111-1120.

72. Karjalainen J, Mantysaari M, Viitasalo M, Kujala U. (1997) Left ventricular mass, geometry, and filling in endurance athletes: association with exercise blood pressure. J Appl Physiol (1985), 82: 531-537.

73. Zemva A, Rogel P. (2001) Gender differences in athlete's heart: association with 24-h blood pressure. A study of pairs in sport dancing. Int J Cardiol, 77: 49-54.

74. Pavlik G, Olexo Z, Banhegyi A, Sido Z, Frenkl R. (1999) Gender differences in the echocardiographic characteristics of the athletic heart. Acta Physiol Hung, 86: 273-278.

75. Whyte GP, George K, Sharma S, Firoozi S, Stephens N, Senior R, McKenna WJ. (2004) The upper limit of physiological cardiac hypertrophy in elite male and female athletes: the British experience. Eur J Appl Physiol, 92: 592-597.

76. Pelliccia A, Maron BJ, Culasso F, Spataro A, Caselli G. (1996) Athlete's heart in women. Echocardiographic characterization of highly trained elite female athletes. J Am Med Assoc, 276: 211-215.

77. Wiebe CG, Gledhill N, Warburton DE, Jamnik VK, Ferguson S. (1998) Exercise cardiac function in endurance-trained males versus females. Clin J Sport Med, 8: 272-279.

78. Rawlins J, Carre F, Kervio G, Papadakis M, Chandra N, Edwards C, Whyte GP, Sharma S. (2010) Ethnic differences in physiological cardiac adaptation to intense physical exercise in highly trained female athletes. Circulation, 121: 1078-1085.

79. D'Aloisio AA, Schroeder JC, North KE, Poole C, West SL, Travlos GS, Baird DD. (2009) IGF-I and IGFBP-3 polymorphisms in relation to circulating levels among African American and Caucasian women. Cancer Epidemiol Biomarkers Prev, 18: 954-966.

80. Mosen H, Steding-Ehrenborg K. (2014) Atrial remodelling is less pronounced in female endurance-trained athletes compared with that in male athletes. Scand Cardiovasc J, 48: 20-26.

81. Zheng ZJ, Croft JB, Giles WH, Mensah GA. (2001) Sudden cardiac death in the United States, 1989 to 1998. Circulation, 104: 2158-2163.

82. Van Camp SP, Bloor CM, Mueller FO, Cantu RC, Olson HG. (1995) Nontraumatic sports death in high school and college athletes. Med Sci Sports Exerc, 27: 641-647.

83. Harmon KG, Asif IM, Maleszewski JJ, Owens DS, Prutkin JM, Salerno JC, Zigman ML, Ellenbogen R, Rao AL, Ackerman MJ, Drezner JA. (2015) Incidence, Cause, and Comparative Frequency of Sudden Cardiac Death in National Collegiate Athletic Association Athletes: A Decade in Review. Circulation, 132: 10-19.

84. Corrado D, Basso C, Thiene G. (2009) Letter by Corrado et al regarding article, "sudden deaths in young competitive athletes: analysis of 1866 deaths in the United States, 1980-2006". Circulation, 120: e143.

85. Corrado D, Basso C, Thiene G, McKenna WJ, Davies MJ, Fontaliran F, Nava A, Silvestri F, Blomstrom-Lundqvist C, Wlodarska EK, Fontaine G, Camerini F. (1997) Spectrum of clinicopathologic manifestations of arrhythmogenic right ventricular cardiomyopathy/dysplasia: a multicenter study. J Am Coll Cardiol, 30: 1512-1520.

86. Maron BJ, Shirani J, Poliac LC, Mathenge R, Roberts WC, Mueller FO. (1996) Sudden death in young competitive athletes. Clinical, demographic, and pathological profiles. J Am Med Assoc, 276: 199-204.

87. Gersh BJ, Maron BJ, Bonow RO, Dearani JA, Fifer MA, Link MS, Naidu SS, Nishimura RA, Ommen SR, Rakowski H, Seidman CE, Towbin JA, Udelson JE, Yancy CW. (2011) 2011 ACCF/AHA guideline for the diagnosis and treatment of hypertrophic cardiomyopathy: a report of the American College of Cardiology Foundation/American Heart Association Task Force on Practice Guidelines. J Thorac Cardiovasc Surg, 142: e153-203.

88. Maron BJ, Gardin JM, Flack JM, Gidding SS, Kurosaki TT, Bild DE. (1995) Prevalence of hypertrophic cardiomyopathy in a general population of young adults. Echocardiographic analysis of 4111 subjects in the CARDIA Study. Coronary Artery Risk Development in (Young) Adults. Circulation, 92: 785-789.

89. Teare D. (1958) Asymmetrical hypertrophy of the heart in young adults. Br Heart J, 20: 1-8.

90. Maron BJ, Olivotto I, Spirito P, Casey SA, Bellone P, Gohman TE, Graham KJ, Burton DA, Cecchi F. (2000) Epidemiology of hypertrophic cardiomyopathy-related death: revisited in a large non-referral-based patient population. Circulation, 102: 858-864.

91. Primo JJ. (2001) Efficacy of implantable cardioverter-defibrillators for the prevention of sudden death in patients with hypertrophic cardiomyopathy. Rev Port Cardiol, 20: 225-228.

92. Zorzi A, Perazzolo Marra M, Rigato I, De Lazzari M, Susana A, Niero A, Pilichou K, Migliore F, Rizzo S, Giorgi B, De Conti G, Sarto P, Serratosa L, Patrizi G, De Maria E, Pelliccia A, Basso C, Schiavon M, Bauce B, Iliceto S, Thiene G, Corrado D. (2016) Nonischemic Left Ventricular Scar as a Substrate of Life-Threatening Ventricular Arrhythmias and Sudden Cardiac Death in Competitive Athletes. Circ Arrhythm Electrophysiol, 9: 1-14.

93. Fluechter S, Kuschyk J, Wolpert C, Doesch C, Veltmann C, Haghi D, Schoenberg SO, Sueselbeck T, Germans T, Streitner F, Borggrefe M, Papavassiliu T. (2010) Extent of late gadolinium enhancement detected by cardiovascular magnetic resonance correlates with the inducibility of ventricular tachyarrhythmia in hypertrophic cardiomyopathy. J Cardiovasc Magn Reson, 12: 30.

94. Maron BJ, Rowin EJ, Casey SA, Link MS, Lesser JR, Chan RH, Garberich RF, Udelson JE, Maron MS. (2015) Hypertrophic Cardiomyopathy in Adulthood Associated With Low Cardiovascular Mortality With Contemporary Management Strategies. J Am Coll Cardiol, 65: 1915-1928.

95. Haugaa KH, Haland TF, Leren IS, Saberniak J, Edvardsen T. (2016) Arrhythmogenic right ventricular cardiomyopathy, clinical manifestations, and diagnosis. Europace, 18: 965-972.

96. Akdis D, Brunckhorst C, Duru F, Saguner AM. (2016) Arrhythmogenic Cardiomyopathy: Electrical and Structural Phenotypes. Arrhythm Electrophysiol Rev, 5: 90-101.

97. Herren T, Gerber PA, Duru F. (2009) Arrhythmogenic right ventricular cardiomyopathy/dysplasia: a not so rare "disease of the desmosome" with multiple clinical presentations. Clin Res Cardiol, 98: 141-158.

98. Corrado D, Basso C, Pavei A, Michieli P, Schiavon M, Thiene G. (2006) Trends in sudden cardiovascular death in young competitive athletes after implementation of a preparticipation screening program. J Am Med Assoc, 296: 1593-1601.

99. Tabib A, Loire R, Chalabreysse L, Meyronnet D, Miras A, Malicier D, Thivolet F, Chevalier P, Bouvagnet P. (2003) Circumstances of death and gross and microscopic observations in a series of 200 cases of sudden death associated with arrhythmogenic right ventricular cardiomyopathy and/or dysplasia. Circulation, 108: 3000-3005.

100. Ye D, Edwards WD, Rizkalla W. (2005) Sudden unexpected death in a 31-year-old man caused by arrhythmogenic right ventricular cardiomyopathy. Arch Pathol Lab Med, 129: 1330-1333.

101. Finocchiaro G, Papadakis M, Robertus JL, Dhutia H, Steriotis AK, Tome M, Mellor G, Merghani A, Malhotra A, Behr E, Sharma S, Sheppard MN. (2016) Etiology of Sudden Death in Sports: Insights From a United Kingdom Regional Registry. J Am Coll Cardiol, 67: 2108-2115.

102. Sato PY, Musa H, Coombs W, Guerrero-Serna G, Patino GA, Taffet SM, Isom LL, Delmar M. (2009) Loss of plakophilin-2 expression leads to decreased sodium current and slower conduction velocity in cultured cardiac myocytes. Circ Res, 105: 523-526.

103. Wang L, Liu S, Zhang H, Hu S, Wei Y. (2018) Arrhythmogenic cardiomyopathy: Identification of desmosomal gene variations and desmosomal protein expression in variation carriers. Exp Ther Med, 15: 2255-2262.

104. Sato T, Nishio H, Suzuki K. (2015) Identification of arrhythmogenic right ventricular cardiomyopathy-causing gene mutations in young sudden unexpected death autopsy cases. J Forensic Sci, 60: 457-461.

105. Marcus FI, McKenna WJ, Sherrill D, Basso C, Bauce B, Bluemke DA, Calkins H, Corrado D, Cox MG, Daubert JP, Fontaine G, Gear K, Hauer R, Nava A, Picard MH, Protonotarios N, Saffitz JE, Sanborn DM, Steinberg JS, Tandri H, Thiene G, Towbin JA, Tsatsopoulou A, Wichter T, Zareba W. (2010) Diagnosis of arrhythmogenic right ventricular cardiomyopathy/dysplasia: proposed modification of the Task Force Criteria. Eur Heart J, 31: 806-814.

106. Maron BJ, Udelson JE, Bonow RO, Nishimura RA, Ackerman MJ, Estes NA, 3rd, Cooper LT, Jr., Link MS, Maron MS. (2015) Eligibility and Disqualification Recommendations for Competitive Athletes With Cardiovascular Abnormalities: Task Force 3: Hypertrophic Cardiomyopathy, Arrhythmogenic Right Ventricular Cardiomyopathy and Other Cardiomyopathies, and Myocarditis: A Scientific Statement From the American Heart Association and American College of Cardiology. Circulation, 132: e273-280.

107. Borrione P, Quaranta F, Ciminelli E. (2013) Pre-participation screening for the prevention of sudden cardiac death in athletes. World J Methodol, 3: 1-6.

108. Schwotzer R, Kistler W, Keller DI, Wolber T, Luscher TF, Drechsel S, Villiger B, Schmied C. (2013) "On-site" prevention and education to improve cardiac pre-competition screening in competitive amateur athletes. Swiss Med Wkly, 143: w13785.

109. Kerkhof DL, Gleason CN, Basilico FC, Corrado GD. (2016) Is There a Role for Limited Echocardiography During the Preparticipation Physical Examination? PM R, 8: S36-44.

110. Gottdiener JS. (2001) Overview of stress echocardiography: uses, advantages, and limitations. Prog Cardiovasc Dis, 43: 315-334.

111. Lang RM, Badano LP, Mor-Avi V, Afilalo J, Armstrong A, Ernande L, Flachskampf FA, Foster E, Goldstein SA, Kuznetsova T, Lancellotti P, Muraru D, Picard MH, Rietzschel ER, Rudski L, Spencer KT, Tsang W, Voigt JU. (2015) Recommendations for cardiac chamber quantification by echocardiography in adults: an update from the American Society of Echocardiography and the European Association of Cardiovascular Imaging. Eur Heart J Cardiovasc Imaging, 16: 233-270.

112. Devereux RB, Reichek N. (1977) Echocardiographic determination of left ventricular mass in man. Anatomic validation of the method. Circulation, 55: 613-618.

113. Devereux RB, Alonso DR, Lutas EM, Gottlieb GJ, Campo E, Sachs I, Reichek N. (1986) Echocardiographic assessment of left ventricular hypertrophy: comparison to necropsy findings. Am J Cardiol, 57: 450-458.

114. Lang RM, Bierig M, Devereux RB, Flachskampf FA, Foster E, Pellikka PA, Picard MH, Roman MJ, Seward J, Shanewise J, Solomon S, Spencer KT, St John Sutton M, Stewart W. (2006) Recommendations for chamber quantification. Eur J Echocardiogr, 7: 79-108.

115. Bellenger NG, Burgess MI, Ray SG, Lahiri A, Coats AJ, Cleland JG, Pennell DJ. (2000) Comparison of left ventricular ejection fraction and volumes in heart failure by echocardiography, radionuclide ventriculography and cardiovascular magnetic resonance; are they interchangeable? Eur Heart J, 21: 1387-1396.

116. Jenkins C, Bricknell K, Hanekom L, Marwick TH. (2004) Reproducibility and accuracy of echocardiographic measurements of left ventricular parameters using real-time three-dimensional echocardiography. J Am Coll Cardiol, 44: 878-886.

117. Nikitin NP, Constantin C, Loh PH, Ghosh J, Lukaschuk EI, Bennett A, Hurren S, Alamgir F, Clark AL, Cleland JG. (2006) New generation 3-dimensional echocardiography for left ventricular volumetric and functional measurements: comparison with cardiac magnetic resonance. Eur J Echocardiogr, 7: 365-372.

118. Chang SA, Lee SC, Kim EY, Hahm SH, Jang SY, Park SJ, Choi JO, Park SW, Choe YH, Oh JK. (2011) Feasibility of single-beat full-volume capture real-time three-dimensional echocardiography and auto-contouring algorithm for quantification of left ventricular volume: validation with cardiac magnetic resonance imaging. J Am Soc Echocardiogr, 24: 853-859.

119. Mor-Avi V, Lang RM, Badano LP, Belohlavek M, Cardim NM, Derumeaux G, Galderisi M, Marwick T, Nagueh SF, Sengupta PP, Sicari R, Smiseth OA, Smulevitz B, Takeuchi M, Thomas JD, Vannan M, Voigt JU, Zamorano JL. (2011) Current and evolving echocardiographic techniques for the quantitative evaluation of cardiac mechanics:

ASE/EAE consensus statement on methodology and indications endorsed by the Japanese Society of Echocardiography. Eur J Echocardiogr, 12: 167-205.

120. Leitman M, Lysyansky P, Sidenko S, Shir V, Peleg E, Binenbaum M, Kaluski E, Krakover R, Vered Z. (2004) Two-dimensional strain-a novel software for real-time quantitative echocardiographic assessment of myocardial function. J Am Soc Echocardiogr, 17: 1021-1029.

121. Voigt JU, Pedrizzetti G, Lysyansky P, Marwick TH, Houle H, Baumann R, Pedri S, Ito Y, Abe Y, Metz S, Song JH, Hamilton J, Sengupta PP, Kolias TJ, d'Hooge J, Aurigemma GP, Thomas JD, Badano LP. (2015) Definitions for a common standard for 2D speckle tracking echocardiography: consensus document of the EACVI/ASE/Industry Task Force to standardize deformation imaging. J Am Soc Echocardiogr, 28: 183-193.

122. Cha MJ, Kim HS, Kim SH, Park JH, Cho GY. (2017) Prognostic power of global 2D strain according to left ventricular ejection fraction in patients with ST elevation myocardial infarction. PLoS One, 12: e0174160.

123. Mornos C, Manolis AJ, Cozma D, Kouremenos N, Zacharopoulou I, Ionac A. (2014) The value of left ventricular global longitudinal strain assessed by three-dimensional strain imaging in the early detection of anthracyclinemediated cardiotoxicity. Hellenic J Cardiol, 55: 235-244.

124. Nagy VK, Szeplaki G, Apor A, Kutyifa V, Kovacs A, Kosztin A, Becker D, Boros AM, Geller L, Merkely B. (2015) Role of Right Ventricular Global Longitudinal Strain in Predicting Early and Long-Term Mortality in Cardiac Resynchronization Therapy Patients. PLoS One, 10: e0143907.

125. Lang RM, Badano LP, Tsang W, Adams DH, Agricola E, Buck T, Faletra FF, Franke A, Hung J, de Isla LP, Kamp O, Kasprzak JD, Lancellotti P, Marwick TH, McCulloch ML, Monaghan MJ, Nihoyannopoulos P, Pandian NG, Pellikka PA, Pepi M, Roberson DA, Shernan SK, Shirali GS, Sugeng L, Ten Cate FJ, Vannan MA, Zamorano JL, Zoghbi WA. (2012) EAE/ASE recommendations for image acquisition and display using three-dimensional echocardiography. Eur Heart J Cardiovasc Imaging, 13: 1-46.

126. Lang RM, Badano LP, Tsang W, Adams DH, Agricola E, Buck T, Faletra FF, Franke A, Hung J, de Isla LP, Kamp O, Kasprzak JD, Lancellotti P, Marwick TH,

McCulloch ML, Monaghan MJ, Nihoyannopoulos P, Pandian NG, Pellikka PA, Pepi M, Roberson DA, Shernan SK, Shirali GS, Sugeng L, Ten Cate FJ, Vannan MA, Zamorano JL, Zoghbi WA. (2012) EAE/ASE recommendations for image acquisition and display using three-dimensional echocardiography. J Am Soc Echocardiogr, 25: 3-46.

127. Cao QL, Pandian NG, Azevedo J, Schwartz SL, Vogel M, Fulton D, Marx G. (1994) Enhanced comprehension of dynamic cardiovascular anatomy by three-dimensional echocardiography with the use of mixed shading techniques. Echocardiography, 11: 627-633.

128. Badano LP, Boccalini F, Muraru D, Bianco LD, Peluso D, Bellu R, Zoppellaro G, Iliceto S. (2012) Current clinical applications of transthoracic three-dimensional echocardiography. J Cardiovasc Ultrasound, 20: 1-22.

129. Fenster A, Downey DB, Cardinal HN. (2001) Three-dimensional ultrasound imaging. Phys Med Biol, 46: R67-99.

130. Rankin RN, Fenster A, Downey DB, Munk PL, Levin MF, Vellet AD. (1993) Three-dimensional sonographic reconstruction: techniques and diagnostic applications. AJR Am J Roentgenol, 161: 695-702.

131. Pandian NG, Roelandt J, Nanda NC, Sugeng L, Cao QL, Azevedo J, Schwartz SL, Vannan MA, Ludomirski A, Marx G, et al. (1994) Dynamic three-dimensional echocardiography: methods and clinical potential. Echocardiography, 11: 237-259.

132. Dorosz JL, Lezotte DC, Weitzenkamp DA, Allen LA, Salcedo EE. (2012) Performance of 3-dimensional echocardiography in measuring left ventricular volumes and ejection fraction: a systematic review and meta-analysis. J Am Coll Cardiol, 59: 1799-1808.

133. Caiani EG, Corsi C, Zamorano J, Sugeng L, MacEneaney P, Weinert L, Battani R, Gutierrez-Chico JL, Koch R, Perez de Isla L, Mor-Avi V, Lang RM. (2005) Improved semiautomated quantification of left ventricular volumes and ejection fraction using 3-dimensional echocardiography with a full matrix-array transducer: comparison with magnetic resonance imaging. J Am Soc Echocardiogr, 18: 779-788.

134. Jacobs LD, Salgo IS, Goonewardena S, Weinert L, Coon P, Bardo D, Gerard O, Allain P, Zamorano JL, de Isla LP, Mor-Avi V, Lang RM. (2006) Rapid online

quantification of left ventricular volume from real-time three-dimensional echocardiographic data. Eur Heart J, 27: 460-468.

135. Greupner J, Zimmermann E, Grohmann A, Dubel HP, Althoff TF, Borges AC, Rutsch W, Schlattmann P, Hamm B, Dewey M. (2012) Head-to-head comparison of left ventricular function assessment with 64-row computed tomography, biplane left cineventriculography, and both 2- and 3-dimensional transthoracic echocardiography: comparison with magnetic resonance imaging as the reference standard. J Am Coll Cardiol, 59: 1897-1907.

136. Chuang ML, Beaudin RA, Riley MF, Mooney MG, Mannin WJ, Douglas PS, Hibberd MG. (2000) Three-dimensional echocardiographic measurement of left ventricular mass: comparison with magnetic resonance imaging and two-dimensional echocardiographic determinations in man. Int J Card Imaging, 16: 347-357.

137. Mor-Avi V, Sugeng L, Weinert L, MacEneaney P, Caiani EG, Koch R, Salgo IS, Lang RM. (2004) Fast measurement of left ventricular mass with real-time three-dimensional echocardiography: comparison with magnetic resonance imaging. Circulation, 110: 1814-1818.

138. Jenkins C, Chan J, Bricknell K, Strudwick M, Marwick TH. (2007) Reproducibility of right ventricular volumes and ejection fraction using real-time three-dimensional echocardiography: comparison with cardiac MRI. Chest, 131: 1844-1851.

139. Badano LP, Ginghina C, Easaw J, Muraru D, Grillo MT, Lancellotti P, Pinamonti B, Coghlan G, Marra MP, Popescu BA, De Vita S. (2010) Right ventricle in pulmonary arterial hypertension: haemodynamics, structural changes, imaging, and proposal of a study protocol aimed to assess remodelling and treatment effects. Eur J Echocardiogr, 11: 27-37.

140. Sugeng L, Mor-Avi V, Weinert L, Niel J, Ebner C, Steringer-Mascherbauer R, Bartolles R, Baumann R, Schummers G, Lang RM, Nesser HJ. (2010) Multimodality comparison of quantitative volumetric analysis of the right ventricle. JACC Cardiovasc Imaging, 3: 10-18.

141. van der Zwaan HB, Helbing WA, McGhie JS, Geleijnse ML, Luijnenburg SE, Roos-Hesselink JW, Meijboom FJ. (2010) Clinical value of real-time three-dimensional

echocardiography for right ventricular quantification in congenital heart disease: validation with cardiac magnetic resonance imaging. J Am Soc Echocardiogr, 23: 134-140.

142. Leibundgut G, Rohner A, Grize L, Bernheim A, Kessel-Schaefer A, Bremerich J, Zellweger M, Buser P, Handke M. (2010) Dynamic assessment of right ventricular volumes and function by real-time three-dimensional echocardiography: a comparison study with magnetic resonance imaging in 100 adult patients. J Am Soc Echocardiogr, 23: 116-126.

143. Medvedofsky D, Addetia K, Patel AR, Sedlmeier A, Baumann R, Mor-Avi V, Lang RM. (2015) Novel Approach to Three-Dimensional Echocardiographic Quantification of Right Ventricular Volumes and Function from Focused Views. J Am Soc Echocardiogr, 28: 1222-1231.

144. Monaghan MJ. (2006) Role of real time 3D echocardiography in evaluating the left ventricle. Heart, 92: 131-136.

145. Shiota T. (2014) Role of modern 3D echocardiography in valvular heart disease. Korean J Intern Med, 29: 685-702.

146. Shiota T. (2015) Clinical application of 3-dimensional echocardiography in the USA. Circ J, 79: 2287-2298.

147. Espinola-Zavaleta N, Lozoya-Del Rosal JJ, Colin-Lizalde L, Lupi-Herrera E. (2014) Left atrial cardiac myxoma. Two unusual cases studied by 3D echocardiography. BMJ Case Rep, 2014.

148. Mart CR. (2012) Three-dimensional echocardiographic evaluation of the Fontan conduit for thrombus. Echocardiography, 29: 363-368.

149. Stefani L, Galanti G, Toncelli L, Manetti P, Vono MC, Rizzo M, Maffulli N. (2008) Bicuspid aortic valve in competitive athletes. Br J Sports Med, 42: 31-35; discussion 35.

150. Stefani L, De Luca A, Toncelli L, Pedrizzetti G, Galanti G. (2014) 3D Strain helps relating LV function to LV and structure in athletes. Cardiovasc Ultrasound, 12: 33.

151. Kalam K, Otahal P, Marwick TH. (2014) Prognostic implications of global LV dysfunction: a systematic review and meta-analysis of global longitudinal strain and ejection fraction. Heart, 100: 1673-1680.

152. Auger DA, Zhong X, Epstein FH, Spottiswoode BS. (2012) Mapping right ventricular myocardial mechanics using 3D cine DENSE cardiovascular magnetic resonance. J Cardiovasc Magn Reson, 14: 4.

153. Maffessanti F, Muraru D, Esposito R, Gripari P, Ermacora D, Santoro C, Tamborini G, Galderisi M, Pepi M, Badano LP. (2013) Age-, body size-, and sex-specific reference values for right ventricular volumes and ejection fraction by three-dimensional echocardiography: a multicenter echocardiographic study in 507 healthy volunteers. Circ Cardiovasc Imaging, 6: 700-710.

154. Pavlik G, Major Z, Varga-Pinter B, Jeserich M, Kneffel Z. (2010) The athlete's heart Part I (Review). Acta Physiol Hung, 97: 337-353.

155. Szauder I, Kovacs A, Pavlik G. (2015) Comparison of left ventricular mechanics in runners versus bodybuilders using speckle tracking echocardiography. Cardiovasc Ultrasound, 13: 7.

156. Kusunose K, Kwon DH, Motoki H, Flamm SD, Marwick TH. (2013) Comparison of three-dimensional echocardiographic findings to those of magnetic resonance imaging for determination of left ventricular mass in patients with ischemic and non-ischemic cardiomyopathy. Am J Cardiol, 112: 604-611.

157. Muraru D, Cecchetto A, Cucchini U, Zhou X, Lang RM, Romeo G, Vannan M, Mihaila S, Miglioranza MH, Iliceto S, Badano LP. (2018) Intervendor Consistency and Accuracy of Left Ventricular Volume Measurements Using Three-Dimensional Echocardiography. J Am Soc Echocardiogr, 31: 158-168.

158. D'Ascenzi F, Pelliccia A, Solari M, Piu P, Loiacono F, Anselmi F, Caselli S, Focardi M, Bonifazi M, Mondillo S. (2017) Normative Reference Values of Right Heart in Competitive Athletes: A Systematic Review and Meta-Analysis. J Am Soc Echocardiogr, 30: 845-858.

159. Lakatos B, Kovacs A, Tokodi M, Doronina A, Merkely B. (2016) Assessment of the right ventricular anatomy and function by advanced echocardiography: pathological and physiological insights. Orv Hetil, 157: 1139-1146.

160. Chivulescu M, Haugaa K, Lie OH, Edvardsen T, Ginghina C, Popescu BA, Jurcut R. (2018) Right ventricular remodeling in athletes and in arrhythmogenic cardiomyopathy. Scand Cardiovasc J, 52: 13-19.

161. Kovacs A, Olah A, Lux A, Matyas C, Nemeth BT, Kellermayer D, Ruppert M, Torok M, Szabo L, Meltzer A, Assabiny A, Birtalan E, Merkely B, Radovits T. (2015) Strain and strain rate by speckle-tracking echocardiography correlate with pressure-volume loop-derived contractility indices in a rat model of athlete's heart. Am J Physiol Heart Circ Physiol, 308: H743-748.

162. Kooreman Z, Giraldeau G, Finocchiaro G, Kobayashi Y, Wheeler M, Perez M, Moneghetti K, Oxborough D, George KP, Myers J, Ashley E, Haddad F. (2018) Athletic Remodeling in Female College Athletes, the "Morganroth Hypothesis" Revisited. Clin J Sport Med.

163. Kovacs A, Apor A, Nagy A, Vago H, Toth A, Nagy AI, Kovats T, Sax B, Szeplaki G, Becker D, Merkely B. (2014) Left ventricular untwisting in athlete's heart: key role in early diastolic filling? Int J Sports Med, 35: 259-264.

164. Sanchis L, Sanz-de La Garza M, Bijnens B, Giraldeau G, Grazioli G, Marin J, Gabrielli L, Montserrat S, Sitges M. (2017) Gender influence on the adaptation of atrial performance to training. Eur J Sport Sci, 17: 720-726.

165. Kouri EM, Pope HG, Jr., Katz DL, Oliva P. (1995) Fat-free mass index in users and nonusers of anabolic-androgenic steroids. Clin J Sport Med, 5: 223-228.

166. Schutz Y, Kyle UU, Pichard C. (2002) Fat-free mass index and fat mass index percentiles in Caucasians aged 18-98 y. Int J Obes Relat Metab Disord, 26: 953-960.

167. La Gerche A, Roberts T, Claessen G. (2014) The response of the pulmonary circulation and right ventricle to exercise: exercise-induced right ventricular dysfunction and structural remodeling in endurance athletes (2013 Grover Conference series). Pulm Circ, 4: 407-416.

168. Roy A, Doyon M, Dumesnil JG, Jobin J, Landry F. (1988) Endurance vs. strength training: comparison of cardiac structures using normal predicted values. J Appl Physiol (1985), 64: 2552-2557.

169. Pelliccia A, Culasso F, Di Paolo FM, Maron BJ. (1999) Physiologic left ventricular cavity dilatation in elite athletes. Ann Intern Med, 130: 23-31.

170. Baggish AL, Wang F, Weiner RB, Elinoff JM, Tournoux F, Boland A, Picard MH, Hutter AM, Jr., Wood MJ. (2008) Training-specific changes in cardiac structure and function: a prospective and longitudinal assessment of competitive athletes. J Appl Physiol (1985), 104: 1121-1128.

171. Levine BD, Baggish AL, Kovacs RJ, Link MS, Maron MS, Mitchell JH. (2015) Eligibility and Disqualification Recommendations for Competitive Athletes With Cardiovascular Abnormalities: Task Force 1: Classification of Sports: Dynamic, Static, and Impact: A Scientific Statement From the American Heart Association and American College of Cardiology. J Am Coll Cardiol, 66: 2350-2355.

172. Abergel E, Chatellier G, Hagege AA, Oblak A, Linhart A, Ducardonnet A, Menard J. (2004) Serial left ventricular adaptations in world-class professional cyclists: implications for disease screening and follow-up. J Am Coll Cardiol, 44: 144-149.

173. Richand V, Lafitte S, Reant P, Serri K, Lafitte M, Brette S, Kerouani A, Chalabi H, Dos Santos P, Douard H, Roudaut R. (2007) An ultrasound speckle tracking (two-dimensional strain) analysis of myocardial deformation in professional soccer players compared with healthy subjects and hypertrophic cardiomyopathy. Am J Cardiol, 100: 128-132.

174. Pagourelias ED, Kouidi E, Efthimiadis GK, Deligiannis A, Geleris P, Vassilikos V. (2013) Right atrial and ventricular adaptations to training in male Caucasian athletes: an echocardiographic study. J Am Soc Echocardiogr, 26: 1344-1352.

175. Major Z, Csajagi E, Kneffel Z, Kovats T, Szauder I, Sido Z, Pavlik G. (2015) Comparison of left and right ventricular adaptation in endurance-trained male athletes. Acta Physiol Hung, 102: 23-33.

176. Prakken NH, Velthuis BK, Teske AJ, Mosterd A, Mali WP, Cramer MJ. (2010) Cardiac MRI reference values for athletes and nonathletes corrected for body surface area, training hours/week and sex. Eur J Cardiovasc Prev Rehabil, 17: 198-203.

177. La Gerche A, Burns AT, D'Hooge J, Macisaac AI, Heidbuchel H, Prior DL. (2012) Exercise strain rate imaging demonstrates normal right ventricular contractile reserve and

clarifies ambiguous resting measures in endurance athletes. J Am Soc Echocardiogr, 25: 253-262.

178. Moceri P, Duchateau N, Baudouy D, Schouver ED, Leroy S, Squara F, Ferrari E, Sermesant M. (2017) Three-dimensional right-ventricular regional deformation and survival in pulmonary hypertension. Eur Heart J Cardiovasc Imaging, 19: 450-458.

179. Yusen RD, Edwards LB, Dipchand AI, Goldfarb SB, Kucheryavaya AY, Levvey BJ, Lund LH, Meiser B, Rossano JW, Stehlik J, International Society for H, Lung T. (2016) The Registry of the International Society for Heart and Lung Transplantation: Thirty-third Adult Lung and Heart-Lung Transplant Report-2016; Focus Theme: Primary Diagnostic Indications for Transplant. J Heart Lung Transplant, 35: 1170-1184.

180. Stobierska-Dzierzek B, Awad H, Michler RE. (2001) The evolving management of acute right-sided heart failure in cardiac transplant recipients. J Am Coll Cardiol, 38: 923-931.

181. Badano LP, Miglioranza MH, Edvardsen T, Colafranceschi AS, Muraru D, Bacal F, Nieman K, Zoppellaro G, Marcondes Braga FG, Binder T, Habib G, Lancellotti P. (2015) European Association of Cardiovascular Imaging/Cardiovascular Imaging Department of the Brazilian Society of Cardiology recommendations for the use of cardiac imaging to assess and follow patients after heart transplantation. Eur Heart J Cardiovasc Imaging, 16: 919-948.

182. D'Andrea A, Riegler L, Nunziata L, Scarafile R, Gravino R, Salerno G, Amarelli C, Maiello C, Limongelli G, Di Salvo G, Caso P, Bossone E, Calabro R, Pacileo G, Russo MG. (2013) Right heart morphology and function in heart transplantation recipients. J Cardiovasc Med (Hagerstown), 14: 648-658.

183. Bacal F, Pires PV, Moreira LF, Silva CP, Filho JR, Costa UM, Rosario-Neto MA, Avila VM, Cruz FD, Guimaraes GV, Issa VS, Ferreira SA, Stolf N, Ramires JA, Bocchi E. (2005) Normalization of right ventricular performance and remodeling evaluated by magnetic resonance imaging at late follow-up of heart transplantation: relationship between function, exercise capacity and pulmonary vascular resistance. J Heart Lung Transplant, 24: 2031-2036.

184. Raina A, Vaidya A, Gertz ZM, Susan C, Forfia PR. (2013) Marked changes in right ventricular contractile pattern after cardiothoracic surgery: implications for post-surgical assessment of right ventricular function. J Heart Lung Transplant, 32: 777-783.

185. Sakuma M, Ishigaki H, Komaki K, Oikawa Y, Katoh A, Nakagawa M, Hozawa H, Yamamoto Y, Takahashi T, Shirato K. (2002) Right ventricular ejection function assessed by cineangiography--Importance of bellows action. Circ J, 66: 605-609.

186. Muraru D, Spadotto V, Cecchetto A, Romeo G, Aruta P, Ermacora D, Jenei C, Cucchini U, Iliceto S, Badano LP. (2016) New speckle-tracking algorithm for right ventricular volume analysis from three-dimensional echocardiographic data sets: validation with cardiac magnetic resonance and comparison with the previous analysis tool. Eur Heart J Cardiovasc Imaging, 17: 1279-1289.

187. Clemmensen TS, Eiskjaer H, Logstrup BB, Andersen MJ, Mellemkjaer S, Poulsen SH. (2016) Echocardiographic assessment of right heart function in heart transplant recipients and the relation to exercise hemodynamics. Transpl Int, 29: 909-920.

188. Nyhan DP, Redmond JM, Gillinov AM, Nishiwaki K, Murray PA. (1994) Prolonged pulmonary vascular hyperreactivity in conscious dogs after cardiopulmonary bypass. J Appl Physiol (1985), 77: 1584-1590.

189. Erickson KW, Costanzo-Nordin MR, O'Sullivan EJ, Johnson MR, Zucker MJ, Pifarre R, Lawless CE, Robinson JA, Scanlon PJ. (1990) Influence of preoperative transpulmonary gradient on late mortality after orthotopic heart transplantation. J Heart Transplant, 9: 526-537.

190. Bhatia SJ, Kirshenbaum JM, Shemin RJ, Cohn LH, Collins JJ, Di Sesa VJ, Young PJ, Mudge GH, Jr., Sutton MG. (1987) Time course of resolution of pulmonary hypertension and right ventricular remodeling after orthotopic cardiac transplantation. Circulation, 76: 819-826.

191. Bourge RC, Kirklin JK, Naftel DC, White C, Mason DA, Epstein AE. (1991) Analysis and predictors of pulmonary vascular resistance after cardiac transplantation. J Thorac Cardiovasc Surg, 101: 432-444.

192. Tedford RJ, Beaty CA, Mathai SC, Kolb TM, Damico R, Hassoun PM, Leary PJ, Kass DA, Shah AS. (2014) Prognostic value of the pre-transplant diastolic pulmonary

artery pressure-to-pulmonary capillary wedge pressure gradient in cardiac transplant recipients with pulmonary hypertension. J Heart Lung Transplant, 33: 289-297.

193. Murata M, Tsugu T, Kawakami T, Kataoka M, Minakata Y, Endo J, Tsuruta H, Itabashi Y, Maekawa Y, Murata M, Fukuda K. (2016) Prognostic value of three-dimensional echocardiographic right ventricular ejection fraction in patients with pulmonary arterial hypertension. Oncotarget, 7: 86781-86790.

194. Kind T, Mauritz GJ, Marcus JT, van de Veerdonk M, Westerhof N, Vonk-Noordegraaf A. (2010) Right ventricular ejection fraction is better reflected by transverse rather than longitudinal wall motion in pulmonary hypertension. J Cardiovasc Magn Reson, 12: 35.

195. Brown SB, Raina A, Katz D, Szerlip M, Wiegers SE, Forfia PR. (2011) Longitudinal shortening accounts for the majority of right ventricular contraction and improves after pulmonary vasodilator therapy in normal subjects and patients with pulmonary arterial hypertension. Chest, 140: 27-33.

196. Bittner HB, Chen EP, Milano CA, Kendall SW, Jennings RB, Sabiston DC, Jr., Van Trigt P. (1995) Myocardial beta-adrenergic receptor function and high-energy phosphates in brain death--related cardiac dysfunction. Circulation, 92: 472-478.

197. Ferrera R, Hadour G, Tamion F, Henry JP, Mulder P, Richard V, Thuillez C, Ovize M, Derumeaux G. (2011) Brain death provokes very acute alteration in myocardial morphology detected by echocardiography: preventive effect of beta-blockers. Transpl Int, 24: 300-306.

198. Schwarz K, Singh S, Dawson D, Frenneaux MP. (2013) Right ventricular function in left ventricular disease: pathophysiology and implications. Heart Lung Circ, 22: 507-511.

199. Fritz T, Wieners C, Seemann G, Steen H, Dossel O. (2014) Simulation of the contraction of the ventricles in a human heart model including atria and pericardium. Biomech Model Mechanobiol, 13: 627-641.

200. Unsworth B, Casula RP, Kyriacou AA, Yadav H, Chukwuemeka A, Cherian A, Stanbridge Rde L, Athanasiou T, Mayet J, Francis DP. (2010) The right ventricular annular

velocity reduction caused by coronary artery bypass graft surgery occurs at the moment of pericardial incision. Am Heart J, 159: 314-322.

201. Tamborini G, Muratori M, Brusoni D, Celeste F, Maffessanti F, Caiani EG, Alamanni F, Pepi M. (2009) Is right ventricular systolic function reduced after cardiac surgery? A two- and three-dimensional echocardiographic study. Eur J Echocardiogr, 10: 630-634.

202. Maffessanti F, Gripari P, Tamborini G, Muratori M, Fusini L, Alamanni F, Zanobini M, Fiorentini C, Caiani EG, Pepi M. (2012) Evaluation of right ventricular systolic function after mitral valve repair: a two-dimensional Doppler, speckle-tracking, and three-dimensional echocardiographic study. J Am Soc Echocardiogr, 25: 701-708.

203. Schuuring MJ, Bolmers PP, Mulder BJ, de Bruin-Bon RA, Koolbergen DR, Hazekamp MG, Lagrand WK, De Hert SG, de Beaumont EM, Bouma BJ. (2012) Right ventricular function declines after cardiac surgery in adult patients with congenital heart disease. Int J Cardiovasc Imaging, 28: 755-762.

204. Hedman A, Alam M, Zuber E, Nordlander R, Samad BA. (2004) Decreased right ventricular function after coronary artery bypass grafting and its relation to exercise capacity: a tricuspid annular motion-based study. J Am Soc Echocardiogr, 17: 126-131.

205. Lindqvist P, Holmgren A, Zhao Y, Henein MY. (2012) Effect of pericardial repair after aortic valve replacement on septal and right ventricular function. Int J Cardiol, 155: 388-393.

206. Peura JL, Zile MR, Feldman DS, VanBakel AB, McClure C, Uber W, Haynes H, Pereira NL. (2005) Effects of conversion from cyclosporine to tacrolimus on left ventricular structure in cardiac allograft recipients. J Heart Lung Transplant, 24: 1969-1972.

207. Wink J, de Wilde RB, Wouters PF, van Dorp EL, Veering BT, Versteegh MI, Aarts LP, Steendijk P. (2016) Thoracic Epidural Anesthesia Reduces Right Ventricular Systolic Function With Maintained Ventricular-Pulmonary Coupling. Circulation, 134: 1163-1175.

208. Buendia-Fuentes F, Almenar L, Ruiz C, Vercher JL, Sanchez-Lazaro I, Martinez-Dolz L, Navarro J, Bello P, Salvador A. (2011) Sympathetic reinnervation 1 year after heart

transplantation, assessed using iodine-123 metaiodobenzylguanidine imaging. Transplant Proc, 43: 2247-2248.

209. Bernardi L, Bianchini B, Spadacini G, Leuzzi S, Valle F, Marchesi E, Passino C, Calciati A, Vigano M, Rinaldi M, et al. (1995) Demonstrable cardiac reinnervation after human heart transplantation by carotid baroreflex modulation of RR interval. Circulation, 92: 2895-2903.

210. Beniaminovitz A, Savoia MT, Oz M, Galantowicz M, Di Tullio MR, Homma S, Mancini D. (1997) Improved atrial function in bicaval versus standard orthotopic techniques in cardiac transplantation. Am J Cardiol, 80: 1631-1635.

211. Clemmensen TS, Logstrup BB, Eiskjaer H, Poulsen SH. (2016) Serial changes in longitudinal graft function and implications of acute cellular graft rejections during the first year after heart transplantation. Eur Heart J Cardiovasc Imaging, 17: 184-193.

212. Sera F, Kato TS, Farr M, Russo C, Jin Z, Marboe CC, Di Tullio MR, Mancini D, Homma S. (2014) Left ventricular longitudinal strain by speckle-tracking echocardiography is associated with treatment-requiring cardiac allograft rejection. J Card Fail, 20: 359-364.

213. Pichler P, Binder T, Hofer P, Bergler-Klein J, Goliasch G, Lajic N, Aliabadi A, Zuckermann A, Syeda B. (2012) Two-dimensional speckle tracking echocardiography in heart transplant patients: three-year follow-up of deformation parameters and ejection fraction derived from transthoracic echocardiography. Eur Heart J Cardiovasc Imaging, 13: 181-186.

12. BIBLIOGRAPHY OF CANDIDATE`S PUBLICATIONS

12.1 Publications related to the present thesis

Doronina A, Édes I, Ujvari A, Kántor Z, Lakatos B, Tokodi M, Sydó N, Kiss O, Abramov A, Kovács A, Merkely B.

The female athlete's heart: comparison of cardiac changes induced by different types of exercise training using 3D echocardiography.

BioMed Research International. 2018; DOI: 10.1155/2018/3561962
IF: 2.476

Ujvári A, Komka Zs,Kántor Z, Lakatos,Tokodi M, **Doronina A**, Babity M, Bognár Cs, Kiss O, Merkely B, Kovács A.

Kajakos és kenus élsportolók bal és jobb kamrai analízise 3D echokardiográfia segítségével.

Cardiologia Hungarica 2018; 48: 13–19

Lakatos BK, Tokodi M, Assabiny A, Tősér Z, Kosztin A, **Doronina A**, Rácz K, Koritsánszky KB, Berzsenyi V, Németh E, Sax B, Kovács A, Merkely B.

Dominance of free wall radial motion in global right ventricular function of heart transplant recipients.

Clin Transplant. 2018; DOI: 10.1111/ctr.13192
IF: 1.865

12.2 Publications not related to the present thesis

Lakatos B, Tősér Z, Tokodi M, **Doronina A**, Kosztin A, Muraru D, Badano LP, Kovács A, Merkely B

Quantification of the relative contribution of the different right ventricular wall motion components to right ventricular wall motion components to right ventricular ejection fraction: the ReVISION method.

Cardiovasc Ultrasound. 2017;15(1):8.
IF: 1.598

Lakatos B, Kovács A, Tokodi M, **Doronina A**, Merkely B.

Assessment of the right ventricular anatomy and function by advanced echocardiography: pathological and physiological insights.

Orv Hetil. 2016; 157(29):1139-46
IF: 0.349